URJA 2014-15

Electrical & Electronics Engineering Department E-Magazine

Research Papers
Lightning strike
Engineering work is challenging
Large selection of engineering paths gives career flexibility

CONTENTS

Editorial Board

- Faculty Coordinator:Ms.Ankita Singh
- Editor- in-Chief:Ms. Harshita Gupta
- Co-Editors :Lavina Kanjani

Principal Message

Institute of Engineering and Science, IPS Academy is a leading, premium institution devoted to imparting quality engineering education since 1999. The sustained growth with constant academic brilliance achieved by IES is due to a greater commitment from management, dynamic leadership of the president, academically distinctive and experienced faculty, Disciplined students and service oriented supporting staff. The Institute is playing a key role in creating and ambiance for the creation of novel ideas, knowledge, and graduates who will be the leaders of tomorrow.The Institute is convinced that in order to achieve this objective, we will need to pursue a strategy that fosters creativity, supports interdisciplinary research and education. This will also provide the students with an understanding and appreciation not only of the process of knowledge creation, but also of the process by which technology and knowledge may be used to create wealth as well as achieve social economicgoals.

I am delighted to note that the engineering graduates of this institute have been able to demonstrate their capable identities in different spheres of life and occupied prestigious position within the country and abroad. The excellence of any institute is a measure of achievements made by the students and faculty.

Dr. Archana Keerti Chowdhary
Principal

HOD Message

Our Country is passing through a critical phase of growth. If you take an over view of this growth, we find that we are developing new energy dimension and electrical energy plays the most vital part in total energy context. In fact, electricity is taking the role of indispensible energy form of our daily life. Ours is the sixth largest country in terms of global energy consumption. The last decades of economic growth of our country has brought an unprecedented demand for energy. The installed electrical generating capacity of our country stands at 162366 Megawatts in 2010, and is projected to be 950000 MW by 2030. This large scale use of electrical energy will definitely demand a large team of electrical engineers to manage its use. All the same there is continuous pressure of balancing our ecology especially in context to global warming. This is forcing to ensure efficient use of electrical energy. Electronic power control is offering new tools in management of electrical energy.

Electrical and Electronics engineering together is a dedicated branch of engineering to fulfill all challenges of electrical energy futures.

Prof. B.N. Phadke

HOD

FFICIENCY LED DRIVING CIRCUIT BASED LED

[1]Raj Roushan, [2] Rajvardhan Jain , [3]Bhavana Rohit
Electrical & Electronics Engineering Department
IES,IPS Academy
[1]rajroushan10@gmail.com
[2] rajvivek0001@gmail.com
[3]bhavanarohit@gmail.com

***Abstract*- A high efficiency LED (Light Emitting Diode) driver based on AC-DC converter without using transformer, which could operate under a wide AC input voltage range (150 V - 240 V) and drive a series of high power LEDs, is presented in this paper. The operation principles, power loss factors of the LED driver in this study are analyzed and discussed in detail and some effective ways to improve efficiency are proposed through system design considerations. To verify the feasibility, a laboratory prototype is also designed and tested for an LED lamp which consists of 30 LEDs in series. Experimental results show that a high efficiency of 94% at *Io* = 250 mA can be achieved and the studied driver might be practical for driving high power LEDs. In the last, the over-all efficiency over 92% is gained through some experiments under variable input and output voltages and verifies the validity of the designed driver.**

***Keywords:* LED Driver, High Efficiency, Rectifier circuit without transformer**

I. INTRODUCTION

Among the many artificial lighting sources, high power LED characterized by high luminous intensity, superior longevity, cost-effective and less environment impact, is one of the most competitive to replace the conventional incandescent lamp and fluorescent lamp and gradually becomes a commonly used solid-state lighting source in many lighting applications [1-3]. It has been extensively used in the offline lighting field, such as automotive illuminations, liquid crystal display (LCD) backlights and street lighting, where multiple strings of LED driving techniques are often needed. The increased popularity of high power LED has given a requirement for electronic engineers to propose a series of driving circuits with high efficiency and low-cost.

LED dimming control methods could be simply di-vided into two categories: analog dimming and pulse width modulation (PWM) dimming regulators [4-7]. Analog dimming method is not a good candidate due to colour variation, even though it is simple and cost effective. To avoid colour variation and get accurate current control over full range, PWM dimming regulators in which the pulse current is kept constant. To research the overall efficiency of LED lighting, a driver is chosen in this paper as shown in Fig. 1, and the power dissipation factors are analyzed with all the particulars, then a detailed LED driver example with high power efficiency is designed and implemented.

II. DRIVER

The circuit diagram was designed to create a power supply without utilizing any transformer circuit. This circuit illustrates the advantages as well as the safety precautions to keep in mind. Power supplies are devices accustomed to provide electrical or other sort of energy to a load or cluster of load. A type of power supply that makes use of a transformer is the AC powered linear power supply. The voltage from the wall socket is converted by the transformer to produce a normally

lower voltage. Switched-mode and AC/DC power supplies are the types that does not utilize the presence of transformers. These transformers are responsible for transmitting electrical supply from one circuit to another through its coils (windings).

Designing a transformer less power supply makes it more suitable for smaller installations, in any location, where the area may be limited. The circuit can manage the high current coming from the mains by supplying 90 Volts at 250mA. The reason behind using capacitive reactance rather than resistance is the fact the type of current flowing into the circuit is alternating. It can also be used with fluctuating DC supply. The reactance adapts with the way the components react in the circuit in terms of frequencies. A fusible resistor can also be used to provide more safety.As an output device, optical sensors are preferred by measuring the intensity change of light when the power is increased among other controllers like temperature controllers, light switches or timers. The capacitor C1 are connected across the mains supply to act as restrainer. These capacitors are usually tagged with safety standard measures, although they are usually more expensive type rather than ordinary capacitors. Placing two capacitors in parallel or increasing the value can give way to additional current. The two zener diodes are responsible for supplying the low voltage because these types of diodes controls the output by setting their breakdown or desired voltage, as they flow to the rectifier. The rectifier is responsible for converting the AC to DC. Opposite conversion form DC to AC uses an inverter. If the circuit would require an output higher than 200mA, transformers would be more significant to use.

The comparison between transformerless and transformer-based power supplies is not easy to identify due to the technologies that each one offers in the market. But the primary difference between the two are the physical dimension, noise, efficiency and the intensity of harmonic distortion that they produce.

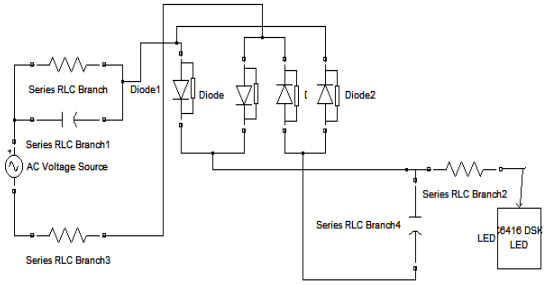

Fig. 1. Simulink model of driver circuit

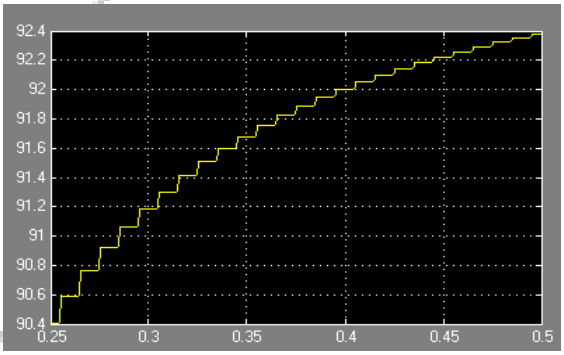

Fig.2. Output wave form

III. DESIGN AND EXPERIMENTAL RESULTS

In this section, an LED constant current driver with high power efficiency is designed and implemented according to the following configuration:

- Input voltage: AC 150 - 240V
- LED string voltage: DC 50 - 90 V
- LED current: 250 mA
- Expected efficiency: 92%

An LED constant current topology driving a input DC supply voltage range from 50 V to 90 V is chosen as a controller and the schematic diagram

shown in Fig. 1. And it is used to drive an LED string with 30 LED with a 3 V working voltage.

The AC 220 V input voltage is converted to 90V DC after following through the rectifier bridge and the filtering capacitors. The system output voltage is $Vo=n*V_{LED}=90$ V. High switching frequency will reduce the size of the inductor *L*, but it will increase the circuit's switch dissipation. The oscillator frequency of is from 20 kHz to 150 kHz and we choice a typical constant switching frequency 40 kHz. The timing resistor should be 620 kΩ and connect to the ground re-ferring. Next to choose the capacitance values of C1 and C2. In order to satisfy the stability requirements at constant switching frequency, the maximum LED string voltage must be less than the half of the minimum input voltage. The minimum input voltage is shown in Equation (1):

$$Vin(min)=2*Vo(max)=150\ V \quad \ldots\ldots(1)$$

The capacitance value C1 should be calculated at the minimum AC input voltage, and the nominal voltage should be larger than the input peak voltage as shown in the following Equations (2) and (3)

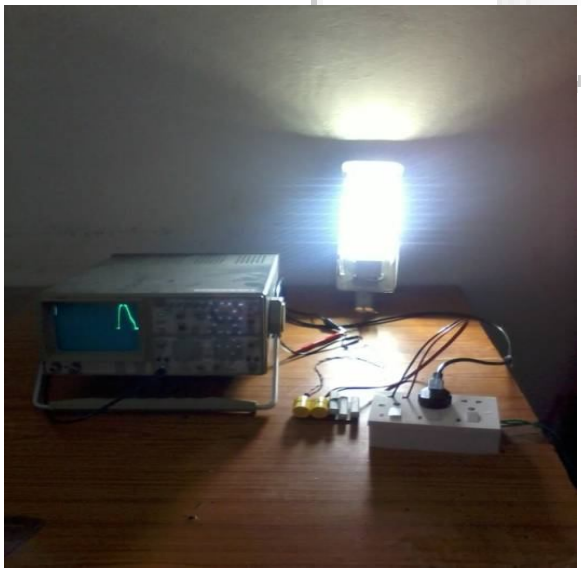

Fig.5 Experiment model

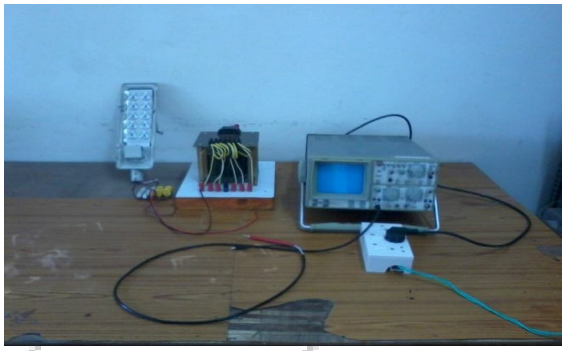

Fig.5 Experiment model

$$C_1 \geq \frac{I_{O(\max)} \times V_{O(\max)}}{\left(2 \times V_{i(\min)}^2 - V_{IN(\min)}^2\right) \times f_s \times \eta} \Rightarrow C_1 \geq 11.67\ \mu F$$

…(2)

$$V_{C_1(\max)} \geq \sqrt{2} \times V_{i(\max)} \Rightarrow V_{C_1(\max)} \geq 375\ V$$

…….(3)

From the mentioned above, we choose a electrolytic capacitor with 33 uF, 240 V. The stability of the electrolytic capacitor is good. However, it is not suitable for high frequency ripple current absorption. So a metalized polypropylene capacitor in parallel with the electrolytic capacitor is used to absorb the high frequency ripple current. The high frequency capacitance 0.47 uF and withstanding voltage 220 V is determined by the following equation:

$$C_2 \geq \frac{0.25 \times I_{O(\max)}}{\left(0.05 \times V_{IN(\min)}\right) \times f_s} \Rightarrow C_2 \geq 0.365\ \mu F$$

…… (4)

Next to calculate the inductance value which is deter-mined by the permissible ripple current and we assume that the existence of LED ripple current is allowed ±15% (total ripple is 30%).

IV. CONCLUSIONS

LED constant current drive circuit efficiency is deter- mined by several factors, and these factors are inter- related and influenced. To optimize and improve the efficiency of the driving system, the circuit performance and the appropriate components selections must be taken into consideration. In this paper, a high efficiency LED driver with AC input voltage range from 85 V to 265 V, which could drive an LED lamp consists of 30 LUMILEDS LEDs, is designed and tested. The measured results on a laboratory prototype show a high efficiency of 92% at I=250mA . Next, a series of experiments results under variable input and output voltages show that the efficiency is over 90% and reach the design re-quirements.

REFERENCES

[1]. Y. K. Cheng and K. W. E. Cheng, "General Study for Using LED to replace Traditional Lighting Devices," 2*nd International Conference on Power Electronics Systems and Applications*, Hong Kong, 12-14 November 2006, pp. 173-177. doi:10.1109/PESA.2006.343093.

[2]. E.-W. Wu, T.-Fu. Wu, J.-R. Tsai, Y.-M. Chen and C.-C. Chen, "Multistring LED Backlight Driving System for LCD Panels with Color Sequential Display and Area Control," *IEEE Transactions on Industrial Electronics*, Vol. 54, No. 10, 2008, pp. 3791-3800.

[3]. M. Rico-Secades, A. J. Calleja, J. Ribas, E. L. Corominas, J. M. Alonso, J. Cardesin and J. Garcia-Garcia, "Evalua-tion of a Low-Cost Permanent Emergency Lighting Sys-tem Based on High-Efficiency LEDs," *IEEE Transactions on Industry Applications*, Vol. 41, No. 5, 2005, pp. 1386-1390. doi:10.1109/TIA.2005.853389.

[4]. K. H. Loo, W.-K. Lun, S.-C. Tan, Y. M. Lai and C. K. Tse, "On Driving Techniques for LEDs: Toward a Gen-eralized Methodology," *IEEE Transactions on Power Electronics*, Vol. 24, No. 12, 2009, pp. 2967-2976. doi:10.1109/TPEL.2009.2021183

[5]. M. Nishika, Y. Ishizuka, H. Matsuo, *et al.*, "An LED Drive Circuit with Constant Output Current Control and Constant Luminance Control," 28*th Telecommunications Energy Conference*, Providence, September 2006, pp. 1-6.

[6]. H. V. D. Broeck, G. Sauerlander and M. Wendt, "Power Driver Topologies and Control Schemes for LEDs," *Twenty Second Annual IEEE of Applied Power Electron-ics Conference*, Anaheim, 25 February-1 March 2007, pp. 1319-1325.

[7]. F.-F. Ma, W.-Z. Chen and J.-C. Wu, "A Monolithic Cur-rent-Mode Buck Converter with Advanced Control and Protection Circuits," *IEEE Transactions on Power Electronics*, Vol. 22, No. 5, 2007, pp. 1836-1846. doi:10.1109/TPEL.2007.904237

[8]. H.-J. Chiu, Y.-K. Lo, J.-T. Chen, S.-J. Cheng, C.-Y. Lin and S.-C. Mou, "A high-Efficiency Dimmable LED Driver for Low-Power Lighting Applications," *IEEE Transactions on Industrial Electronics*, Vol. 57, No. 2, 2010, pp. 735-743. doi:10.1109/TIE.2009.2027251

[9]. D. Gacio, J. M. Alonso, A. J. Calleja, J. Garcia and M. Rico-Secades, "A Universal-Input Single-Stage High- Power-Factor Power Supply for HB-LEDs Based on In-tegrated Buck-Flyback Converter," *Twenty-Fourth Annual IEEE of Applied Power Electronics Conference and Exposition*, Washington, DC, 15-19 February 2009 pp. 570-576.

[10]. Y. Hu and M. M. Jovanovic, "LED Driver with Self- Adaptive Drive Voltage," *IEEE Transactions on Power Electronics*, Vol. 23, No. 6, 2008, pp. 3116-3125.

[11]. L. Zhao and A. Q. Zhu, “Design of Energy-Saving Intel-ligent LED Illumination System,” *Semiconductor Tech-nology,* Vol. 33, No. 2, 2008, pp. 137-140.

Analysis of separately excited DC Motor Using Matlab/Simulation

[1] Harsh Gujrati, [2] Ketan Patel,

Electrical & Electronics Engineering Department
IES,IPS Academy
[1]harshgujrati@gmail.com
[2] ketan99.2010@rediffmail.com

Abstract— This paper present comparison between separately excited DC motor characteristics using MATLAB/Simulink to practically dc drive characteristics. This paper describes a MATLAB/Simulink ac-dc converter fed dc motor speed and current comparison to practically work separately excited dc motor. The harmonics are presence in both model. In this paper show the efficiency of motor is reduced.

Keywords converter, DC motor, Speed control, MATLAB

I. INTRODUCTION

There are two types of single-phase diode rectifier that convert a single-phase ac supply into a dc voltage, namely, single-phase half-wave rectifiers and single-phase full-wave rectifiers. In the following paper, the operations of these rectifier circuits are examined and their performances. is generally valid for the case of diode rectifiers that use the mains, a low-frequency source, as the input, and when the forward voltage drop is small compared with the peak voltage of the mains.

Full wave circuits have the advantage that there is only one conducting device in series with the load, which was much more of an important consideration when mercury arc rectifiers were used, since they could have arc drops of 30V or more. However, modern thyristors lose only a volt or two, so that this is important only when working from abnormally low supply voltages. Generally, bridge circuits have better transformer utilization and are more frequently used. The paper describes the principles of unidirectional and bi-directional converters, followed by the effects of discontinuous load current and source reactance on their operation. The performance factors used in the analysis of these converter circuits are then obtained, and the chapter concludes with a description of gate-control and voltage multiplication circuits, which is a special application of rectification.

MATLAB with its toolboxes such as Simulink and Sim Power Systems is one of the most popular software packages, which has been used to support and enhance electric machinery courses. There are many methods of speed control of DC motors, namely field control, armature voltage control, and armature resistance control methods. In practice, the commonly method used to control the DC motor

speed is the armature voltage control method. In this method, a power electronic converter controllable rectifier or PWM chopper will supply the DC motors. This paper presents a Simulation model of a DC motor and practical motor model.

II. MODELLING OF DC MOTOR

The dc motor is basically a torque transducer that converts electrical energy into mechanical energy. The torque developed on the motor shaft is directly proportional to field flux and the armature current. A current carrying conductor is established in a magnetic field with flux ø and the conductor is located at a distance r from the centre of rotation the relationship among the developed torque flux and current I_a is-Where T_e is electromagnetic torque, ϕ is magnetic flux, I_a is armature current and K_m is proportional constant. The back emf and the shaft velocity is-

$$E_b = k_\phi \qquad \text{....(1)}$$

Where E_b = back emf

$$T_e = k_\phi I_a \qquad \text{.....(2)}$$

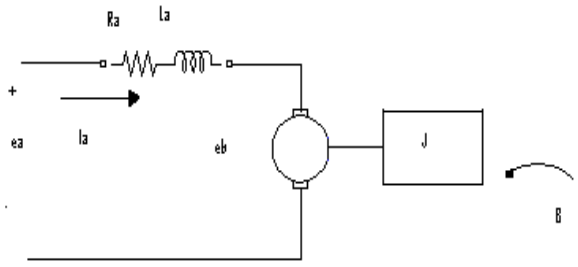

Fig.1. dc motor

The armature winding has a resistance R_a, a shaft inductance L_a, and an induced emf. The terminal relationship is-

$$E_b = I_a R_a + L_a \qquad \text{.....(3)}$$

In steady state the armature current is constant and hence the rate of change of the armature current is zero hence

$$V = E_b - I_a R_a \qquad \text{.....(4)}$$

Torque and speed is

$$T_e = \frac{E_b I_a}{\omega} = K_\phi I_a \qquad (5)$$

$$E_b = k_\phi \omega \qquad \text{.....(6)}$$

$$T_e = k_\phi I_a \qquad \text{.....(7)}$$

Where- I_a is the armature current

R_a is the armature resistance

L_a is the armature inductance

E_b is the is back emf

T_e is the electromagnetic torque

ω is the angular velocity

P_a is the air gap power

k_ϕ is the flux constant

The load is modeled as a moment of inertia J Kg m^2/sec^2 with a viscous friction coefficient, B_1 in Nm/(rad/sec). Then the acceleration torque T_a Nm drives the load is given by-

$$J\frac{d\omega}{dt} + B_1 = T_e - T_L = T_a \qquad \text{.....(8)}$$

Where – T_L is the load torque

T_a is the acceleration torque

B_1 = is the viscous friction

J = is the moment of inertia

From equation (1)

$$\frac{dI_a}{dt} = \frac{V}{L_a} - \frac{K_\phi \omega}{L_a} - \frac{I_a R_a}{L_a} \qquad \text{.....(9)}$$

From equation (2)

$$\frac{d\omega}{dt} = \frac{B_1}{J} + \frac{K_\phi I_a}{J} - \frac{T_L}{J} \qquad \text{.....(10)}$$

From equation (6) and from equation (7) written in matrix from as-

$$\begin{bmatrix} I_a \\ \omega \end{bmatrix} = \begin{bmatrix} -R_a/L_a & -K_\Phi/L_a \\ K_\Phi/J & -B_1/J \end{bmatrix} \begin{bmatrix} I_a \\ \omega \end{bmatrix} + \begin{bmatrix} 1/L_a & 0 \\ 0 & -1/J \end{bmatrix} \begin{bmatrix} V \\ T_L \end{bmatrix}$$

$$\frac{dX}{dt} = AX + BU \qquad \text{.....(11)}$$

$$Y = CX + DU \qquad \text{.... (12)}$$

Where-

X= [I_a, ω], U= [V T_L],

X is the state vector

U is the input vector

Y is the input vector

A, B, C, D is coefficient of appropriate dimension.

Taking Laplace Transform of equation (1)

$$V = E_b + I_a R_a + L_a I_a \qquad \text{....(13)}$$

Taking Laplace Transform of equation (2)

$$\frac{d\omega}{dt} + B_1 = T_e - T_L \qquad \text{..... (14)}$$

$$\omega_m = K_\phi I_a - \frac{T_L}{J} + B_1 \qquad \text{.....(15)}$$

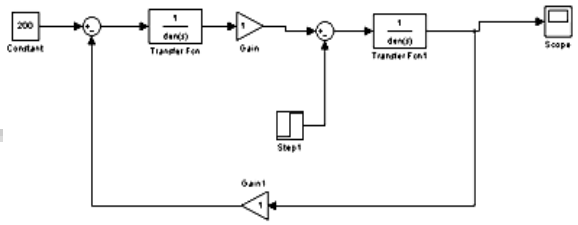

Fig.2. Transfer function model of dc motor

III. SIMULINK MODEL OF SEPARATE EXCITED DC MOTOR

Single phase AC/DC semi and full converters are presented and the performance of the DC motor drive is analyzed. A 5-HP DC motor of 240-V rating 1220 rpm is used in the simulation model. Fig. 3 shows the Simulink realization of the semi converter drive. The armature circuit is supplied from a single phase full wave converter in which a power diode is used as an electronic switch.

The field circuit is separately excited from an ideal DC voltage source. A DC motor block of SimPowerSystems toolbox is used. Where, Fig. 4 shows the Simulink realization of the full converter drive. The armature circuit is supplied from a single phase full converter in which a diode is used as an electronic switch. The field circuit is separately excited from an ideal DC voltage source. A DC motor block of SimPowerSystems toolbox is used.

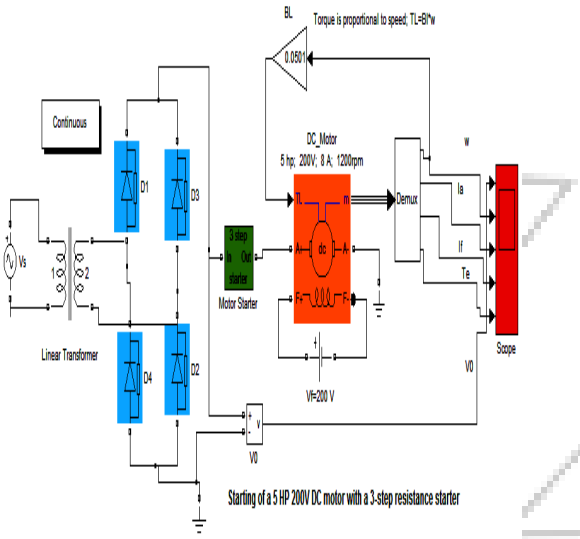

Fig.3 Simulink model

Where

V_t – Supply voltage (V)

E_b – Back emf (V)

R_a – Armature resistance (ohm)

L_a – Armature inductance (H)

R_f – Field resistance (ohm)

L_f – Field inductance (H)

I_f – Field current (A)

I_a – Armature current (A)

W_m – Speed (rad/s)

J – Rotor inertia of motion (kgm2)

D_m – Viscous friction of motor (Nms)

IV. SIMULATION RESULTS

Simulation has been performed with the help of the software named Simulink. The Simulink model of the system used for the simulation is given in Fig**.** This communication between Simulink and dedicated program is carried out via the blocks (To Workspace and From Workspace) given in Fig. once in every sampling period. In this study, 200 V, 5 hp, 1200 rpm a separately excited DC motor having the following parameters is used: Ra=l ohm, La=46mH**,** J=0.02 kgm2, B_v=0.0501 Nt-m/rd/sec.. The other parameters used in the simulation are as follows: Amplitude of AC input is 300V and linear transformer are used. The power of transformer is 10KVA and primary voltage of transformer is 300V and the secondary is 220V. A full wave AC –DC converter are used for DC voltage. In this converter power diode are used. Fig.4 & 5. shows the variation of the armature current and rotor speed in time obtained from the simulation of the system. The ripple on the current waveform, torque and speed is shows that the harmonics are presence because filter circuit are not used.

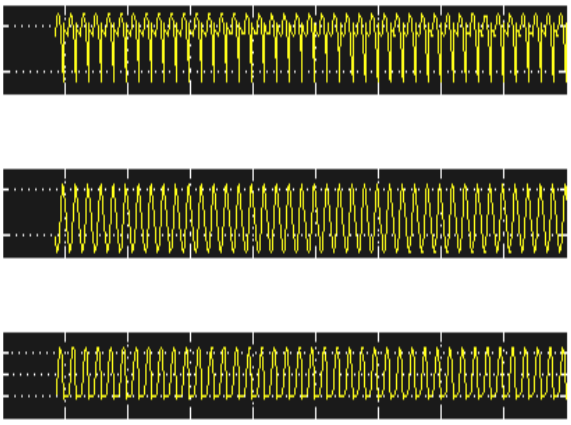

Fig.4 Output waveform of Speed and armature current

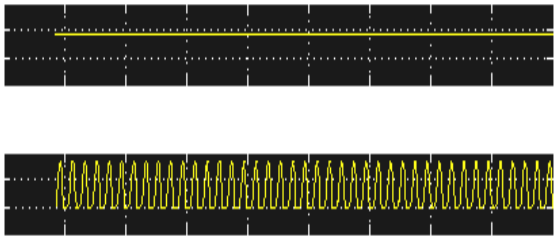

Fig.5 Output waveform of Torque and field current

In order to investigate the effect of armature voltage on the torque-speed characteristic, Four different armature voltages with average values *Vt* = 220 V,applied while the voltage applied to the field circuit is kept constant at its nominal value 200 V. A constant 240 V,50 HZ AC is applied to the input of single phase semi converter. The torque-speed, armature current and field current is shown in fig. It is clear that torque-speed and current wave form are pulsating.

V. PRACTICAL MODEL OF SEPERETELY EXCITED DC MODEL

The purpose of the full-wave rectifier is basically the same as that of the halfwave rectifier but full-wave rectifiers have some fundamental advantages. There are two types of full-wave rectifiers that are the bridge rectifier and the center-tapped rectifier as shown in Fig6 and Fig.7. The lower peak diode voltage in the bridge rectifier which consists of four diodes arranged makes it more suitable for high voltage applications. Thus, the center-tapped transformer rectifier in addition to including electrical isolation has only one diode voltage drop between the source and load making it desirable for low-voltage and high current applications. DOL starting is sometimes used to start small water pumps, compressors, fans and conveyor belts. In the case of an asynchronous motor, such as the 3-phase squirrel-cage motor, the motor will draw a high starting current until it has run up to full speed. This starting current is typically 6-7 times greater than the full load current. To reduce the inrush current, larger motors will have reduced-voltage starters or variable speed drives in order to minimise voltage dips to the power supply.

Fig.6 Rectifier circuit diagram

Fig.7 Complete setup of DC motor

VI. CONCLUSION

In this paper present comparison between separately excited DC motor output current, speed waveform using MATLAB/Simulink to practically dc drive. This paper describes a MATLAB/Simulink ac-dc converter fed dc motor speed and current comparison to practically work separately excited dc motor. The harmonics are presence in both model. In this paper show the efficiency of motor is reduced.

REFERENCES

[1] GOPAL K. DUBEY, "FUNDAMENTALS OF ELECTRIC DRIVES", .NAROSA PUBLISHING HOUSE NEW DELHI,1989.

[2] Muhammad H. Rashid, ''Power Electronics Circuits, Devices, and Applications," Prentice Hall, 3rdedition, 2003.

[3] Kumara MKSC, Dayananda PRD, Gunatillaka MDPR, Jayawickrama SS, "PC based speed controlling of a dc motor", A fmal year report University of Moratuwa Illiniaus USA, 2001102.

[4] J. Chiasson, Nonlinear Differential-Geometric Techniquesfor Control of a Series DC Motor, IEEE Transactionson Control Systems Technology.vol 2, p. 35-42,1994.

[5] A Khoei Kh.Hadidi, "MicroProcessor Based Closed- Loop Speed Control System for DC Motor Using Power MOSFET", 3rd IEEE international conference on Electronics, Circuits and Systems(1996) vol.2, pp.1247-1250.

[6] M.H. Rashid, "Power Electronics circuits, drives and application", 3rd Ed., 2007, Pearson Prentice Hall.

[7] S. K. Pillai, “A first course on electrical drives”, II[nd] Ed. 2004, New Age International Publication.

[8] Bimal K. Bose, “High Performance control and estimation in A.C. drives”, IEEE IECON Conf. Rec., pp. 377-385, 1997

[9] Micromaster440 user manual by Siemens.Simrog dc mater user manual by Siemens.

[11] J. M. D. Murphy, F. G. Turnbull, “Power Electronic control of A.C. motors”, Pergamon Press Using Simulink. . Natick, MA: MathWorks Inc., 2001.

[12] S. Li and R. Challoo, “Restructuring an electric machinery coursewith an integrativ approach and computer-assisted teaching methodology,” IEEE Transactions on Education., vol. 49, pp. 16- 28, Feb. 2006.

[13] W. M. Daniels and A. R. Shaffer, “Re-inventing the electrical machines curriculum,” IEEE Transactions on Education, vol. 41, pp. 92-100, May 1998.

Comparison Of Simulation Technique And Results For Three Phase DC-AC Converters Using Matlab & Psim

[1]Jitendra Pachoriya, [2]Neha Singh,
Electrical & Electronics Engineering Department
IES,IPS Academy
[1]ashishverma2012@yahoo.in
[2]anupma.singh04@gmail.com

Abstract:-

This paper presents the performance & comparison of modeling & Simulation of a 120˚ & 180˚ conduction DC-AC converters (Inverter) using SIMULINK/PSIM software. The power electronic DC-AC conversion system consisting of switches (SCR, IGBT, and MOSFET) and dc supply. A simple PWM switching method is used to model the DC-AC converters (Inverters). The model of the power electronic converters has been constructed in SIMULINK/PSIM. The performance of the system has been studied. It has been demonstrated that SIMULINK can effectively used for power electronic system studies.

Keyword- Inverter, PWM, MATLAB, PSIM, 120˚ & 180˚ conduction

1. Introduction:-

Various types of power electronic converters are increasingly used in almost all power levels, from HVDC links for bulk power transmission to motor drives in domestic appliances. The analysis and design of a power electronic converter and the associated control system could be time-consuming and expensive without a good modeling and simulation study; therefore, simulation plays an important role in the design and analysis of power electronic converters and their controllers**.** Three phase six-switch inverters are used in many industries. For this reason, many researchers have been presented recently investigating different types of fault that commonly occur in these inverters. Of these, the improvement of the output waveform and reduce harmonic distortion is very important . Therefore, using electronic devices, various types of inverters are presented with different structures, which can reduction harmonic and can lead to improve the output voltage too.

Although, this inverters increase he quality of output voltage and current, but lead to other disadvantages, including increased size, weight and price. Therefore, three phase six switch inverters are important, still, but these inverters have been used in particular conductive angles such as 120° & 180° in published papers.

MATLAB is a high-performance language for technical computing. It integrates computation, visualization, and programming in an easy-to-use environment where problems and solutions are expressed in familiar mathematical notation. Typical uses include Math and computation Algorithm development Data acquisition Modeling, simulation, and prototyping Data analysis, exploration, and visualization Scientific and engineering graphics Application development, including graphical user interface building.

In the cases of PSIM, the power conversion circuits can be schematically expressed by using actual power semiconductor device models and passive elements. Also, the control algorithm can be implemented by analog components. PSIM are suitable for design at the circuit level, i.e.,

power system configuration, snubber circuit, resonant network, and auxiliary circuit for the main power circuit. However, these models are described as a nonlinear controlled source by means of functions that contain exponential terms, resulting in slow execution times, large amounts of generated data, and convergence problems.

INVERTERS

A device that converts dc power to ac power at desired output voltage and frequency is called an inverter. Inverters can broadly classified into two types : VSI and CSI .A VSI, is one in which the dc source has small or negligible impedance. In other words a voltage source inverter has stiff dc voltage source at its input terminals. A CSI is fed with an adjustable current from a dc source of high impedance, i.e from a stiff dc current source. In a CSI fed with stiff current source, output current waves are not affected by the load. In VSIs using thyristors, some type of forced commutation is usually required. In case VSIs are made up of using GTOs, power transistors, power MOSFETs or IGBTs, self commutation with base or gate drive signals is employed for their turn-on and turn-off.

180 ˚ conduction:-

In this circuit each IGBT conduct for 180˚. Three IGBT remain on at any instant of time. When IGBT1 is switch on, terminal a is connected to the positive terminal of the dc input voltage. When IGBT4 is switched on, terminal a is brought to the negative terminal of the DC source . There are six modes of operation in a cycle and the duration of each mode is 60˚. The IGBT are numbered in the sequence of getting the IGBT (123,234,345,456,561,612). The gating signal shown in fig. are shifted from each other by 60˚ to obtain 3 phase balanced (fundamental) voltages.

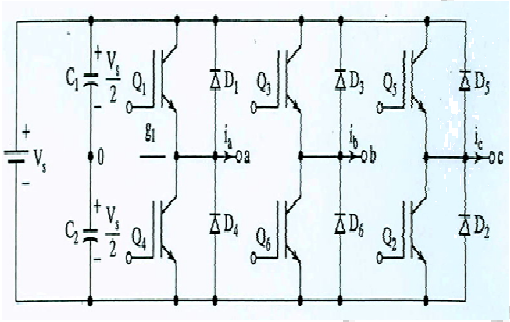

TABLE 6.2 Switch States for Three-Phase Voltage-Source Inverter (VSI)

State	State No.	Switch States	v_{ab}	v_{bc}	v_{ca}
S_1, S_2, and S_6 are on and S_4, S_5, and S_3 are off	1	100	V_S	0	$-V_S$
S_2, S_3, and S_1 are on and S_5, S_6, and S_4 are off	2	110	0	V_S	$-V_S$
S_3, S_4, and S_2 are on and S_6, S_1, and S_5 are off	3	010	$-V_S$	V_S	0
S_4, S_5, and S_3 are on and S_1, S_2, and S_6 are off	4	011	$-V_S$	0	V_S
S_5, S_6, and S_4 are on and S_2, S_3, and S_1 are off	5	001	0	$-V_S$	V_S
S_6, S_1, and S_5 are on and S_3, S_4, and S_2 are off	6	101	V_S	$-V_S$	0
S_1, S_3, and S_5 are on and S_4, S_6, and S_2 are off	7	111	0	0	0
S_4, S_6, and S_2 are on and S_1, S_3, and S_5 are off	8	000	0	0	0

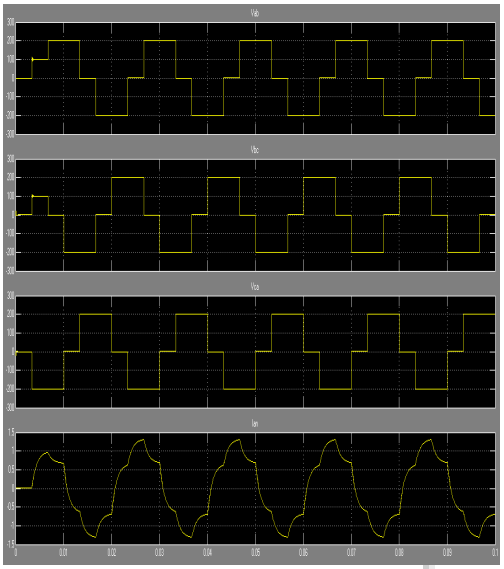

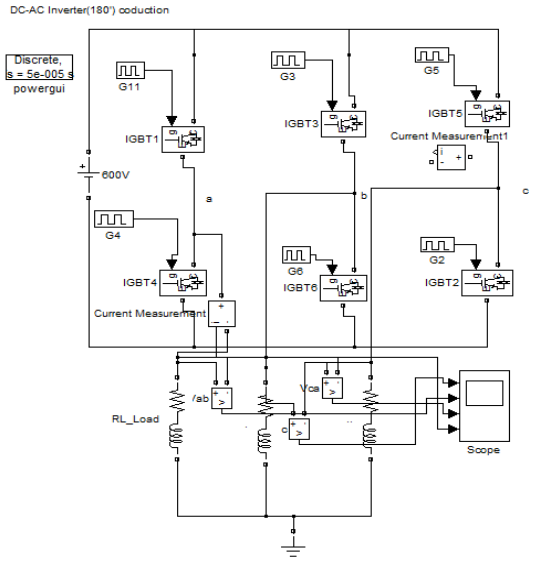

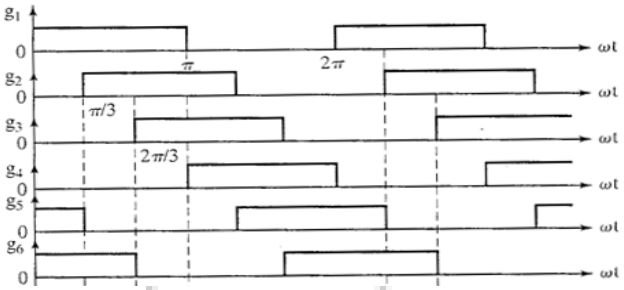

The load may be connected in wye or delta as shown in fig. for a delta connected load , the phase current can be obtained directly from the line to line voltages. Once the phase current is known, the line current can be determined. For a wye connected load, the line to neutral voltage must be determined to find the line (or phase) current. There are three modes of operation in a half cycle and the equivalent circuit is shown in fig. For a wye connected load.

120˚ conduction:-

In this circuit each IGBT conduct for 120˚. Only two IGBT remain on at any instant of time. The gating signal are shown in fig. the conduction sequence of IGBT is 61,12,23,34,45,56,61. There are three modes of operation in one half cycle and the equivalent circuit for a wye connected load are shown in fig.

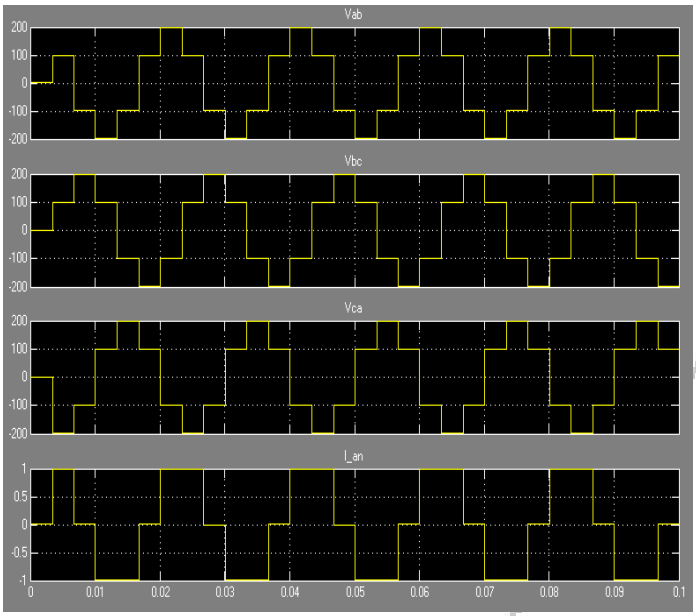

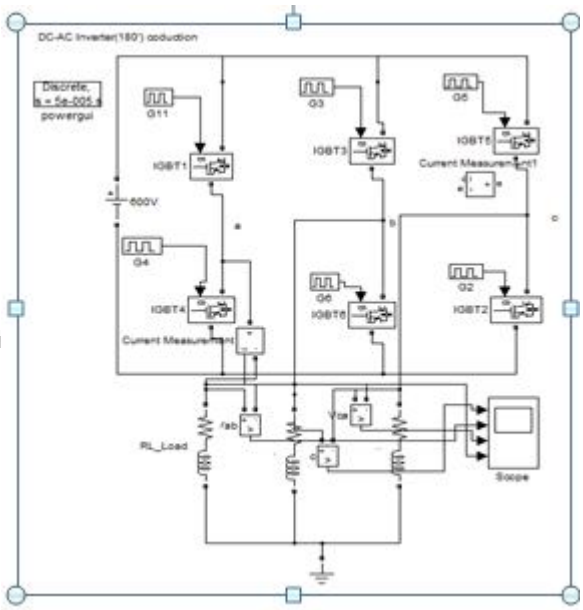

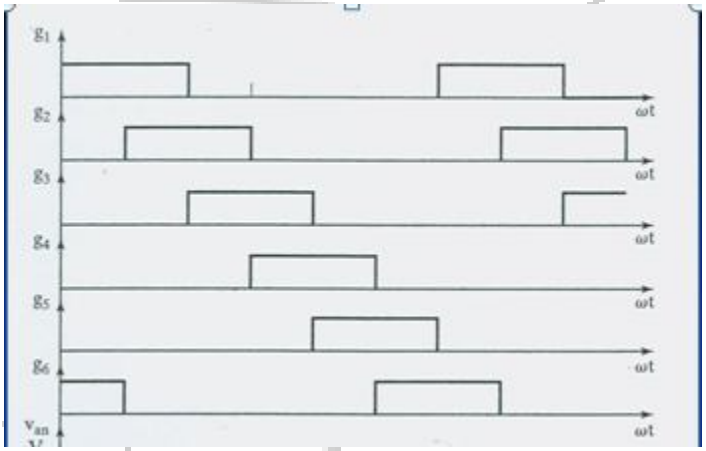

Merits and Demerits of 120 ° mode inverter over 180 ° mode inverter

1. In the 180° mode inverter, when the gate signal is turned off to turn off S1 at 180°, gating signal to S4 is simultaneously applied to turn on S4 in the same leg. In practice interval must exist between the removal of gating signal to S1 and application of gating signal to S4, because otherwise source would experience a direct short circuit through S1 and S4 in the same leg. This difficulty is overcome considerably in 120° mode inverter. In this inverter there is a 60° interval between the turning off of S1 and turning on of S4. During this 60° interval, S1 is commutated safely. In general, this angular interval of 60° exists between the turning off of one device and turning on of the complementary device in the same leg.2. In the 120° mode inverter, the potentials of only two output terminals connected to the dc source are defined at any time of the cycle. The potential of the third terminal, pertaining to a particular leg in which neither device is conducting, is not well defined; its potential therefore depends on the nature of the load circuit.

Thus, the analysis of the performance of this inverter is complicated for a general load circuit. For a balanced resistive load, the potential of all the three terminals is, however, well defined. For the simulation of the permanent magnet synchronous motor in this project we use a six step inverter in 120° mode because of its advantages over 180° mode.

Comparison between MATLAB & PSIM Software

- In PSIM, the simulation time of execution of program is less as compared to MATLAB software.
- For same input values and same element value, in PSIM, gets output in multiple pulses form but in MATLAB output is in rectangular form.
- In MATLAB, circuit consist in block and in block switches option are given, but in PSIM some circuit block are available and block switches option are not given.
- In MATLAB, zoom in and zoom out option are presence, but in PSIM this option are not presence.
- In MATLAB, we need Scope to have output result, but in PSIM we don't need any Scope for output.
- In MATLAB, we get elements from its Simulink Library Brochure so it takes time in the circuit draw. But in PSIM all elements are available from its Dialog Box so doing work in this software is easy & proper.
- In MATLAB, concern parameters are with full detailed information in understanding of circuits as compare to PSIM because it can't contain detailed information.
- In PSIM, for showing the flow of current in the circuit, given current flag in the element parameters. But in MATLAB, for showing flow of current we have to place a separate ammeter.
- In PSIM, the figure of circuit diagram is seen simpler & easy as compared to MATLAB.
- In MATLAB, the simulink library is too big so by the help of that any program should be executed so easily as compared to PSIM library because its library can't contain that much elements.

Conclusion

In this paper present comparison of simulation technique and results for basic power electronics converters. In both software, Models of the power electronic system are developed and the control system is described. The modelling system is constructed in SIMULINK and PSIM. The performance of the system has been studied by simulation.

It has been demonstrated that SIMULINK can effectively be used for power electronic system analysis and the associated control system design.

REFERENCES

[1] Albert Alexander.S and Manigandan.T (2009) Digital Switching Scheme for Cascaded Multilevel Inverters. *Proceedings of Third International Conference on Power Systems*, Indian Institute of Technology, Kharagpur.

[2] Albert Alexander.S and Sivavasath.A (2007) Design, Simulation and Implementation of UPS inverters using Artificial Neural Network Controller. *Proceedings of International Conference on Trends in Industrial Measurements and Automation*, National Institute of Technology, Trichy.

[3] Dakshina M. Bellur and Marian K. Kazimierczuk (2008) PSpice and MATLAB Applications in Teaching Power Electronics to Graduate Students at Wright State University. *Proceedingsof the 2008 ASEE North Central Section Conference, American Society for Engineering Education.*

[4] Elena Niculescu, E. P. Iancu, M. C. Niculescu and Dorina-Mioara Purcaru (2006) Analysis of PWM Converters Using MATLAB. *Proceedings of the 6th WSEAS International Conference on Simulation, Modeling and Optimization,* Lisbon, Portugal, September, 507-512.

[5] De Doncker, R.W.A.A.; Divan, D.M.; Kheraluwala, M.B.; "A three-phase soft-switched high-power density DCDC converter for high-power applications" IEEE Transactions on Industry Applications, Volume: 27, Issue: 1, Jan.-Feb. 1991 Pages 53 ~ 73.

[6] Kunrong Wang, Fred C. Lee, Jason Lai, Operation principle of bi-directional full- bridge DC-DC converter with unified soft-switching scheme and soft-switching capability, APEC 2000, pp.l I I-I *18*

[7] M. H. Rashid, *SPICE for Circuits and Electronics Using PSpice*. Englewood Cliffs, NJ: Prentice-Hall, 1990.

[8] Power Electronics: Computer Simulation, Analysis and Education Using PSpice Schematics by Prof. NED MOHAN.

[9] Power Electronics: converters, applications and design by MOHAN.UNDELAND.ROBBINS

[10] S.Raghuwanshi, A.Singh Indian Journal of Technical Education & ISTE Education "Performance & Comparison of Singe Phase Controlled Converters using MATLAB & PSIM".April 2012, p.g. 107-111

[11] S.Raghuwanshi, A.Singh, Y.Mokhriwale "A Comparison and Performance of Simulation tools MATLAB/SIMULINK,PSIM & PSPICE for power electronic circuit", "International Journal of Advanced Research in Computer Science and Software Engineering", Vol. 2, issue 3, March 2012, p.g. 187-191.

[12] D. Maksimovic, A. M. Stankovic, V. J. Thottuvelil, and G. C.Verghese, "Modeling and simulation of power electronic converters," *Proc. IEEE*, vol. 89, no. 6, pp. 898– 912, Jun. 2001.

[13] B. K. Bose," Power electronics - an emerging technology," IEEE Trans. On Ind.Electron., vol. 36, no. 3, pp. 403-412, 989.

DESIGN AND ANALYSIS OF IGBT BASED CHOPPER FED DC DRIVE USING MATLAB

[1]Dulendra Tembhre, [2]Chhotelal Sahu, [3]Ritesh Solanki

Electrical & Electronics Engineering Department
IES,IPS Academy
[1] pin2.2309@gmail.com
[2] chhote.sahu93@gmail.com
[3]riteshsolanki @gmail.com

Abstract— This paper presence speed of separately excited DC motor can be controlled from below and up to rated speed using chopper as a converter. The chopper firing circuit receives signal from controller and then chopper gives variable voltage to the armature of the motor for achieving desired speed. There are closed control loops are used for speed control. The controller used is Proportional-Integral type which removes the delay and provides fast control. Modelling of separately excited DC motor is done. After obtaining the complete model of DC drive system, the model is simulated using MATLAB(SIMULINK).The simulation of DC motor drive is done and analysed under varying speed and varying load torque conditions like rated speed and load torque, half the rated load torque and speed, step speed and load torque and stair case load torque and speed.

Keywords **— Chopper Circuit, DC motor, Speed control, IGBT.**

I.INTRODUCTION

Although the dc machine is more expensive, the control principles and the converter equipment required are somewhat simpler compared to ac machines. The simplicity and flexibility of control of dc motors have made them suitable for adjustable speed drive applications. Also fast torque response has favored their use in high performance servo drives. Class-C type chopper is widely used especially in the speed control of dc motors in industry as a drive circuit. The dc motor fed by a chopper is usually modelled by the average value of the armature terminal voltage [11]. However this modelling does not include the ripples due to chopping of the armature voltage.

II .PRINCIPAL OF DC MOTOR

The dc motor is basically a torque transducer that converts electrical energy into mechanical energy. The torque developed on the motor shaft is directly proportional to field flux and the armature current. A current carrying conductor is established in a magnetic field with flux Φ and the conductor is located at a distance r from the centre of rotation the relationship among the developed torque flux Φ and current I_a is-

$$I_a = K \phi / Te$$

Where T_e is electromagnetic torque,Φ is magnetic flux, I_a is armature current and K_m is proportional constant. The back emf and the shaft velocity is-

$$E_b = k \phi \quad \text{..... (1)}$$

Where

E_b = back emf

ω_m=Shaft velocity

$$T_e = k_\phi I_a \quad \text{..... (2)}$$

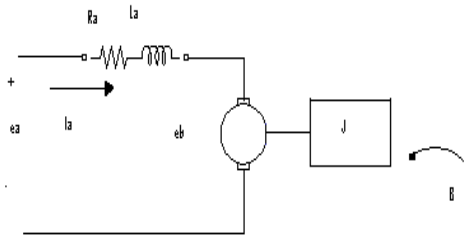

Fig. 1-"dc motor"

The armature winding has a resistance R_a, a shaft inductance L_a, and an induced emf. The terminal relationship is-

$$E_b = I_a R_a + L_a \quad \text{..... (3)}$$

In steady state the armature current is constant and hence the rate of change of the armature current is zero hence

$$V = E_b - I_a R_a$$

Torque and speed is

$$T_e = \frac{E_b I_a}{\omega} = K_\phi I_a \quad \text{..... (4)}$$

$$E_b = k_\phi \omega$$

$$T_e = k_\phi I_a$$

Where-

I_a is the armature current

R_a is the armature resistance

L_a is the armature inductance

E_b is the is back emf

T_e is the electromagnetic torque

ω_m is the angular velocity

P_a is the air gap power

$K_e \Phi$ is the flux constant

The load is modelled as a moment of inertia J Kg m^2/sec^2 with a viscous friction coefficient, B_1 in Nm/(rad/sec). Then the acceleration torque T_a Nm drives the load is given by-

$$J \frac{d\omega}{dt} + B_1 = T_e - T_L = T_a \quad \text{..... (5)}$$

Where –

T_L is the load torque

T_a is the acceleration torque

B_1 = is the viscous friction

J = is the moment of inertia

From equation (1)

$$\frac{dI_a}{dt} = \frac{V}{L_a} - \frac{K_\phi \omega}{L_a} - \frac{I_a R_a}{L_a} \quad \text{.....(6)}$$

From equation (2)

$$\frac{d\omega}{dt} = \frac{B_1}{J} + \frac{K_\phi I_a}{J} - \frac{T_L}{J} \quad \text{.....(7)}$$

From equation (6) and from equation (7) written in matrix from as-

$$\begin{bmatrix} I_a \\ \omega \end{bmatrix} = \begin{bmatrix} -R_a/L_a & -K_\Phi/L_a \\ K_\Phi/J & -B_1/J \end{bmatrix} \begin{bmatrix} I_a \\ \omega \end{bmatrix} + \begin{bmatrix} 1/L_a \\ 0 \end{bmatrix} V + \begin{bmatrix} 0 \\ -1/J \end{bmatrix} T_l$$

$$\frac{dX}{dt} = AX + BU \quad (8)$$

$$Y = CX + DU \quad (9)$$

Where-

X= [I_a Φ], U= [V T_L],

X is the state vector

U is the input vector

Y is the input vector

A, B, C, D is coefficient of appropriate dimension.

Taking Laplace Transform of equation (1)

$$V = E_b + I_a R_a + L_a I_a \quad \text{..... (10)}$$

Taking Laplace Transform of equation (2)

$$\frac{d\omega}{dt} + B_1 = T_e - T_L \quad \text{.....(11)}$$

$$\omega_m = K_\phi I_a - \frac{T_L}{J} + B_1 \quad \text{.....(12)}$$

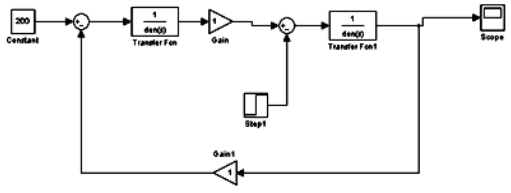

Fig.e2 –"Transfer function model of dc motor"

III. STATE SPACE MODEL OF DC MOTOR

Consider the state- space model of dc motor then it behaves as an open-loop function. There is no feedback path of the model. The main draw back of open loop function, if output is not that desired value then there is no feedback for given in reference signal but in close loop system path is available which gives that output as a feedback in reference signal compare this feedback value with the actual value and given into the controller.

Basic State space equation is –

$$\frac{dX}{dt} = AX + BU$$

$$Y = CX + DU$$

$$A = \begin{bmatrix} -R_a/L_a & -K_\Phi/L_a \\ K_\Phi/J & -B_1/J \end{bmatrix}$$

$$B = \begin{bmatrix} 1/L_a \\ 0 \end{bmatrix}$$

C = [0 1]

D = [0 0]

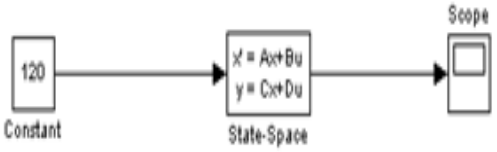

Fig 3 – "State - space Model of dc motor"

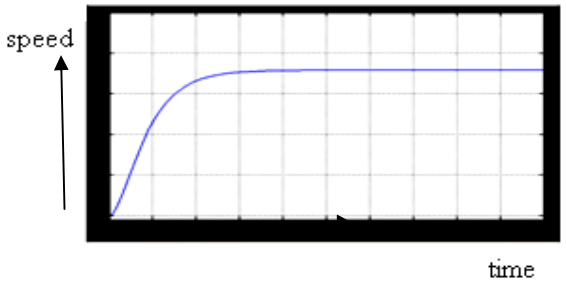

Fig 4- "Waveform of State space Model of dc motor"

Rise time = 0.0788

Settling time = 0.1386

Settling Min = 0.1386

Settling Max = 0.8953

Overshoot = 0

Undershoot = 0

Peak = 0.8953

Peak time = 0.3635

T_m = 3.47e+001

IV. MODELING OF THE CHOPPER

In this study, chopper whose load voltage is positive whereas load current is both positive and negative is considered. The chopper circuit and its output PWM voltage waveform is given in Figure 3. In the circuit, the time ton in which load is connected to input voltage can be changed via control signals i_{Cl} and $i_{C2.}$ In the closed-loop system, i_{C1} and iC_2 are related to the current controller output signal (E,) and the peak value of saw- tooth signal **(E_{sw})** as being seen in Figure, and the following equations can be

$$t_{on} = \frac{T}{E_{sw}}.E \qquad \text{for } o \le E \le E_{sw} \qquad (13)$$

$$t_{on} = T \qquad \text{for } E \ge E_{sw} \qquad \text{……..(14)}$$

Therefore, the problem in the simulation of the system is to generate the real time modeling period is known. If it is assumed that the PWM signal is high at the beginning of a period, PWM waveform over one period whose amplitude is K_{pwm} Volts .

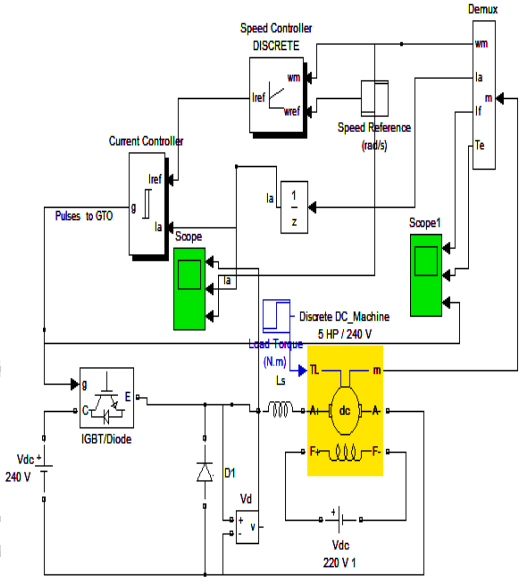

Fig 5-"Block diagram representation of the Simulink model"

The speed control circuit of a SEDM using Simulink is shown in Fig.

Where

V_t – Supply voltage (V)

E_b – Back emf (V)

R_a – Armature resistance (ohm)

L_a – Armature inductance (H)

R_f – Field resistance (ohm)

L_f – Field inductance (H)

I_f – Field current (A)

I_a – Armature current (A)

W_m – Speed (rad/s)

J – Rotor inertia of motion (kgm2)

D_m – Viscous friction of motion (Nms)

V. SIMULATION RESULTS

Simulation has been performed with the help of the software named Simulink [5]. The Simulink model of the system used for the simulation is given in Figure. The discrete transfer functions of the speed and current controllers in the Simulink model are given in Equations The blocks "Step Fun" and "Step Fun" represent the reference speed and the load torque respectively. The subsystem named "DC Motor" consists of the transfer functions given in Figure. The PWM waveform at the output of the chopper has been generated by comparing the output of current controller to the sawtooth waveform. This comparison is performed by receiving the value of E, from the simulation program. The computation of the duty cycle depending on this value and peak value of sawtooth wave is made in a dedicated program written in Matlab. Receiving the duty cycle as a result of this computation, the PWM waveform has been generated as mentioned and the data is transferred to the Simulink in order to continue to the simulation of the system. This communication between Simulink and dedicated program is carried out via the blocks (To Workspace and From Workspace) given in Fig. **4,** once in every sampling period.

In this study, 220 V, 5 hp, 1400 rpm a separately excited DC motor having the following parameters is used: Ra=0.5 ohm, La=1.25H**,** J=0.050 kgm2, B_v=0.02 Nt-m/rd/sec, K=0. 55 V/rad/sec. The other parameters used in the simulation are as follows: Amplitude of PWM armature voltage (K_{Pm}) =240 **V**. Figure shows the variation of the armature current and rotor speed in time obtained from the simulation of the system for the chopping frequency of 1 KHz. Figure shows the change of the armature current and the rotor speed obtained from the average value model. The ripple on the current waveform in Fig. 5 is a result of the discrete modelling of PWM; however, the smooth variation of the same waveform in Figure 6 reflects the continuous change of armature voltage in average value modelling. Fig. 6. shows the waveform at the armature terminal generated from Equation in simulation.

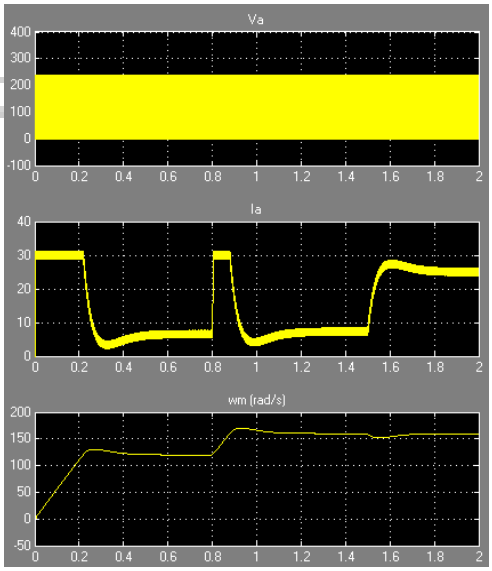

Fig.6. Armature current and speed(rad/sec)

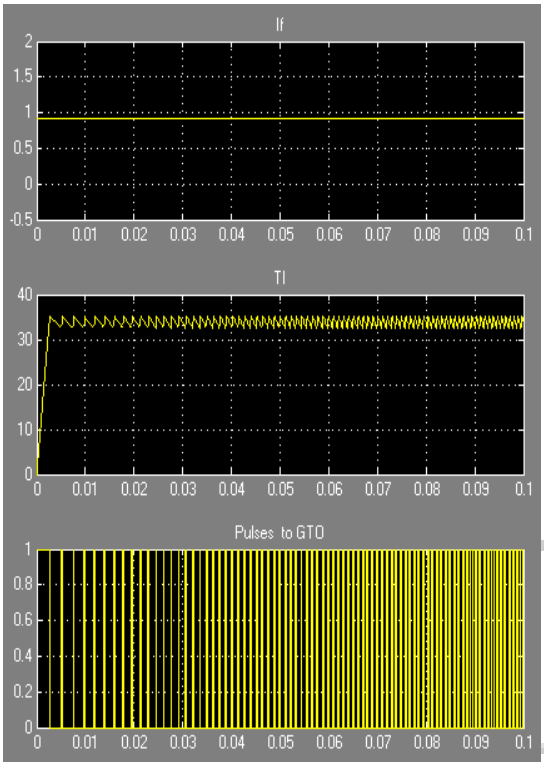

Fig.7 -"Result from the field current, torque and gate pulse

VI. CONCLUSION

After results analysis, we can say the speed control of separately excited DC motor can be controlled from below and up to rated speed using chopper as a converter. The chopper firing circuit receives signal from controller and then chopper gives variable voltage to the armature of the motor for achieving desired speed. There are closed control loops are used for speed control. The controller used is Proportional-Integral type which removes the delay and provides fast control. Modelling of separately excited DC motor is done.

REFERENCES

[1]. S. Raghuwanshi "Modelling & Simulation of a DC-DC Converters using MATLAB & PSIM" National Conference on ECOMM-11 in SDBCT, Indore.

[2]. S. Raghuwanshi "Performance & Comparision Of Igbt And Mosfet Switches Based Dc-Dc Converters Using Matlab" National Conference on NCRTEEE-11 in MITM, Indore.

[3]. S.Raghuwanshi, A.Singh Indian Journal of Technical Education & ISTE Education "Performance & Comparison of Singe Phase Controlled Converters using MATLAB & PSIM".April 2012, p.g. 107-111

[4]. Wester, G. W. & Middle brook, R. D. "Low- Frequency Characterization of Switched dc-dc Converters", IEEE Transactions on Aerospace and Electronic Systems, vol. AES-9, n.3, pp.376-385, 1973.

[5]. Krause, P.C. "Analysis of Electrical Machinery", Mc Graw-Hill, 1986.

[6]. Phillips, C.L. & Nagle, H.T. "Digital Control System Analysis and Design", Prentice-Hall, 1984.

[7]. M.GAUTIER,P.M.ROBFZPT.C.BERGMANN," Modelling and Simulation of DC-Motor Chopper Drive for Robots".

[8]. Franc Mihali¡c. and Dejan Kos "Randomized PWM for conductive EMI reduction in dc-dc choppers,"HAIT Journal of Science and Engineering B, Volume 2, Issues 5-6, pp.

[9]. Dubey, G.K., Fundamentals of Electrical Drives. New Delhi, Narosa Publishing House, 2009.

[10]. Gopal,M., Control Systems, Principles and Design. New Delhi, Tata McGraw Hill Publishing Company Ltd, 2008.

[11]. Mohan, Ned, Electrical Drives-An Integrated Approach. Minneapolis, MNPERE, 2003.

[12]. Bose B.K., Power electronics and motor drives recent technology advances, Proceedings of the IEEE International Symposium on Industrial Electronics, IEEE, 2002, pp 22-25.

[13]. MATLAB and SIMULINK Version 2009, the Maths works Inc, USA.

[14]. Zuo Z. Liu, Fang L. Luo, and Muhammad H. Rashid, "High performance nonlinear MIMO field weakening controller of a separately excited dc motor," Electric Power Systems Research, vol. 55, issue 3, Sep. 2000, pp. 157-164.

[15]. Nabil A. Ahmed, "Modelling and simulation of ac dc buck-boost converter fed dc motor with uniform PWM technique," Electric Power Systems Research, vol.73, issue 3, Mar. 2005, pp. 363-372.

[16]. N. Barakat and R. Rajagopalan, "Speed control of a DC motor using a feed forward computed torque control scheme," in Proc. 1996 Int. Sym. On Intelligent control, 15-18 Sept. 1996, pp. 432-437.

Duality Analysis and Improving the Capacity of Multi-Input Multi-Output Channel using Dirty Paper Coding Technique

[1]Himanshu Bhawsar, [2]Monika Mishra,

Electrical & Electronics Engineering Department
IES,IPS Academy
[1] h.631@rediffmail.com
[2] monika_mishra11@rediffmail.com

Abstract

In wireless communication, Multi- Input Multi-Output (MIMO) technology offers significant increase in data throughput and link range without additional bandwidth. The dirty paper coding (DPC) achieves the sum rate capacity of Gaussian MIMO broadcast channel. The dirty paper coding is a technique for efficient transmission of digital data through a channel that is subject to some interference that is known to the transmitter. This technique consists of precoding the data so as to cancel the effect of interference .The duality relationship between BC and MAC channel has been studied and The Sato upper bound and Marton's inner bound on the capacity of Broadcast channel has been considered and applied this capacity to the MAC channel by showing the duality. The use of dirty paper coding closely achieves the sum-rate capacity region of broadcast channel. MIMO is abbreviation of Multiple Input Multiple Output. In MIMO fading environment, the so called degenerating channels or keyholes may exist that exhibit low partial fading correlation at both ends of the link but still have poor rank properties, and hence low ergodic capacity. The performance of dirty-paper coding over MIMO keyhole channels has been analyzed. The capacity and the probability of error of a MIMO system with Binary phase shift keying (BPSK) over keyhole channel. This paper also proves the intuitive result that the capacity under keyhole condition can be improved using Dirty paper coding.

Keywords: MIMO, DPC, BER, BPSK

1.Introduction

Multiple-Input Multiple-Output (MIMO) system has been one of the key to achieve high data rate and high reliability over wireless downlink (broadcast channel). Broadcast is a communication scenario where a single transmitter sends independent information to multiple un-cooperative receivers. The downlink of a multiuser transmission is called broadcast channel (BC) and the reverse; many to one uplink are known as multiple access channel (MAC). There is duality between achievable region of BC and capacity region of MAC exists.

Dirty Paper Coding is used to achieve the capacity region of MIMO broadcast channel. DPC in fact achieves the full capacity region of MIMO BC. However, DPC is rather new and complicated scheme and yet to be implemented in practical system. Basically DPC states that if the transmitter has perfect, non causal knowledge of additive interference in the channel then the capacity of the channel is same as if there was no interference. In MIMO BC, this technique is used at the transmitter to choose code words for different receivers. DPC emerged out as new topic of research as it is also used in digital watermarking and it outperforms TDMA scheme in cellular system.

Tomlinson-Harashima Precoding (THP) is the technique used for the implementation of DPC.THP was originally proposed for ISI channel. By using THP, the capacity of channel does not decrease if the receiver observes the transmitted signal in the presence of interference, provided that the transmitter knows

this interference non-causally. But due to modulo loss THP technique does not perform well in low SNR region.

1.1 Use of Dirty Paper Coding

We next consider the dirty paper coding strategy of Costa for broadcast channels [1]. Dirty paper coding exploits the known interference between users in a broadcast channel to pre subtract out this interference. We apply this coding strategy to broadcast channels with multiple antennas at the transmitter and receiver (the MIMO channel). This shows that dirty paper coding provides significant rate gains over the high-data-rate (HDR) strategy used in current cellular systems. Here, establishment of a duality between the achievable region of the MIMO broadcast channel using dirty paper coding and the capacity region of the dual MIMO multiple-access channel has been done. Then it show that dirty paper coding achieves sum-rate capacity of the MIMO broadcast channel. The proof exploits duality, dirty paper coding, and clever upper bounding techniques.

1.2 Duality Relationship

The capacity region of a fading or constant Gaussian BC is equal to the union of the capacity regions of the dual Gaussian MAC where the union is taken over power constraints on the individual users of the MAC that sum up to the BC power constraint. This result allows us to directly compute the capacity region of a Gaussian BC from the capacity region of its dual Gaussian MAC. It is also show that the capacity region of the Gaussian MAC equals the intersection of capacity regions of the dual Gaussian BC where the intersection is taken over appropriately scaled channel gains and the total BC power equals the sum of powers of the dual MAC users. The duality relationships between the capacity regions of the Gaussian MAC and BC are quite powerful and interesting. First they indicate a direct connection between known capacity results for dual MAC and broadcast channels. More importantly, there are several BCs and MACs where the capacity region and optimal transmission strategy for one channel is either unknown or very hard to compute, whereas the regions are known and easy to compute for the dual channel. In these cases we can use duality to obtain new capacity results. In particular, we will show that the minimum rate capacity region and optimal transmission strategy for a fading MAC can be obtained from the dual BC capacity region, yet no direct method exists to compute this region.

The capacity of a broadcast channel with multiple antennas at the transmitter and receiver (the MIMO BC) is an open problem due to the lack of a general theory on the capacity of non-degraded broadcast channels. Pioneering work in this area by Caire and Shamai [8] developed an achievable set of rates for a broadcast channel with two transmit antennas and one receive antenna at each node based on the dirty paper coding result of Costa [1]. This coding strategy allows a channel with interference known at the transmitter to achieve the same data rate as if the interference did not exist. The original coding strategy was described as writing on dirty paper, where the structure introduced by the ‘dirt’ is exploited in the code design. Computing the corresponding set of achievable rates for the MIMO BC is extremely complex, especially for a larger number of antennas at either the transmitter or the receivers. We establish a duality between the achievable region of the MIMO BC obtained using dirty paper coding and the capacity region of the dual MIMO MAC for any number of transmit and receive antennas. This result greatly simplifies calculation of the achievable region for the MIMO BC obtained with dirty paper coding, since we can use recently developed iterative water filling techniques to obtain the capacity region for the dual MIMO MAC capacity region [4] and then apply duality [3]. We also show that dirty paper coding achieves the sum-rate point of the MIMO BC channel capacity region (maximum achievable sum of all users' rates).

1.3 Multi-Input Multi-Output Key-Hole Effect

The performance of a multiple-input multiple-output (MIMO) channel is severely degraded under the so-called keyhole or pinhole effect [10]. Under this condition, the channel loses its spatial degrees of freedom, and the channel matrix becomes rank-deficient [11]. This can happen even when the MIMO component channels are uncorrelated [12]. Under the keyhole condition, the capacity scaling of the MIMO channel, with respect to signal-to-noise

ratio (SNR), is no better than a single-input single-output (SISO) channel. Thus, under the keyhole condition, MIMO coding techniques cannot yield the same impressive capacities that are available in rich scattering environments. With the decreased performance, one naturally wishes to use techniques that compensate the key- hole effect. To compensate the effect of MIMO key-hole effect we use the dirty paper coding and we see the surprising result that DPC not only compensate the keyhole effect but it also improves the capacity of 2x2 MIMO channel without any effect.

2. MIMO Broadcast Channel

In radio, multiple- input and multiple- output (MIMO) technology is the use of multiple antennas at both the transmitter and receiver to improve communication performance which is one of several forms of smart antenna technology. In multi user MIMO systems, the multiple transmitter and receiver share the same communication medium and cause mutual interference to each other. However, cooperation between multiple transmitter and receiver is possible to deal with the interference. When transmitter cooperates and receiver does not, the channel scenario is called the MIMO broadcast channel. The other channel scenario is called multiple access channel (MAC) where transmitter do not cooperate and receivers do.

2.1 Multi-Input Multi-Output Model

Consider MIMO channel model shown below:

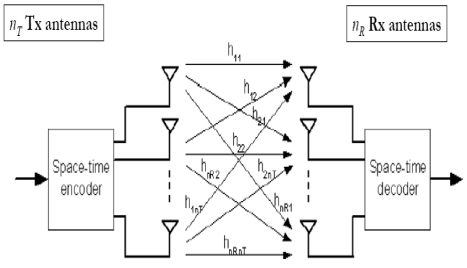

$$\begin{bmatrix} y_1 \\ \vdots \\ y_{n_R} \end{bmatrix} = \begin{bmatrix} h_{11} & \cdots & h_{1n_T} \\ \vdots & \ddots & \vdots \\ h_{n_R1} & \cdots & h_{n_Rn_T} \end{bmatrix} \begin{bmatrix} x_1 \\ \vdots \\ x_{n_T} \end{bmatrix} + \begin{bmatrix} n_1 \\ \vdots \\ n_{n_R} \end{bmatrix}, \quad \mathbf{y} = \mathbf{Hx} + \mathbf{n}, \quad \mathbf{n} \sim N(0, \sigma^2 I)$$

Fig.1. MIMO channel model

As shown in Fig.1, MIMO channel consist of n_T transmitting antennas and n_R receiving antenna and after that input is provided at space time encoder which is transmitted through channel by transmitted antennas and at receiving side receiving antennas receive and decode signal through space- time decoder. Here y is output vector, x is input vector of the model, H is channel transition matrix and n is the noise vector which is AWGN.

2.2 Duality between BC and MAC

Consider the achievable capacity region of MIMO broadcast channel which is equal to the capacity region of the dual MIMO MAC.

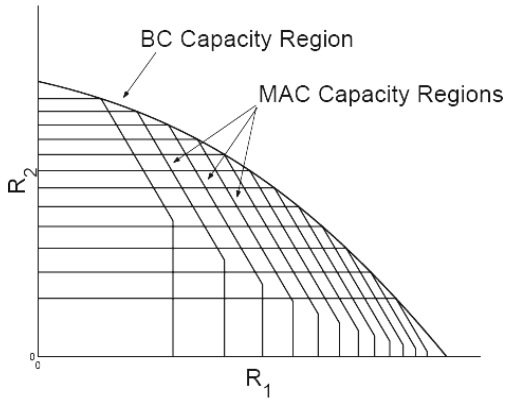

Fig.2. Gaussian BC capacity region as a union of duality MAC region.

The capacity region of a constant Gaussian BC with power P is equal to the union of the capacity region of duality MAC with power P_1 and P_2 such that $P_1+P_2= P$ as shown in Fig.2 and the boundary of each MAC capacity region touches the boundary of BC region at different points and each point along the BC capacity region boundary is intersected by a different MAC capacity region boundary.

The relation between capacity of BC region and capacity of MAC from Fig.2 is given by:

$$C_{BC}(P; h_1, h_2) = \bigcup_{0 \le p_1 \le p_2} C_{MAC}(P_1, PP_1; h_1, h_2)$$

(1)The capacity region of a Gaussian MAC is equal to the intersection of the capacity region of scale dual BC over all scaling.

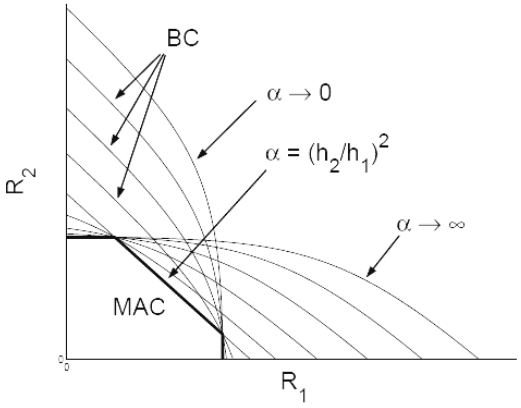

Fig.3. Gaussian MAC capacity region as intersection of dual BC region

The relation between MAC region and BC region from Fig.3 is given by

$$C_{MAC}(P_1, P_2; h_1, h_2) = \bigcap_{\alpha \rangle 0} C_{BC}\left(\frac{P_1}{\alpha} + P_2; \alpha h_1, h_2\right)$$

(2)

The optimal power allocation and decoding order for the MAC can be obtained by reversing the dual BC encoding order and applying the power constraint. Thus the optimal transmission strategy to achieve any point on the capacity region can be obtained from dual BC channel. Since MAC region a pentagon, the broadcast channels characterized by $\alpha = 0$, $\alpha = h_2/h_1$ and $\alpha = \infty$ are sufficient to form a pentagon. If $\alpha = h_2/h_1$, the channel gains of both users are the same and the capacity BC region is bounded by a straight line because the capacity region can be achieved by time sharing. All scaled BC capacity region except the $\alpha = h_2/h_1$ channel intersect MAC at exactly one of the two corner point of the MAC region and also intersect the MAC region along its time-sharing line.

3. Dirty Paper Coding

In 1983, Costa gives the idea of dirty paper coding and proves that, if the transmitter has perfect, non causal knowledge of additive interference in channel, then the capacity of channel is the same as if there was no additive interference in the channel [1]. According to Costa, a piece of paper covered with independent dirt spots and a written message on it with a limited amount of ink, the dirty paper, with the message on it, is then send to someone else and acquires more dirt along the way. If the recipient cannot distinguish between the ink and dirt, then it can send just as much information on such a dirty piece of paper and gave away to get that capacity.

The dirty paper code is a way for the writer to adapt his message to the dirt already on the paper the writer and the reader agree ahead of time on which dirty paper code they will use for the messages.

The Costa channel is shown below:

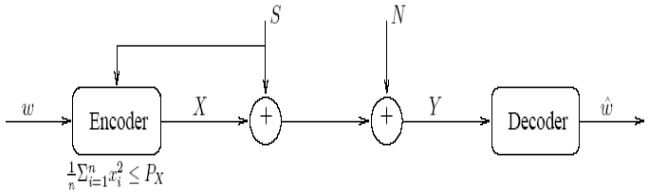

Fig.4. Dirty Paper Channel

The received signal is

$$Y = X + S + N \quad (3)$$

Where, S is arbitrarily interference non-causally known to at transmitter is independent Gaussian random variable with variance P_n and P_x is the power constraint on the transmitted signal .The output of the encoder given as X which obeys the transmitter power constraints. The Costa's results, shows that the capacity of this channel is the same as if the interference is not present:

$$C_{DPC} = \tfrac{1}{2} \log (1+P_x/P_n) \quad (4)$$

Dirty paper coding now a day's used in various applications, recent research shows that DPC combined with 2x2 MIMO can potentially achieve spectral efficiency gain of 0.8 b/s/Hz over 2x2 MIMO alone and 1.35 b/s/Hz over 4x4 MIMO. DPC outperforms the frequency reuse scheme. Its require vector quantization at transmitter and receiver. DPC use iterative type of decoder i.e. viterbi, turbo or successive trellis decoder.

In wireless network, often a transmitter has different messages, and each one needs to be sent to different person. The sum-rate capacity of a system that transmit all message at the same time and uses the dirty paper codes to reduce interference between messages can be many times the sum-rate capacity of similar system that only can sends one message at a time (TDMA). Any one receiver is only concerned with the messages for that receiver all the other messages the transmitter is simultaneously sending to everyone else are to that receiver irrelevant noise that only interferes with the desired message.

3.1 Implementation of Dirty Paper Coding

In high SNR regime, dirty paper coding can be approximated by Tomlinson-Harashima precoding (THP).THP was originally introduced in the context of ISI channel. The basic idea is illustrated in Fig.5. As shown; the system intends to send a message v from transmitter to compensate the interference in the channel to the receiver through AWGN channel which is corrupted by interferences.

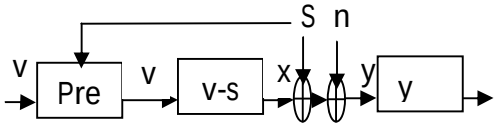

Fig.5. DPC implementation with THP

The TH precoder involves two stages. In the first stages the interference s is subtracted directly from the source v to compensate the interference in the channel but the power of v-s may exceed the transmitter power constraint. A modulo operator is lied to sustain the power constraint at transmitter. At the receiver, another modulo operation is performed to recover the intended message v.

Transmitter: The encoder sends:

$$X = (v - s - u) \bmod \Lambda \quad (5)$$

Receiver: The receiver computes:

$$= (y + u) \bmod \Lambda. \quad (6)$$

u is the common dither shared by the receiver and the transmitter and is uniformly distributed over $(\Lambda/2,-\Lambda/2)$, which makes sure that the channel input x has uniform distribution. From Fig-4.2, it is seen that

$$y = x + s + n + u = (v - s - u) \bmod \Lambda + s + n = v + n - m\Lambda \quad (7)$$

where m is an integer. Then we have,

$$= y \bmod \Lambda = (v + n) \bmod \Lambda. \quad (8)$$

The quantizer Λ is chosen to meet the power constraints without causing any ambiguity in v. In the absence of noise, the message v can be fully recovered at the receiver. From the expression of , it is clear that quantization introduces extra noise in demodulation.

The basic premise of dirty paper coding is that if interference to a given user is known in advance, the encoding strategy can exploit the structure of the interference such that the capacity is the same as if there was no interference at all. The encoding strategy cleverly distributes the codeword's based on the interference, and the decoder must know how to read these codewords. Dirty paper coding is a natural technique to use on the broadcast channel since the interference between all users is known. An achievable region for the MIMO BC based on dirty paper coding was first proposed in [5].

3.2 Dirty paper coding in multi-user MIMO downlink channel

The traditional additive Gaussian noise channel is modified to include an additive interference term that is known at the transmitter:

Received signal = Transmitted signal + Interference +Noise. (9)

The simplest thing to do in such a scenario would be to set the transmitted signal equal to the desired data minus the interference, but such an approach requires increased power. Costa proved the surprising result that the capacity of this channel is the same as if the interference was not present; no more power is needed to cancel the interference than is used in a nominal additive Gaussian noise channel. To use Costa's analogy, writing on dirty paper is information theoretically equivalent to writing on clean paper when one knows in advance where the dirt is. Costa's approach is theoretical, however, and does not provide a practical technique for approaching capacity. The application of this principle to downlink transmission in multi-user MIMO channels was proposed in [19]. Because the transmitter in Fig.6 has CSI, it knows what interference user 1's signal will produce at user 2, and hence can design a signal for user 2 that avoids the known interference. This concept has been used to characterize the sum-capacity and capacity region [20] of the multi-antenna multi-user channel.

The most well-known dirty paper technique for the MIMO downlink uses a QR decomposition of the channel, which we write here as the product of a lower triangular matrix L with a unitary matrix H = LQ. The signal to be transmitted is precoded with the Hermitian transpose of Q, resulting in the effective channel L. The first user of this system sees no interference from other users; its signal may be

chosen without regard for the other users. The second user sees interference only from the first user; this interference is known and thus may be overcome using dirty paper coding. Another approach applies dirty paper techniques directly, rather than for individual users. An important difference between the multi-user MIMO channel and the interference channels for which dirty paper techniques are designed is that the interference depends on the signal being designed. In the previous section this problem is solved using QR-type decomposition, so the interference for any particular user depends only on the interference generated by previous users. Dirty paper coding is then applied to cancel this interference. An alternate technique is to design all the signals jointly; this is the approach taken in [13], where matrix algebra is used to solve for the signal to be transmitted. The simple dirty paper technique of applying a modulo operation to the transmitted and received data is shown to operate close to the sum capacity.

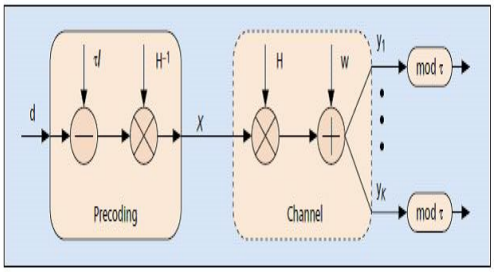

Fig.6. A modulo precoding technique (vector chosen to minimize the signal power is added to the data to be transmitted)

Fig.6 illustrates this technique, referred to as vector precoding. It can be seen as a modification of channel inversion, where the desired signal d is offset by a vector l of integer values chosen to minimize the power in the transmitted signal, $x = H^{-1}(d + \tau l)$:

$$L = \text{argmin} \| H{-}1(d + \tau l \| \quad (10)$$

Where τ is chosen in the same way as for the successive algorithm described above. As with basic channel inversion, this encoding results in the kth receiver seeing an additive Gaussian channel $y_k = d_k + \tau_k + w_k$. The integer offset lk is removed by applying a modulo function at the receiver, resulting in a signal that looks very much like an additive noise channel:

$$y_k \bmod \tau = (d_k + \tau l_k + w_k) \bmod \tau$$
$$= (d_k + w_k) \bmod \tau \quad (11)$$

A modification of this technique uses a regularized inverse at the encoder rather than simple channel inversion. The transmitted signal in this case is $x = H^*(HH^* + K/PI)^{-1}(d + \tau l)$, where the vector l is again chosen to minimize the norm of x. Decoding occurs in the same way as for the non regularized approach.

3.4 Algorithm to Compute Bit Error Rate Performance of 2x2 MIMO channel

Let us Consider 2×2 MIMO channel, in a 2×2 MIMO channel, probable usage of the available 2 transmit antennas can be as follows:

1) Consider a transmission sequence.

2) In normal transmission, we will send in the first time slot, second time slot, and so on.

3) However, we now have 2 transmit antennas; we make group symbols of two time slot each. In the first time slot, send one sequence from the first and second antenna. In second time slot, send second sequence from the first and second antenna, and repeat same for next and so on.

4) Notice that as we are grouping two symbols and sending them in one time slot, we need only time slots to complete the transmission – data rate is doubled)

5) This forms the simple explanation of a probable MIMO transmission scheme with 2 transmit antennas and 2 receive antennas.

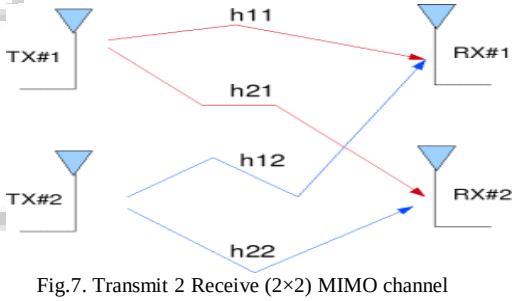

Fig.7. Transmit 2 Receive (2×2) MIMO channel

Let us consider a MIMO channel with H as channel matrix is given by:

$$Y = H x + n \quad (12)$$

to solve for x the MIMO channel with zero forcing technique for meeting the constraint

$W^*H = I$ is given by:

$$W = (H^H H)^{-1} H^H \quad (13)$$

Now to cancel the effect of interference we apply the dirty paper technique which uses the successive interference cancellation technique.

We have the estimated sequence

$$X_1\hat{} = h^H * r / h^H * h \quad (14)$$

This estimated sequence is detected in Rayleigh channel for BPSK modulation for 2x2 MIMO in different cases.

4. TOMLINSON–HARASHIMA PRECODING

Tomlinson-Harashima precoding (THP) was originally proposed for ISI channel, now it used in implementation of dirty paper coding.THP states that if the channel response is known to transmitter, the equalizer can be placed at the transmitter end of communication system. Thus, the noise enhancement that is generally inherent when the equalizer (linear or DFE) is placed at the receiver is avoided. This approach has the advantage that the problem of error propagation due to incorrect decision in the feedback filter is completely eliminated.

The Fig.8 illustrates a general system with additive interference and AWGN noise. Interference is non-causally known at the transmitter and its probability density function (PDF) known at the receiver.

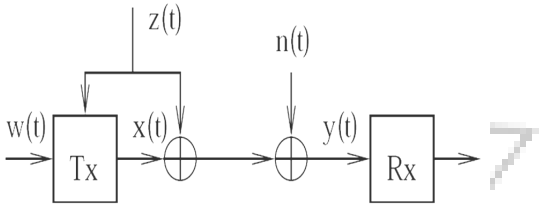

Fig.8. System configuration THP

4.1 System configuration of Tomlinson-Harasima Precoding (THP)

The channel output is given by

$$y(t) = x(t) + z(t) + n(t) \quad (15)$$

where x (t), y(t) , z(t), n(t) denotes the transmitted signal , the received signal ,the interference and the AWGN channel at time instant t respectively. The transmitted signal x is output of the encoder given the information signal w and the interference z, and therefore denoted by x (w,z) the information signal w is a symbol from an M-ary pulse amplitude modulation(M-PAM) constellation with uniform spacing. The interference z may be Gaussian.

The basic strategy of Tomlinson- Harashima precoding is to subtract the interference z from the source signal w, and then pass the resulting signal (w-z) through a modulo operator. Given a real valued variable a, the modulo operation "mod Λ" outputs a new real valued variable b which falls in to the region [Λ /2,- Λ /2] ,where Λ is called modulo range. After this modulo operation, the output signal x = (w - z) mod Λ is transmitted through noisy channel. The received signal y can be expressed by:

$$y = x + z + n = (w - z) \bmod \Lambda \quad (16)$$

where the modulo range Λ can be adjusted to achieve the best performance while maintaining the power constraint. Tomlinson–Harashima Precoding (THP) could largely decrease the transmit power while maintaining the same communication quality , both in the mutual information sense and in terms of bit error rate. With optimized parameters, THP can eliminate most of the effect brought in by known interference, regardless of whether it consists of discrete symbol or Gaussian components. Tomlinson-Harashima Precoding (THP) [2] is a well known method to eliminate error propagation in a DFE which has been adopted in a wide variety of modern communication systems with reliable feedback channels. In this paper, we study the effect THP on the source distribution and blind equalization performance. We show that THP bounds the higher-order statistics of the transmitted signal.

4.2 The Blind-THP Scenario

This gives combination of blind equalization and THP. In this, is to study the performance of blind equalization algorithms for Tomlinson-Harashima Precoded (THP) signals in a communication system as shown in Fig. 9.

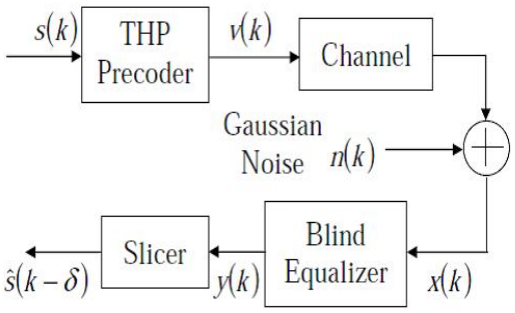

Fig.9. Blind equalization model for THP system.

Such a system might arise in the following scenarios:

a) In modern digital broadcasting or point-to-multipoint systems, such as VDSL, THP can be used to implement spectral masks to prevent egress noise. At the same time, to increase the overall bandwidth efficiency of the system, receiver set-top boxes can be blindly initialized, instead of using a trained sequence-based adaptive algorithm.

b) Another scenario is in a MIMO-based broadcast system with users blindly trained to the broadcast signal at different times. By using spatial information, a MIMO system can increase the system robustness and capacity. If the precoding is done in the transmitter, then adding a new user which uses a blind algorithm at the receiver side again, increases the bandwidth efficiency of the overall system. In [6] and [17] THP is implemented for MIMO systems, yielding good noise reduction performance.

c) A final scenario is in military applications, where an operator wants to intercept a precoded signal without a training sequence. Blind equalization would enable the interception of an encrypted or scrambled signal.

4.3 THP in Single-Input Single-Output (SISO) System

In a THP system the equalization is done in the transmitter using an inverse modulo filter. Therefore, error correction coding techniques can be applied in the same way as for channels without interference. Note that to construct the optimal modulo filter, the channel transfer function needs to be known at the transmitter both for SISO and MIMO systems. Fig. 10 is a general representation of a SISO THP system. Modulo adder basically wraps around the signal constellation so that the signal does not expand infinitely, increasing the transmit power. If data signal is drawn from an M-point one-dimensional PAM signal set A = {±1, ±3, . . . ,±(M −}, for even M, then the modulo adder makes sure that the signal set does not go beyond the interval [-M, +M].

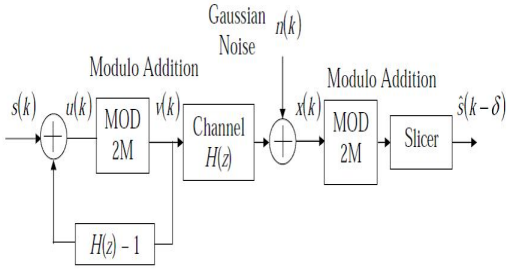

Fig. 10. SISO Tomlinson-Harashima Precoder

The following algorithm:

a) If the result of the summation is greater than M,

2M is deducted from it until it is less than M.

b) If the result of the summation, u(k) is less than -

M, 2M is added to it until it is greater than or equal to −M.

If the data symbols are drawn from an M-ary square QAM signal set A = {a+j b | a, b ∈ ±1,±3, ··±(√M −1)}, then the modulo adder makes sure that the real and imaginary parts of the precoded symbols lie in the interval [-√M, +√M). Due to the modulo operation, all the points spaced by integer multiples of 2√M in real or imaginary part represent the same data.

4.4 THP in Multi-Input Multi-output (MIMO) System

The concept of Tomlinson-Harashima Precoding (THP) for SISO channels can be easily extended to MIMO channels. Fig.11 shows a generalized MIMO THP system for a zero-forcing (ZF) system.

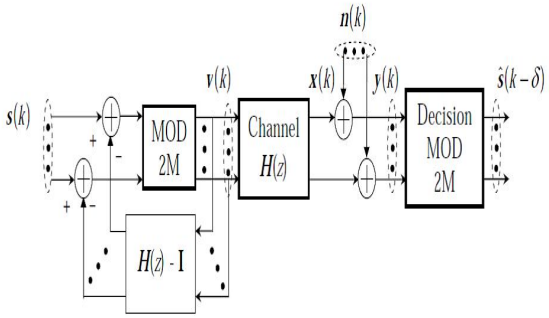

Fig.11. MIMO Tomlinson-Harashima Precoder.

Similar to the SISO case, the direct realization of THP requires advanced knowledge of the Channel State Information (CSI) matrix H(z). One result of implementing SISO or MIMO THP is the input data is scrambled into a pseudorandom sequence [17]. This scrambling spreads the frequency spectrum of the data, and so reduces the intermodulation effects, but it colors the data unlike a conventional scrambler which has a whitening effect. As the input data sequence is modified because of modulo addition, the receiver needs to apply the same modulo operation to the received data to retrieve the original transmitted symbol. So, the received sequence is passed through the modulo adder based on the same algorithm as in the transmitter before it is passed through the slicer.

Tomlinson- Harashima precoding slightly increases average transmitted power. This

precoding loss is only relevant for "small" signal sets and vanishes completely as the number M of signal points goes to infinity. Additionally, the number of nearest neighbor points increases slightly due to the periodic extension of the constellation. Using MIMO precoding, the major drawbacks of decision feedback equalization are avoided. No error propagation may occur since the feedback filter is located at the transmitter where the signals are perfectly known. Additionally, channel coding can be applied in a straightforward manner. Using precoding, no immediate decisions at the receiver are required for equalization, which is irreconcilable with the principle of channel coding.

5. SIMULATION MODEL

Consider a multiple antenna system with M transmit antennas (say, M=2) and N receive antennas (say, N=2) surrounded by scatters & these antennas are assumed to be uncorrelated. Under normal situation, this would yield a channel matrix of full rank and size N x M. Suppose a screen with small hole in it separates these two sets of antennas. The only way for the transmit signal is to pass through the key hole. It appears like concatenation of multiple-input single-output (MISO) and single input multiple-output (SIMO). Recently, the dirty paper coding has emerged as a building block in multiuser communication. A 2Tx-2Rx simulation model is shown in Fig.12. In this model, the message will be modulated using BPSK modulation. After pre-subtraction of the known interference, it is transmitted through an AWGN channel or a Rayleigh fading channel. The received signal is chosen based on selection diversity technique where the strongest and highest signal power is selected.

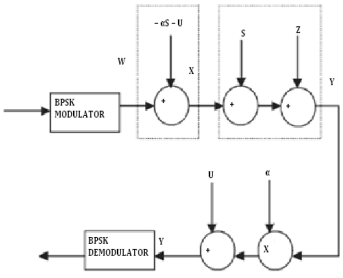

Fig.12. A 2Tx-2Rx antenna system model

5.1 Proposed Algorithm

In this work, we extend the approach by using dirty paper coding over the MIMO keyhole fading channel. The encoder sends:

$$V = X - \alpha S - U \quad (17)$$

and hence $V = X + \alpha S + U$ (18)

The received signal is

$$Y = X + S + Z \quad (19)$$

with Z distributed according to Z(0, N).

At the input of the BPSK demodulator, we have the signal

$$Y = U + Ay \quad .. \quad (20)$$

$$= U + \alpha (X + S + Z)$$

$$= U + \alpha (W - \alpha S - U + S + Z)$$

$$= (\alpha W - \alpha^2 S + \alpha S) + (1 - \alpha) U + \alpha Z$$

$$= W + Z \quad (21)$$

where

$$Z = (1 - \alpha) U + \alpha Z \quad (22)$$

One can measure the channel H1 from transmitter to keyhole & the channel H2 from keyhole to receiver, and finally concatenate the two. The MISO channel matrix (transmitter-to-keyhole) is represented by

$$H1 = (h_1, h_2, \ldots\ldots\ldots\ldots, h_M) \quad .. \quad (23)$$

The channel capacity can be obtained as

$$C = log2(1 + \sum_{j=1}^{M} |hj|^2 Et/MN \quad (24)$$

If the channel coefficients are equal and normalized as

$$\sum_{j=1}^{M} |h_j = M \quad (25)$$

Then, the capacity of MISO becomes

$$C = \log_2(1 + Es/N_0) \quad (26)$$

On the other hand , if channel is known to transmitter , the capacity is given by

$$C = \log_2(1 + M*Es/N_0) \quad (27)$$

In case of SIMO (keyhole to receiver) with one transmit antenna & N receive antennas , the channel matrix is represented as column matrix:

$$H_2 = (h_1, h_2, \ldots\ldots\ldots\ldots h_M)^T \quad (28)$$

The capacity is given by :

$$C = \log_2 \det (I_M + E_s/MN_0 * H^H H)$$

Now $H^H H = \sum_{j=1}^{M} |h_j$ and M = 1

Hence

$$C = log2 \det(1M + \sum_{j=1}^{N} |hj|^2 Et/N_0)$$

If

$$|h_1|^2 = |h_2|^2 = \ldots\ldots\ldots\ldots\ldots\ldots\ldots\ldots = |h_N|^2$$

The capacity of SIMO channel is given by

$$C = \log_2 \det (1 + N*Es/N_0) \quad (29)$$

The system achieves diversity gain of N.

Now consider the MIMO keyhole system with M = N =2. The effective channel H is given by

$$H = H_2 H_1^T \quad (30)$$

Where, $H_1 = [h_1 \; h_2]$ with h_1, h_2 as channel coefficient corresponding to transmitted signals and $H2 = [h_3 \; h_4]^T$ with h_3 and h_4 as the channel coefficient corresponding to the first and second receiving antenna respectively. Since the transmitted signal m_2 acts as an interference to signal m_1 (and vice versa) and the two capacities is given by

$$C_1 = log2\frac{|H_1 Q_1 H_1^T + I}{N_1} \quad (31)$$

$$C_2 = log2\frac{|H_2 Q_2 H_2^T + I}{H_2 Q_2 H_2^T + I} \quad (32)$$

6.SIMULATION RESULTS AND PERFORMANCE ANALYSIS

In this paper, the performance of MIMO system with two transmit antenna and two receive antennas has been compared**.**

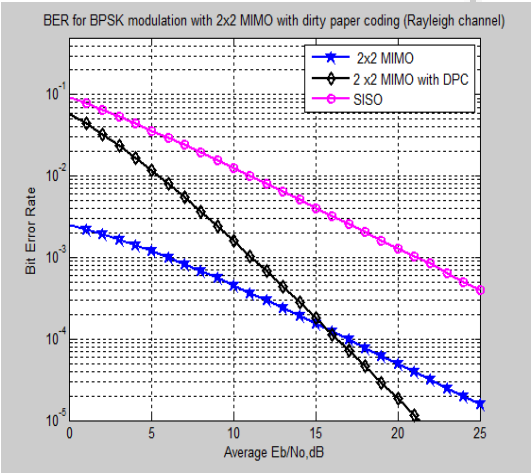

Fig.13. Bit Error Performance of SISO,2x2 MIMO and 2x2 MIMO with DPC(Improved Performance)

In the simulations, it is assumed that the receiver has perfect CSI and that the fading between transmit and receive antennas is mutually independent. As we have seen throughout this paper our emphasis on the improvement of performance of the MIMO channel. This improvement of MIMO performance is achieved by the interference cancellation technique, Dirty paper coding and the implementation of DPC is done by Tomlinson-Harashima Precoding (THP). All simulation results have been done on MATLAB.

Fig.13 shows the Bit error rate performance of 2x2 MIMO with BPSK modulation in Rayleigh Channel. As we see in Fig.13 pink line shows the performance of SISO where single antenna at transmitter end and single antenna at receiver end, which shows the poor bit error rate, so to improve this performance we take 2 Tx antenna and 2 Rx antenna. Blue line shows the performance of 2x2 MIMO. Now if we use dirty paper coding with 2x2 MIMO as we see from the figure at low SNR region and approximately 5 dB gain has been achieved with using DPC at BER of 10^{-5}.

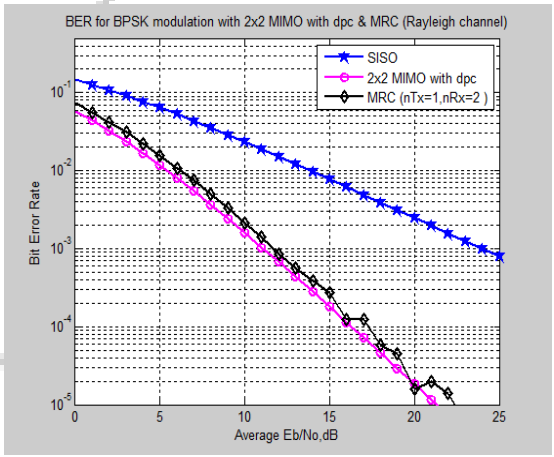

Fig.14. Bit error rate performance of 2x2 MIMO with DPC and Maximal ratio combining

Fig.14 shows the Bit error rate performance of 2x2 MIMO using DPC with bpsk modulation in Rayleigh Channel and its comparison with the performance of Maximal ratio combining (MRC) which is receiver diversity technique where multiple antenna at receiver. Here we take 1x2 MRC and as we have seen from the Fig. 14, the performance of 2x2 MIMO using DPC is very close to the maximal ratio combining.

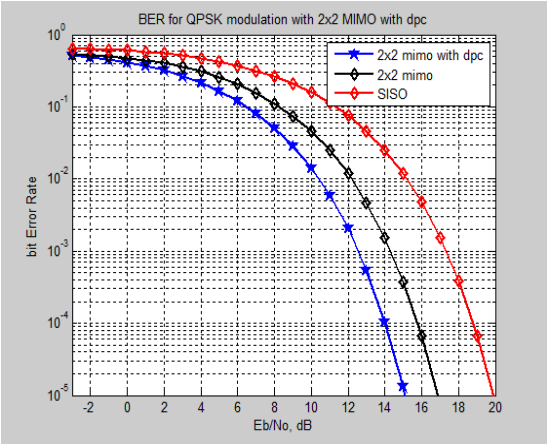

Fig.15.Improved Performance of 2x2 MIMO for QPSK using DPC

To improve the performance we change the modulation technique now we take QPSK in Rayleigh channel. Fig.15 shows the Bit error rate performance of 2x2 MIMO using DPC with QPSK modulation. As we see in the Fig.15, with the using QPSK as modulation technique, the performance has been improved for both SISO and 2x2 MIMO as compared to BPSK technique. And after that by using dirty paper coding approximately 2-dB gain has been achieved. Now we consider the 2x2 MIMO keyhole channel in this case we assume that these two set of antennas are separated by a screen with a small hole in it (keyhole or pinhole effect) so that the transmitted signals pass through the keyhole.

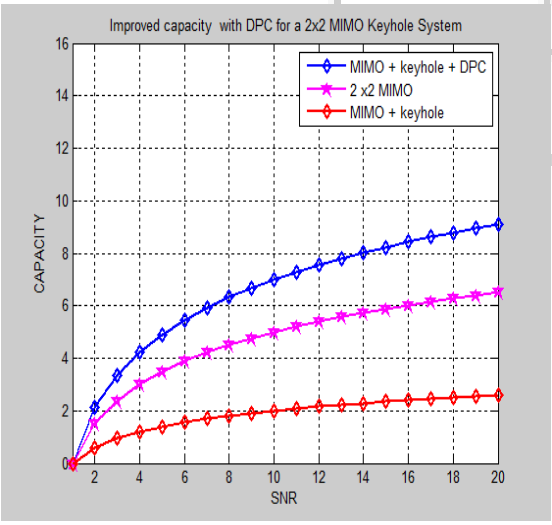

Fig.16. Improved Capacity of MIMO keyhole channel with Dirty paper coding and without DPC

Fig.16 shows the performance of keyhole channel. We observe the drop in capacity compare to regular channel. We observe a significant improvement in the capacity of a MIMO keyhole channel using DPC.

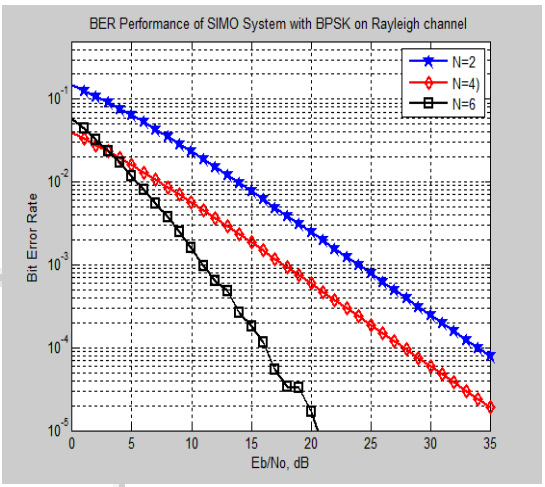

Fig.17. BER performance of SIMO with BPSK in Rayliegh channel with different number of receiving antennas.

Consider N transmit diversity system with a single receive antenna and no feedback. The average bit error probability of the coherent BPSK with N receiver antennas on Rayleigh fading channel shown in Fig 17 .This plot of bit error performance of scheme against Eb/N0 for varying number of receive antenna indicates the effective receive diversity in mitigating the effect of fading . For example, at a BER of 10^{-3}, we achieve a SNR gain of almost 13 dB when the transmit diversity is increased from two to six.

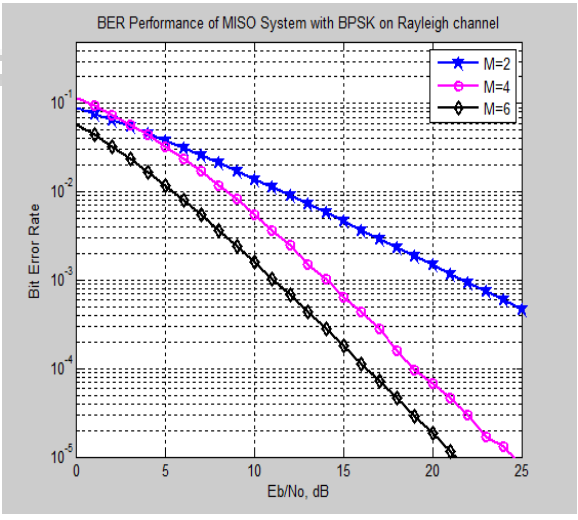

Fig.18. BER performance of MISO with BPSK in Rayleigh channel with different number of transmitting antennas.

In Fig. 18, we plot the bit error rate performance of the MISO system against Eb/No for various numbers of the transmit diversity, M. From this

figure, we can observe that at the BER of 10^{-3} the error performance is improved by about 8 dB and 2 dB, when the transmit diversity is increased from two to four and four to six, respectively. However, the performance curves suggest that a further increase in the transmit diversity can only improve the performance marginally.

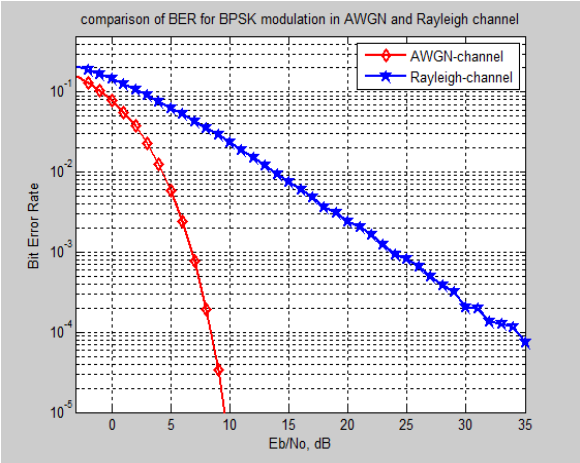

Fig.19. BER comparison of BPSK modulation in AWGN and Rayleigh channel.

It is very clear that the diversity helps in mitigating the effect of fading. Just to illustrate the effect of fading on the BER performance of the system, in the absence of transmit and receive diversity, BER vs. Eb/No plots with and without Rayleigh fading are shown in Fig.19.

7. CONCLUSION

In this paper, the MIMO broadcast channel and its duality with the multiple access channel (MAC) have been studied. Tomlinson-Harashima Precoding (THP) used as simple technique to implement Dirty Paper Coding (DPC). Duality is a power technique to relate capacity regions for broadcast and MAC channels. Duality holds for many notions of capacity, including ergodic, outage, and minimum rate capacity. Duality can be used to show the connection between capacity regions and optimal transmission strategies for BC and MAC channels. It is shown that the degenerate channels, called 'keyholes', may arise under realistic assumptions which have zero correlation between the entries of the channel matrix H and yet only a single degree of freedom. The keyholes present low correlation at both transmitter and receiver. Anticipate that keyhole effect due to real-world waveguides like tunnels or corridors will usually be very weak and the correlation is the major capacity-reducing effect. The diversity order of a MIMO keyhole channel is equivalent to min(N;M). For the case of M > N, the design criteria are unaffected by the keyhole condition, but for M < N the design criteria are indeed affected. The application of dirty paper coding gives capacity gain in the keyhole MIMO channel.

If we observe the simulation result, we find that performance of 2x2 MIMO has been improved to a greater extent by using dirty paper coding. We also observe that by increasing diversity to a given limit a better gain in dB has been achieved, and it also suppressed the effect of fading. So we concluded that dirty paper coding has been emerged out as a very effective technique to overcome the interference in the different channel scenerio.DPC can also be used in digital water marking. In case of MIMO there is open research field to increase the number of antenna, and with the challenge that with increasing the number of antenna leads to increase in interference.

References

[1] M. Costa ,“Writing on dirty paper," IEEE Trans. Inform. Theory, vol. IT-29, no. 3, May 1983.

[2] John. G. Proakis "Digital communications" Fourth edition Mc Graw Hill.

[3] Nihar Jindal, Sriram Vishwanath, Syed Jafar and Andrew Goldsmith, “Duality,dirty paper coding and capacity of multi user wireless channel", IEEE transaction-2006.

[4] N. Jindal, S. Vishwanath, and A. J. Goldsmith, “On the duality of multiple-access and broadcast channels", Proc. IEEE Allerton Conf. Commun. Cont. Comput., Oct. 2001.

[5] P. Viswanath and D. Tse, “Sum capacity of the vector Gaussian broadcast channel and uplink-downlink duality", IEEE Trans. on Information Theory IEEE 2004.

[6] Bin liu, HiuLiu, Sumit Ro, "Structured dirty paper coding with known interference structure at receiver", IEEE Trans. 2005.

[7] Shin-Chun Lin ,Hsaun-Jung Su ,"Practical vector Dirty paper coding for MIMO Gaussian broadcast channels", IEEE Trans. 2009.

[8] G. Caire and S. Shamai, “On the Achievable Throughput of a Multi-antenna Gaussian Broadcast Channel", IEEE Trans. on Inform. Theory, July 2001.

[9] U. Erez , Stephan ten Brink," A Close To Capacity Dirty paper coding scheme", IEEE Trans. 2007.

[10] M. Costa ,“Writing on dirty paper," IEEE Trans. Inform. Theory, vol. IT-29, no. 3, May 1983.

[11] John. G. Proakis "Digital communications" Fourth edition Mc Graw Hill.

[12] Nihar Jindal, Sriram Vishwanath, Syed Jafar and Andrew Goldsmith, “Duality,dirty paper coding and capacity of multi user wireless channel", IEEE transaction-2006.

[13] N. Jindal, S. Vishwanath, and A. J. Goldsmith, “On the duality of multiple-access and broadcast channels", Proc. IEEE Allerton Conf. Commun. Cont. Comput., Oct. 2001.

Efficient Shunt Active Power Filter For HarmonicSuppression -A Matlab/Simulink Approach

[1]Ritvik Kumar, [2] Romita Tiwari , [3] Shishupal Singh Dohare
Electrical & Electronics Engineering Department
IES,IPS Academy
[1]ritvik.kumar7@gmail.com
[2]romita_tiwari@gmail.com
[3]shishupalsinghdohare @gmail.com

***Abstract* - Due to the wide spread of power electronics equipment in modern electrical systems, the increase of the harmonics disturbance in the ac mains currents has became a major concern due to the adverse effects on all equipment. This paper presents the analysis and simulation using Matlab Simulink of a three-phase four wire neutral clamped active power filter (APF) compensating the harmonics and reactive power created by nonlinear balanced and unbalanced low power loads in steady state and in transients. The usefulness of the simulation approach to APF is demonstrated so APF designers have a better insight using Matlab Simulink in order to develop new APFs.**

***Keywords* -Harmonic suppression, Power factor, Shunt Active Power Filter, Total Harmonic Distortion.**

I. INTRODUCTION

Harmonic pollution is not a new phenomenon, issues of harmonic components of voltage and / or current curves occurred early in the industrial use of electricity, the first mention regarding to the use of harmonic analysis as a way of solving a practical electrical engineering problem, was made in 1893 by Steinmetz. Nowadays, in modern industry, about 50% of receivers an industrial customer are supplied using frequency converters (AC and DC adjustable drives), switching mode power supply (for powering computer systems or process controllers) and electronic ballasts. Due to the nonlinear characteristics of these receivers (using diodes,thyristors or transistors to convert AC voltage in DC voltage and DC voltage in AC voltage or DC voltage in DC voltage), in industrial distribution systems harmonic currents occur. These, harmonic currents,leads to the distortion of the voltage curve at the point of common coupling (and in other parts of the distribution system), so are affected and other customers, non-harmonic polluting. Resonance phenomena can increase the harmonic components of voltage that will lead to increase the voltage indifferent parts of the electricity supply system,over loading of transformers and, in particular capacitor. Also, can causing losses increasing in overhead electric lines, cable, transformers and capacitor banks, leading to acceleration of insulation aging and reduction life. In four wire systems, harmonic current with frequency multiple by three will be add up in the neutral conductor, so the current through this reaches high values. Given the negative consequences of harmonic distortion the measures must be taken that would lead to limitation of harmonic pollution in power networks. Measures can be undertaken involving: reduce harmonic currents from customers, changing the resonance frequency and filtering of the harmonic distortion using passive, active or hybrid systems. Passive filters have been used as a conventional solution to solve harmonic currents problems, but they present some challenges such as they only filter the frequencies they are pre-tuned for, their operation cannot be limited to a certain load or

group of loads, resonance can occur due to the interaction between the passive filters and others loads, with unexpected results.

To cope with these disadvantages continuous efforts have been concentrated on the development of active power filters [10-13]. In this paper the development of a shunt & series active filter is proposed, with a control system based on the p-q theory. The filter described effectively compensates the harmonic currents and the reactive power and also balances the power supply currents.

II. PRAPOSED REACTIVE POWER THEORY (P-Q THEORY)

This theory was proposed by (Akagi et al. 1983)[6] for three-phase systems with or without neutral wire, and it is valid for both steady state and transients. It consists in the algebraic transformation of the current and voltage of the system from the abc system to αβ0 system using the Clarke transformation as in equation (1)and(2).

$$\begin{bmatrix} v_0 \\ v_\alpha \\ v_\beta \end{bmatrix} = \sqrt{\frac{2}{3}} \begin{bmatrix} \frac{1}{\sqrt{2}} & \frac{1}{\sqrt{2}} & \frac{1}{\sqrt{2}} \\ 1 & -\frac{1}{2} & -\frac{1}{2} \\ 0 & \frac{\sqrt{3}}{2} & \frac{\sqrt{3}}{2} \end{bmatrix} \begin{bmatrix} v_a \\ v_b \\ v_c \end{bmatrix} \quad \text{.....(1)}$$

$$\begin{bmatrix} i_0 \\ i_\alpha \\ i_\beta \end{bmatrix} = \sqrt{\frac{2}{3}} \begin{bmatrix} \frac{1}{\sqrt{2}} & \frac{1}{\sqrt{2}} & \frac{1}{\sqrt{2}} \\ 1 & -\frac{1}{2} & -\frac{1}{2} \\ 0 & \frac{\sqrt{3}}{2} & \frac{\sqrt{3}}{2} \end{bmatrix} \begin{bmatrix} i_a \\ i_b \\ i_c \end{bmatrix} \quad \text{.....(2)}$$

where ia, ib, ic are the load currents and va, vb and vc are the load voltages. According to the p-q theory, the active, reactive and zero-sequence powers are defined as in equations (3 ,4and5):

$$p = v\alpha i\alpha + v\beta i\beta \quad \text{.....(3)}$$

$$q = v\alpha i\beta - v\beta i\alpha \quad \text{.....(4)}$$

$$p0 = v0i0 \quad \text{.....(5)}$$

The currents, voltages and powers in the α-β system can be decomposed in mean and alternating values, corresponding to the fundamental and harmonic components, as in equation (6)

.

$$x = \bar{x} + \tilde{x} \quad \text{.....(6)}$$

where x can be currents, voltages or powers.

The power components have the following physical meaning (Afonso J.L. et al., 2003):

p0 = zero sequence power. It only exists in three-phase systems with neutral wire. Since it is an undesired power component because it only exchanges energy with the load, it must be compensated. From equation (5) it can be seen that p0=v0i0, but i0*=p0/v0=i0, so there is no need for computing p0.

$\bar{p}$ =mean value of the instantaneous real power. It is the only desired power component to be supplied by the source because it corresponds to the energy transferred from the source to the load.

$\tilde{p}$=alternating value of instantaneous real power. Since it does not involve any energy transfer from the source to the load, it must be compensated.

$\bar{q}$ =mean value of imaginary power. It corresponds to the power exchanged between the phases of the load and is responsible for the existence of undesired current. It must be compensated.

$\tilde{q}$= alternating value of imaginary power. It corresponds to the conventional reactive power. It can be compensated by the APF, depending on the requirements of the system. Since in the p-q theory the voltages are assumed sinusoidal, the power components must be computed using sinusoidal voltages. In the α-β voltage system, the AC components of the voltage are eliminated in order to the IRPT to provide good performance. Conventionally, in IRPT control, are used High Pass (HP) and Low Pass (LP) Filters, but this method has a high error in the phase and magnitude of the harmonics and also is sensitive to high-frequency noise. Even worse, there is a need of five HP or LP filters – for α-β voltage components, and for p,q and p0 power components. This paper presents a control scheme based on the usage of only two self-tuning filters. The powers required to be compensated by the APF are calculated as in equation (7):

$$\begin{bmatrix} p \\ q \end{bmatrix} = \begin{bmatrix} v_\alpha & v_\beta \\ -v_\beta & v_\alpha \end{bmatrix} * \begin{bmatrix} i_\alpha \\ i_\beta \end{bmatrix} \text{.....(7)}$$

The load currents are transformed from three-phase abc to αβ0 components using Clarke transformation, as in equation (8):

$$\begin{bmatrix} i_0 \\ i_\alpha \\ i_\beta \end{bmatrix} = \sqrt{\frac{2}{3}} \begin{bmatrix} \frac{1}{\sqrt{2}} & \frac{1}{\sqrt{2}} & \frac{1}{\sqrt{2}} \\ 1 & -\frac{1}{2} & -\frac{1}{2} \\ 0 & \frac{\sqrt{3}}{2} & \frac{\sqrt{3}}{2} \end{bmatrix} \begin{bmatrix} i_a \\ i_b \\ i_c \end{bmatrix} \text{.....(8)}$$

The compensation strategy based on the p-q theory of all undesired power components (p , p0 and q) can be accomplished with the use of the shunt active power filter.

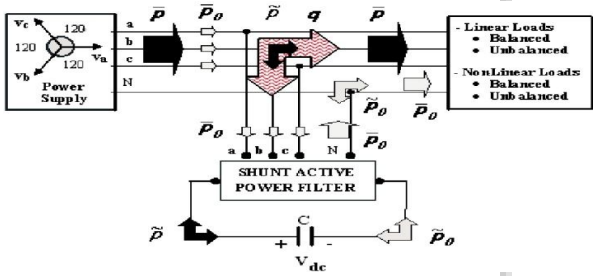

Fig.1: p-q theory power components in a generic three phasepower system with shunt active filter

An important aspect is that only the mean values of the instantaneous real power (p) and of the instantaneous zero-sequence power (p0) must come from the power supply, as they effectively transfer energy to the load.The active filter also permits the power supply to deliver a magnitude p0 to the load from the phases, without the using the neutral wire. All the other power components (p0 ,$p\tilde{}$,pand q) can be compensated with the use of shunt active power filter, as presented in Fig .1

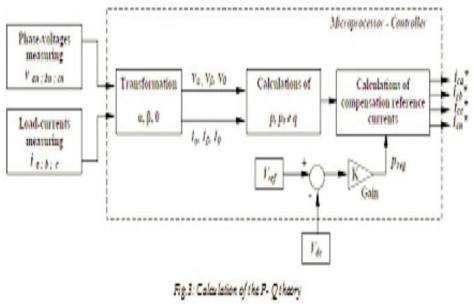

Fig.2: Calculation of the P- Q theory

The p-q controller allows systematic information, to verify the requirement of compensation currents by the active filter. It receives the information of phase voltages, load currents and DC voltage, and proceeds to the calculations based on its control algorithm generating necessary reference compensation currents, which is indicated in Fig.2. The objective of this algorithm is to compensate all undesirable power components. Besides, the source will see the load as if it was a balanced resistive load and the RMS value of the supply currents will be the lower possible to deliver the energy the load needs to work.

III.REFERENCE CURRENT CALCULATION

The control scheme of the Shunt and Series active power filters must calculate the current reference signals from each phase of the inverter using instantaneous real power compensator. The simulation model for calculation of reference current shown in fig.3. In this case a P-Q controller is applied to the System in generating the switching signals.

The Power stage is basically a VSI, controlled similar to a current source. Reference currents calculated by the controller (ica *,icb*,icc*,icn*) is used by the inverter to produce the compensation currents (ica,icb,icc,icn) to compensate harmonics

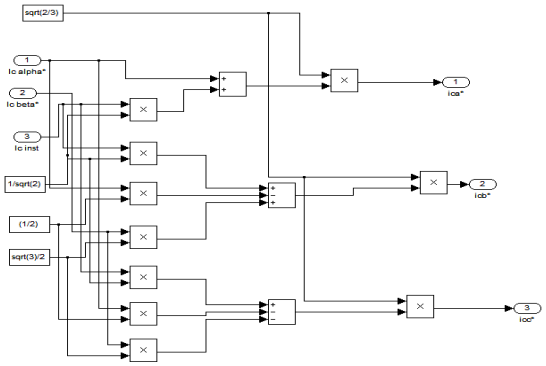

Fig.3: Reference Current Calculation

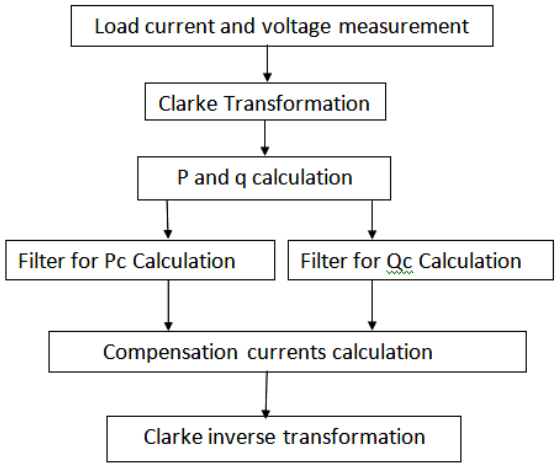

Fig. 4 :Basic control algorithm for Shunt Active Power filter based on P-Q theory

The basic algorithm commonly used for the calculation of the compensating currents is shown in Fig. 4. In this figure, pc and qc are the compensation reference powers. The p-q theory is a suitable tool to the analysis of non-linear three-phase systems and for the control of active filters.

The implementation of active filters based on the p-q theory are cost-effective solutions, allowing the use of a large number of low-power active filters in the same facility, close to each problematic load (or group of loads), avoiding the circulation of current harmonics, reactive currents and neutral currents through the facility power lines.

IV. SIMULINK MODEL OF THE SAPF

The P-Q Theory based with and without Shunt Active Power Filter is implemented for harmoniccompensation and the various models used for simulating and validating its performance are given under in Fig.5 & Fig.6.

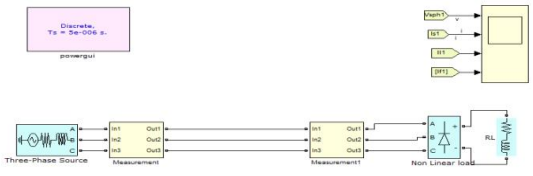

Fig. 5: Simulation model of power system for non- linear load without APF

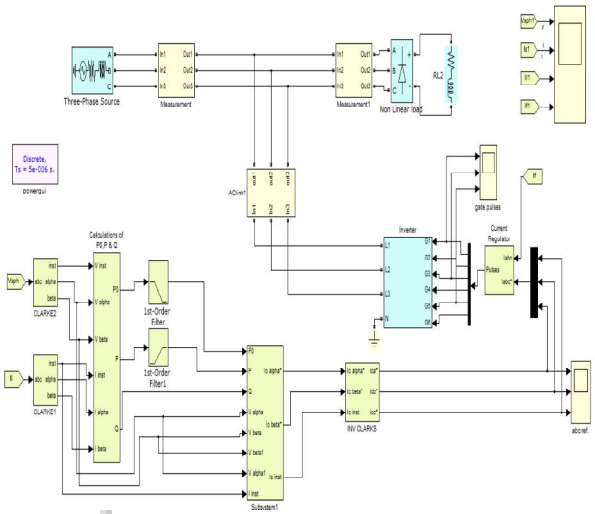

Fig. 6: Simulation model of shunt APF using p-q theory

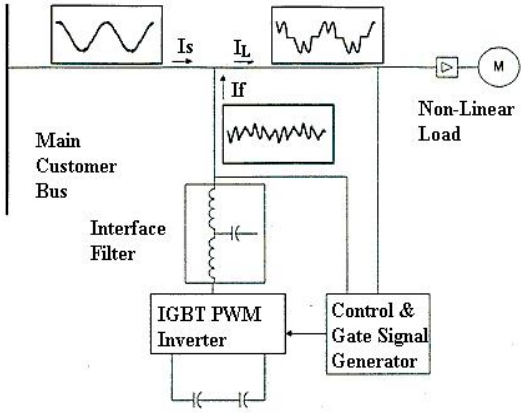

Fig. 7: Test Power System.

Table 1.Circuit Parameters for SAPF

Parameters name	Numerical value
Source Voltage Vab,Vbc,Vca	230*sqrt(2)Vrms(Line-Line)
Source Resistance and Inductance Rs, Ls	0.5 Ω, 1mH
Switching Device	1 mΩ, $1*10^5$ Ω,inf

(IGBT/Diode) Ron,Rs,Cs	
DC Link Capacitor	$3300*10^{-6}$ F
DC Link Capacitor Voltage	400 V
RL non- linear load	R=20 Ω, L=200 mH

This section presents the details of the simulation carried out to demonstrate the effectiveness of the proposed control strategy for the SAPF to reduce the harmonics. Fig.7 shows the test system used to carry out the analysis. The test system consists of a three phase voltage source, and an uncontrolled rectifier with RL load.The values of the circuit elements used in the simulation are listed in **Table 1**. The Matlab/Simulink is used to simulate the test power system with and without the proposed SAPF.

V. SIMULATION RESULTS

The filter topologies discussed in the previous sections were investigated through Matlab®/ Simulink© V-2009b and the results obtained are shown below for an electric network voltage and current responses without Fig.8& Fig.9 and with an APF in Fig.10& Fig 11.

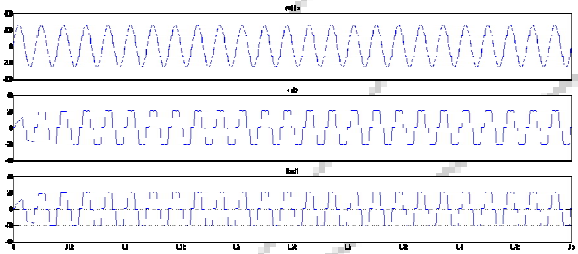

Fig.:8 Waveforms for source & load current before applying APF

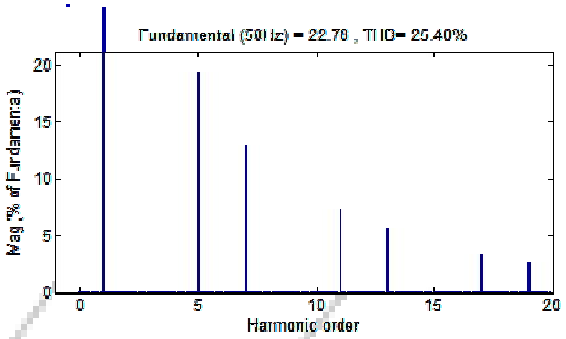

Fig.9: FFT analysis obtained for source current before applying APF (THD % =25.40%)

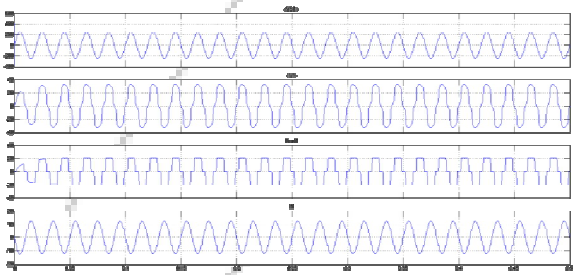

Fig.10 : Waveforms obtained for source voltage, source current , load current, filter current after applying shunt APF

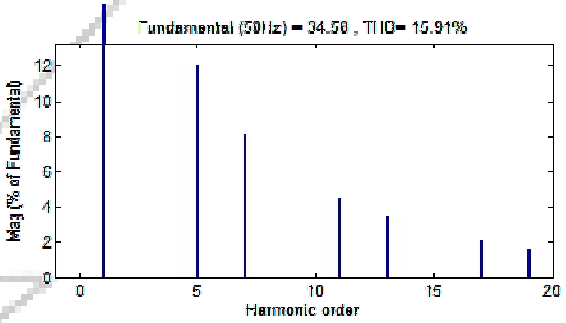

Fig.11 : FFT analysis obtained for source current after applying APF (THD % =15.91%)

As the source current & Voltage are in phase, also the source current is almost sinusoidal (very low THD), it can be said that source is providing only active power required by the circuit. In P-Q theory view, source current is providing only average real power component (P–), while remaining components i.e. real oscillating power P^+,q^+&q– is being provided by APF. From load current and Non linear load RL, it can be said that the effectiveness of APF in compensating of harmonic components of load current depends on the specific load current waveform involved. Two different

waveforms have the same rms harmonic content, but APF may do a better job of compensating for one of the waveforms because of the wave shapes involved. *I*n general the limiting factor for increasing the DC voltage is the voltage withstand capability of the IGBT devices. From harmonic analysis of source current ,it can be seen due to uneven switching of compensator large No. of inter harmonics are introduced. But it should be noted that these components have very less magnitude.It is worth to also to note that P-Q based APFs can be used for complete harmonic elimination not selective harmonic elimination.

VI. CONCLUSION

The validity in terms of eliminating p-q theory in terms of eliminating harmonics and Power Factor improvement is conformed from low THD source current which is in phase with source voltage. But p-q theory utilizes large No. of calculation & demands higher processing power resulting in utility to be complex & expensive. They are predominantly utilized in three phase circuits, thus cannot be used at remote single phase customer. From source currents of both cases, it can be inferred that APF is most effective when the load current waveform does not have abrupt changes. The overall filtering effectiveness depending significantly on the types of loads being compensated and are very effective for voltage source inverter type loads, even when the distortion is high. By comparing reference current & source waveforms, it can be conducted that this controller compensation at the cost of high switching frequency, which can result in high switching losses in practical high power applications.

In p-q theory has some short comings which need to be addressed like mathematical expression of instantaneous power does not follow power conservation and real & imaginary power needed to be more accurately defined as zero sequence instantaneous power cannot be defined by the theory. In practical approach also it can be noted that p-q theory is unable of providing selective harmonic elimination and specific power factor compensation.

ACKNOWLEDGEMENT

The authors would like to thank to all referees for their useful remarks, which helped to improve the work. And would also like to express cordial thankfulness to the entire Department of Electrical Engineering, NIIST, Bhopal (M.P.) , INDIA for providing all necessary and due help for successful attainment of the research objectives.

REFERENCES

[1] T. Mahalalekshami," Current harmonic compensation and power factor improvement by hybrid shunt active power filter", International journal of computer applications(0975-8887) Vol-04, No.3,july 2010.

[2] Vaibhav Purwar,Sanjiv Kr.,"Simulation of Shunt Active power line conditioner (APLC) for three phase AC/DC converters", VSRD-IJEECE Vol.1 ,No.9, 2011,504-513

[3] H. Akagi, "New trends in active power filters for power conditioning",IEEE Trans. Ind. Appli.,vol.IA-vol 32, no 6, pp.1312-1322.1996.

[4] H. Akagi, Y. Kanazawa and A.Nabae,"Instantaneous reactive power compensators comprising switching devices without energy storage compenents", IEEE Trans. Ind Appli.,vol. IA-20, pp.625-630.1984.

[5] Edson H.Watanabe ,Maurício Aredes ,Hirofumi Akagi "The P-Q Theory For Active Filter Control : Some Problems And Solutions",review & automatic control. Vol.15 No.1,2004.

[6] Akagi, H., Kanazawa, Y. and Nabae, A. (1983) "Generalized Theory of the Instantaneous Reactive Power in Three-Phase Circuits," IPEC'83 . Int. Power Electronics Conf., Tokyo, Japan, pp. 1375-1386.

[7] N. Mohan, T. M. Undeland, W. P. Robbins, "Power Electronics:Converters, Applications, and Design," New York, NY, USA, John Wiley & Sons, Inc., 1995.

[8] Handbook of "Power Electronics Circuits,Devices and applications" by M. H.Rashid, ,pearson Education,Singapore 1993

[9] Handbook of Power Electronics by M.D. Singh,K.B. Khanchandani., Tata McGraw Hill Publication,Delhi 2001

[10] Karrupanan P. and Kamalakanta Mahapatra "Cascaded Multilevel inverter based Active Filters for Power line Conditioners using Instantanous Real PowerTheory"IEEE-IICPE2010,International conference on Power Electronics,NSIT-NEW –Delhi, January 28-30 2011.

[11] Leszek S. Czarnecki, Fellow IEEE" Instantaneous Reactive Power p-q Theory and Power Properties of Three-Phase Systems",IEEE transaction on Power Delivery,Vol.21 No.1,Jan 2006, 362-367.

[12] G. Jayakrishna and K.S.R.Anjaneyulu ,"Fuzzy Logic Control based Three Phase Shunt Active Filter for Voltage Regulation and Harmonic Reduction", ",International journal of computer applications(0975-8887)Vol-10, No.5,Nov. 2010.

[13] Musa Yusup Lada,Ismadi Bugis, Md Hairul Nizam Talib "Simulation Shunt Active Power Filter using Matlab/Simulink", The 4th International Power Engineering and Optimization Conf. (PEOCO2010), Shah Alam, Selangor, MALAYSIA: 23-24 June 2010

[14] HandBook of "Electrical Power Systems Quality "by R.C. Dugan, Tata McGraw Hill Publication, Delhi Second Edition.

FIRING ANGLE CONTROL CONVERTERS (AC-DC) USING MATLAB/SIMULINK

[1]Ajay Raj Singh Pawar, [2]Durgesh Mehra,

Electrical & Electronics Engineering Department
IES,IPS Academy
[1]aj786avril@gmail.com
[2]durgeshmehra2010@gmail.com

ABSTRACT-This paper presents the modeling of a power electronic AC-DC converters using MATLAB/SIMULINK software. The power electronic AC-DC conversion system consisting of switches (SCR, IGBT and MOSFET) and ac supply. Several methods for dc voltage control of single-phase pulse width modulation ac/dc voltage-source converters are known. A simple PWM switching method is used to control output voltage for different firing angle. The model of the power electronic converters has been constructed in SIMULINK. The performance of the system has been studied. It has been demonstrated that SIMULINK can effectively used for power electronic system studies.

***KEYWORDS*- AC-DC Converters, MATLAB, PWM**

I. INTRODUCTION

Controlled rectifier circuits had been in use long before power semiconductors were invented, the control element being the mercury arc rectifier, although these have now almost entirely been replaced by the semiconductor switch, primarily the thyristor.

All these circuits can usually be divided as follows:
(i) Bi-directional or unidirectional converters.
(ii) Each of the above converters can then be either push-pull or bridge in configuration, the push-pull arrangement requiring an input transformer.

Half wave converters are capable of inversion in addition to rectification, and this is often a desirable feature. Where it is not required unidirectional converters can be used, the resulting circuit being cheaper and having a smaller d.c. voltage ripple and input 'wattless' current content.

Full wave circuits have the advantage that there is only one conducting device in series with the load, which was much more of an important consideration when mercury arc rectifiers were used, since they could have arc drops of 30V or more. However, modern thyristors lose only a volt or two, so that this is important only when working from abnormally low supply voltages. Generally, bridge circuits have better transformer utilisation and are more frequently used.

The paper describes the principles of unidirectional and bi-directional converters, followed by the effects of discontinuous load current and source reactance on their operation. The performance factors used in the analysis of these converter circuits are then obtained, and the chapter concludes with a description of gate-control and voltage multiplication circuits, which is a special application of rectification.

The advent of fast high-power semiconductor switching devices has made it possible to consider pulse width modulation (PWM) techniques for ac/dc converters in electric power systems. Conventional diode bridge and phase-controlled thyristor converters are incapable of producing input currents with low harmonic content at unity power factor. PWM converters of the voltage-source type are capable of providing near-sinusoidal currents at unity power factor. One promising version is the single-phase PWM ac/dc voltage-source converter . Several control strategies have been devised for single-phase PWM ac/dc voltage source converters.

Pulse width prediction methods based on approximate discrete-time models of the converter have been proposed by Ohnuki et al. (1996) and Nishida et al. (1997). In these methods, the predicted pulse width is a function of the instantaneous value of the input current and the ac-side inductance (L). This makes input current sensing essential for the prediction of a pulse width. However, we have recently introduced a new control method in the continuous-time domain which eliminates the need for input current sensing .In this control method, an error voltage is produced from the comparison of the output voltage with a reference voltage. This error voltage is then utilized by a PI controller to generate a command signal for the input current amplitude.

The PWM converter operated with these control methods is a nonlinear dynamical system. Such a system is stable in the vicinity of the operating point but may not be stable when the system undergoes a large perturbation. Therefore, the PWM converter with the control methods proposed so far cannot guarantee system stability against large-signal disturbances (large load variations). Thus, it is most desirable if a control method which would make the control system globally stable could be developed for the single-phase PWM converter.

II. MATLAB/SIMULINK

This paper is a used matlab software for controllling output voltage of converters. The MATLAB (an abbreviation of MATrix LABoratory) basics, registered trademark of computer software, version 7.0 or later developed by the Math Works Inc. The software is widely used in many of science and engineering fields. MATLAB is an interactive program for numerical computation and data visualization. MATLAB is supported on Unix, Macintosh, and Windows environments. For more information on MATLAB, contact The MathWorks.Com. A Windows version of MATLAB is assumed here. The syntax is very similar for the DOS version. MATLAB integrates mathematical computing, visualization, and a powerful language to provide a flexible environment for technical computing. The open architecture makes it easy to use MATLAB and its companion products to explore data, create algorithms, and create custom tools that provide early insights and competitive advantages. Known for its highly optimized matrix and vector calculations, MATLAB offers an intuitive language for expressing problems and their solutions both mathematically and visually.

Typical uses include:

• Numeric computation and algorithm development

• Symbolic computation (with the built-in Symbolic Math functions)

• Modeling, simulation, and prototyping

• Data analysis and signal processing

• Engineering graphics and scientific visualization

In this paper, we will introduce the MATLAB environment. We will learn how to create, edit, save, run, and debug m-files (ASCII files with series of MATLAB statements). We will see how to create arrays (matrices and vectors), and explore the built-in MATLAB linear algebra functions for matrix and vector multiplication, dot and cross products, transpose, determinants, and inverses, and for the solution of linear equations. MATLAB is based on the language C, but is generally much easier to use. We will also see how to program logic constructs and loops in MATLAB, how to use subprograms and functions, how to use comments (%) for explaining the programs and tabs for easy readability, and how to print and plot graphics both two and three dimensional. MATLAB's functions for symbolic mathematics are presented. Use of these functions to perform symbolic operations, to develop closed form expressions for solutions to algebraic equations, ordinary differential equations, and system of equations was presented. Symbolic mathematics can also be used to determine analytical expressions for the derivative and integral of an expression.

III. SINGLE-PHASE HALF-WAVE RECTIFIER

As shown in Fig.1, the single-phase half-wave rectifier uses a single thyristor to control the load voltage. The thyristor will conduct, ON state, when the voltage Vs is positive and a firing current pulse i_G is applied to the gate terminal. Delaying the firing pulse by an angle α does the control of the load voltage. The firing angle α is measured from the position where a diode would naturally conduct. In Fig. 1. the angle α is measured from the zero crossing point of the supply voltage Vs . The load is resistive and therefore current i_d has the same waveform as the load voltage. The thyristor goes to the non conducting condition, OFF state, when the load voltage and, consequently, the current try to reach a negative value. The load average voltage is given by:

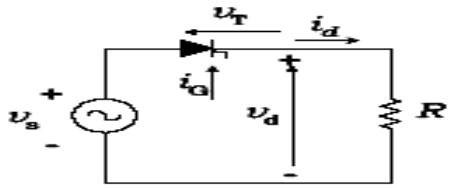

Fig.1 Half wave rectifier

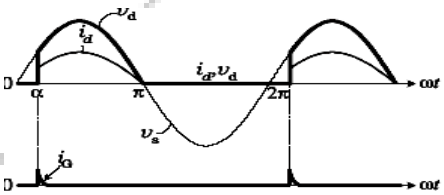

Fig.2. output wave form

$$V_{d\alpha} = \frac{1}{2\pi}\int_{\alpha}^{\pi} V_{\max}\sin\omega t d(\omega t) = \frac{V_{\max}}{2\pi}(1+\cos\alpha) \quad \text{--- (1)}$$

where Vmax is the supply peak voltage. Hence, it can be seen from Eq. (1) that changing the firing angle α controls both the load average voltage and the power flow.. When the thyristor is turned ON, the voltage across the inductance is

$$v_L = v_S - v_R = L\frac{di_d}{dt} \quad \text{--- (2)}$$

The voltage in the resistance R is $V_R = R * i_d$. While $V_S - V_R > 0$, Eq. (2) shows that the load current increases its value. On the other hand, i_d decreases its value when

$V_S - V_R < 0$. The load current is given by

$$i_d(\omega t) = \frac{1}{\omega L}\int_{\alpha}^{\omega t} v_L \, d\theta \qquad \text{---- (3)}$$

A. SCR based Half-Wave Rectifier circuit in MATLAB

As shown in Fig.3, the single-phase half-wave rectifier uses a single thyristor to control the load voltage in MATLAB. The thyristor will conduct, ON state, when the voltage V_s is positive and a firing pulse i_G is applied to the gate terminal. Delaying the firing pulse by an angle α does the control of the load voltage. The firing pulse by an angle α are vary from 0̊,30̊,45̊ and 90̊ does the control of the load voltage.

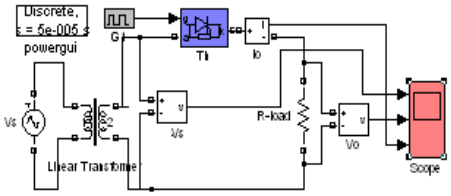

Fig.3 SCR based Half wave rectifier circuit in MATLAB

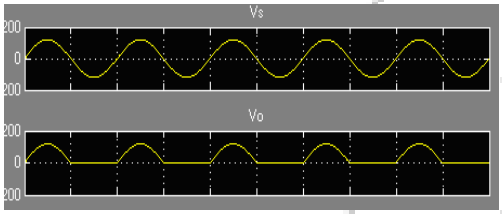

Fig.4. output voltage waveform when α=0̊

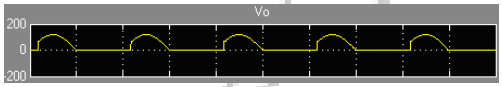

Fig.5. output voltage waveform when α=30̊

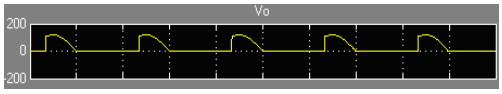

Fig.6. output voltage waveform when α=45̊

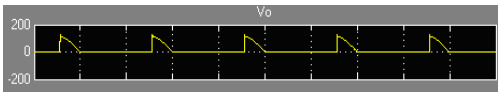

Fig.7. output voltage waveform when α=90̊

Computer simulation and experimental verification In order to demonstrate the feasibility of the proposed control method, the closed-loop system has been tested by both simulations and experiments. In all the simulation and experimental results given, unless otherwise stated, V o =110 V,Operation of the proposed control strategy was experimentally varied on a hardware simulation circuit. Analogue multiplexers are digitally controlled switches and are used to implement the electronic switches of the single-phase PWM converter. In the simulation circuit output voltages are controllrd using different delay angle . Fig.4. shows the delay angle is α=0̊,in this fig show the out put average voltage voltage is 49.51V. Fig.5. shows the delay angle is α=30̊,in this fig show the out put average voltage voltage is 46.20V . Fig.6. shows the delay angle is α=45̊,in this fig show the out put average voltage voltage is 42.26V. Fig.7. shows the delay angle is α=90̊,in this fig show the out put average voltage voltage is 24.75V. we can say in above simulation results the output voltage is control,when control the firing angle of the converters.

IV. SCR BASED MID POINT FULL-WAVE RECTIFIER CIRCUIT IN MATLAB

There are several ways in which it may be extended to full-wave operation, generally these systems falling into two groups:

(i) Mid-point (m-2) converters, which require a tapped transformer input.

(ii) Bridge converters, where an input transformer may be used but is not an essential requirement for correct system operation.

Fig. 8. shows the SCR based mid point converter circuit in MATLAB and Fig.9, gives its output voltage wave forms. It is assumed here that the load current is maintained at a constant d.c. value through the operating cycle. T1 is a centre-tapped transformer whose turns ratio may be adjusted to give any primary to secondary voltage change. When terminal A of the a.c. supply goes positive T1 is forward biased and when the supply polarity reverses T2 becomes forward biased. When either thyristor conducts, the load voltage equals the instantaneous a.c. voltage across half the transformer secondary winding.. The supply current is assumed square (ripple-free load current) and is composed of a fundamental and various higher harmonics.

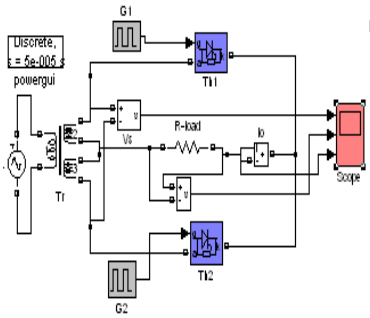

Fig.8 SCR based mid point full wave reactifier in MATLAB

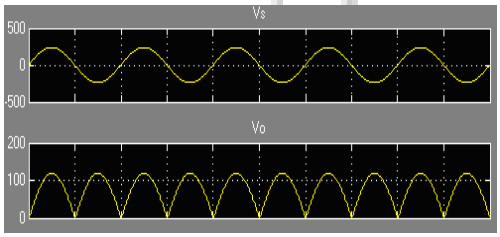

Fig.9. output voltage waveform when α=0°

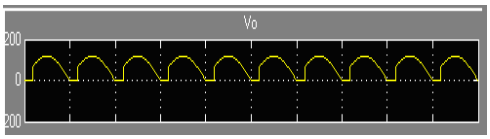

Fig.10. output voltage waveform when α=30°

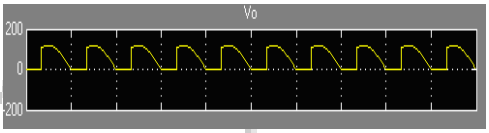

Fig.11. output voltage waveform when α=45°

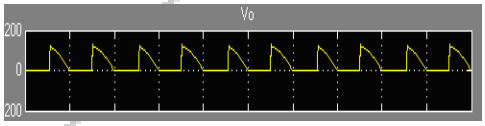

Fig.12. output voltage waveform when α=90°

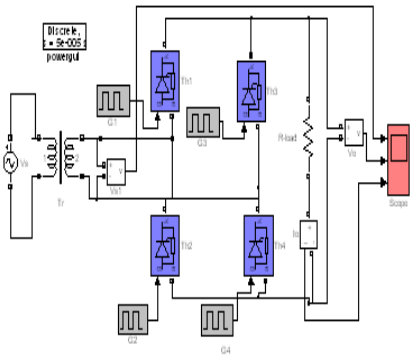

Fig.13 shows the power circuit of the fully controlled single-phase PWM converter in MATLAB

In this circuit taken source voltage is 110V,after simulation output results given, unless otherwise stated, V o =110 V,Operation of the proposed control strategy was experimentally veried on a hardware simulation circuit.in this converter PWM control techniques are used for controlling the output voltage. In the simulation circuit output voltages are controlled using different delay angle . Fig.9. shows the delay angle is α=0°,in this fig show the out put average voltage voltage is 99.03V. Fig.10. shows the delay

angle is α=30°,in this fig show the out put average voltage voltage is 92.40V . Fig.11. shows the delay angle is α=45°,in this fig show the out put average voltage voltage is 84.53V. Fig.12. shows the delay angle is α=90°,in this fig show the out put average voltage voltage is 49.51V. we can say in above simulation results the output voltage is control,when control the firing angle of the converters.

V. SCR BASED FULLY CONTROLLED BRIDGE CONVERTER CIRCUIT IN MATLAB

Fig. 13 shows the power circuit of the fully controlled single-phase PWM converter in MATLAB, which uses four SCR & ac supply. Using a bipolar PWM switching strategy, this converter may have two conduction states:

i) Transistors T1 and T4 in the ON state and T2 and T3 in the OFF state; or

ii) Transistors T2 and T3 in the ON state and T1 and T4 in the OFF state.

In this topology, the output voltage Vo must be higher than the peak value of the ac source voltage Vs in order to ensure proper control of the input current.

The input voltage value Vs= 110v, switching frequency is 1KHz. After simulation the output voltage and current wave form with resistive load is shown in fig. 14. In this wave harmonics are presence.

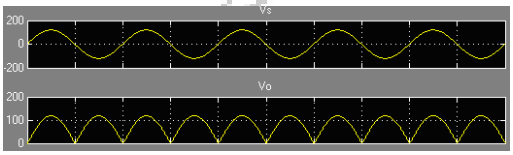

Fig.14. output voltage waveform when α=0°

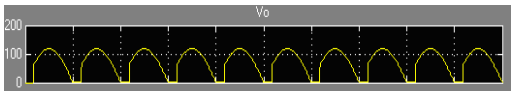

Fig.15. output voltage waveform when α=30°

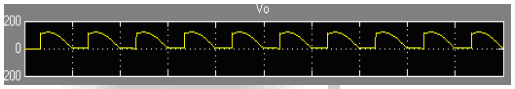

Fig.16. output voltage waveform when α=45°

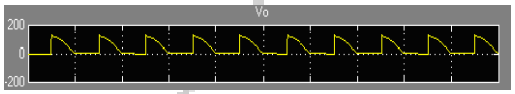

Fig.17 output voltage waveform when α=90°

In this circuit taken source voltage is 110V,after simulation output results given, unless otherwise stated, V o =110 V, Operation of the proposed control strategy was experimentally varied on a hardware simulation circuit.In this converter PWM control techniques are used for controlling the output voltage. In the simulation circuit output voltages are controlled using different delay angle . Fig.9. shows the delay angle is α=0°,in this fig show the out put average voltage voltage is 99.03V. Fig.10. shows the delay angle is α=30°,in this fig show the out put average voltage voltage is 92.40V . Fig.11. shows the delay angle is α=45°,in this fig show the out put average voltage voltage is 84.53V. Fig.12. shows the delay angle is α=90°,in this fig show the out put average voltage voltage is 49.51V. we can say in above simulation results the output voltage is control, when control the firing angle of the converters.

CONCLUSION

This paper presents the modeling of a power electronic AC-DC converters using MATLAB/SIMULINK software. Several methods for dc voltage control of single-phase pulse width modulation ac/dc voltage-source converters are

known. A simple PWM switching method is used to control output voltage for different firing angle. This paper shows the control of output voltage is east to using firing angle control method for any converters.this method is used for speed control of dc motor drives. The efficiency of this method is high and maintance is cheap.

REFERENCES

[1]. S. Raghuwanshi "Modelling & Simulation of a DC-DC Converters using MATLAB & PSIM" National Conference on ECOMM-11 in SDBCT, Indore.

[2]. S. Raghuwanshi "Performance & Comparision Of Igbt And Mosfet Switches Based Dc-Dc Converters Using Matlab" National Conference on NCRTEEE-11 in MITM, Indore.

[3]. S.Raghuwanshi, A.Singh Indian Journal of Technical Education & ISTE Education "Performance & Comparison of Singe Phase Controlled Converters using MATLAB & PSIM".April 2012, p.g. 107-111

[4]. A. Leon-Garcia, Probability and Random Process for Electrical Engineering, Addison-Wesley Publishing Company, 1989.

[5]. B. K. Bose," Power electronics - an emerging technology," IEEE Trans. on Ind.Electron., vol. 36, no. 3, pp. 403-412, 989.

[6]. D. Maksimovic, A. M. Stankovic, V. J. Thottuvelil, and G. C.Verghese, "Modeling and simulation of power electronic converters," Proc. IEEE, vol. 89, no. 6, pp. 898– 912, Jun. 2001.

[7]. E. P.Wiechmann, P. D. Ziogas, and V. R. Stefanovic, "Generalized functional model for three phase PWM inverter/rectifier converters," in Conf. Rrec. IEEE-IAS Annu Meeting, 1985, pp. 984–993.

[8]. Huing-H design of switching converters via MATLAB /SIMULINK" IEEE Transactions on uei Su; Jiann-Jong feedback controller Education, Vol. 45, Issue: 4, Nov. 2002, pp.307 - 315.

[9]. J. Arrillaga, D. A. Bradley. and P. S. Bodger. Power Svstem Harmonics, John Wiley & Sons, 1985.

[10]. M. H. Rashid, SPICE for Circuits and Electronics Using PSpice. Englewood Cliffs, NJ: Prentice-Hall, 1990.

[11]. P. Wood, Theory of Switching Power Converter. New York: Van Nostrand- Reinhold, 1981.

Home Automation Using GSM

[1]Amber Tuteja, [2]Divya Gour,

Electrical & Electronics Engineering Department
IES,IPS Academy
[1]ambertuteja04@gmail.com
[2]gour.divya278@gmail.com

***Abstract*— This project aims to design and implement a cost effective but yet flexible, adaptable, and secure Home automation system. Report presents design and prototype implementation of a basic home automation system based on SMS technology. The proposed system consists of two main components; the GSM modem, which is the communication interface between the home automation system and the user. GSM modem uses SMS technology to exchange data, and signaling between users and home automation system. The second module is the micro controller, which is the core of the home automation system, and acts as the bridge between the GSM network (the user) and sensors and actuators of home automation system. Sensors and actuators are directly connected to hardware micro controller through appropriate interface. System supports a wide range of home automation devices; power management components, security, multimedia applications, and telecommunication devices. System security based on user authentication of each SMS being exchange, as each SMS contains user name and password (beside comments). User can easily configure home automation system setting through RS232 protocol using a user friendly interface.**

Keywords—GSM; ATmega328; style; styling; insert (key words)

Introduction

The home automation refers to domestic Environment that improves the quality of the resident's life by facilitating a flexible, comfortable, healthy, and safe environment. Internet based home automation systems has become the most popular home automation system in international markets. The remote controlling and monitoring of a house using internet requires a computer, which is large in size and heavy to carry around. The most available home automation systems use different wireless communication standard to exchange data and signaling between their components, like Bluetooth, Zig bee, Wi-Fi, and finally the Global System for Mobile Communication (GSM). Wireless based home automation systems decrease installation cost and effort, and enhance system flexibility and scalability. The main features of the GSM based control system is that it uses mobile network and it is battery powered, which makes home automation system safer from internet hacks and power failures. Also, GSM based home automation system makes it suitable for any remote control and monitoring mobile system like automobiles. GSM module can be interfaced with the car ignition system where the owner carries the mobile phone rather than to carry around the key. Recent advances in the GSM based home automation system have been made in billing system for electricity, gas and water using the GSM network and SMS services for

metering service rather than assigning person to visit each house and read meters manually. However, the GSM based home automation has some drawbacks like; the system running cost, as the user need to pay for every single SMS of network connectivity. Generally home automation is facing four significant challenges. These are high cost of ownership, inflexibility, poor manageability, and difficulty achieving security. To overcome these obstacles many researches carried out and focus on eliminating the need for home structural changes during home automation system deployment, and provide end users with a simple, secure, and easily configurable home automation system. Authors hope that the proposed research contributes to overcome these barriers facing home automation systems and will enable a home technology ecosystem that allows people to easily adopt the subset of home automation technology that appeals to their household.

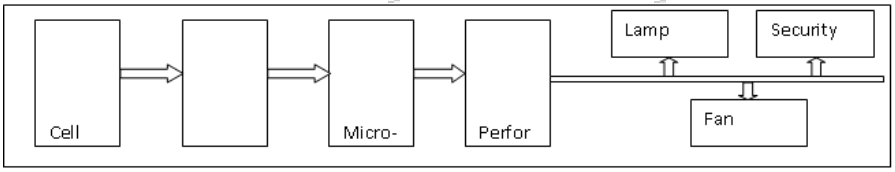

Fig. 1. Block diagram of the system

System Model

Fig. 1 shown is a simple block diagram of the project. It is a simple illustration of how we will try to implement our project and the various parts involved in it. From the above representation, a Mobile station is used as a transmitting section from which the subscriber sends text messages that contain commands and instructions to the second mobile station which is based on a specific area where our control system is located. The received SMS message is stored in the SIM memory of the GSM module and then extracted by the microcontroller and processed accordingly to carry out specific operations. A relay driver can be used to drive the relay circuits which switches the different appliances connected to the interface.

The idea can be summarized as:

- The remote user sends text messages including commands to the receiver.
- GSM receiver receives messages sent from the user cell phone.
- GSM receiver decodes the sent message and sends the commands to the microcontroller.
- Microcontroller issues commands to the appliances and the devices connected will switch ON/OFF.

System Description

GSM (SIM 300)

A GSM (Global System for Mobile communication) module is a specialized type of module which accepts a SIM (Subscriber Identity Module) card, and operates over a subscription to a mobile operator. When a GSM module is connected to a microcontroller (ATmega328), it allows the microcontroller to use the GSM module to communicate over the mobile network. A GSM module exposes an interface that allows applications to send and receive messages over the module interface. To perform these tasks, a GSM module must support an “extended AT command set” for sending/receiving SMS messages.

The AT commands are sent by the microcontroller to the module. The module sends back an Information Response i.e. the information requested by the action initiated by the AT command. This is followed by a Result Code. The result code tells about the successful execution of that command. Text message may be sent through the module by interfacing only three signals of the serial interface of module with microcontroller i.e., TXD, RXD and GND. In this scheme RTS and CTS signals of serial port interface of GSM Modem are connected with each other.

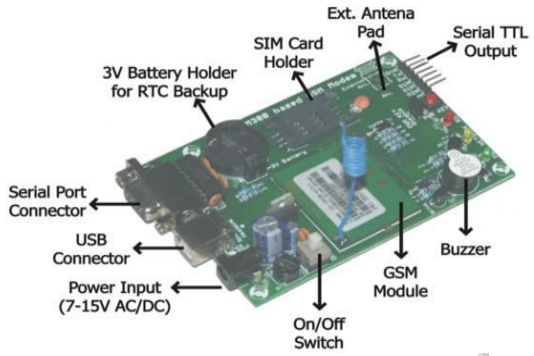

Fig. 1.GSM module

ATmega328

ATmega328 is a microcontroller, can also be used in arduino board which an open-source physical is computing platform based on Atmel microcontrollers, and a development environment for writing software for the board. It can be used to develop interactive process, taking inputs from the combination of switches or sensors, and controlling other physical outputs. A typical ATmega328 has 14 digital input/output pins (of which 6 can be used as PWM outputs), six analog inputs with one 16 MHz crystal oscillator. For Communication purposes, it has a number of facilities for communicating with a computer, or with other microcontrollers. The ATmega328 provides UART TTL serial communication which is available on digital pins 0(RX) and 1(TX).

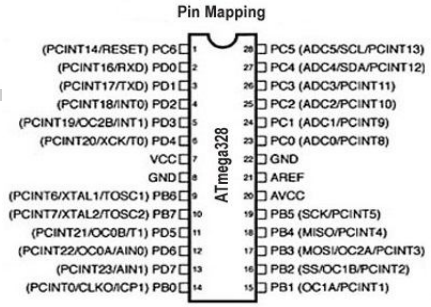

Fig.3

Relays

Relay is an electromechanical switch which is operated by a coil inside it. When we supply a voltage to the coil it develops an electromagnetic field around it. The switch toggles based on potential difference created across the coil. As shown in fig.4. There are 3 terminals in relay as Common (COM), Normally Open (NO), Normally Close (NC). Initially Common terminal is connected to Normally Closed. Whenever the potential difference is created across coil, then the switch toggles to Normally Open terminal.

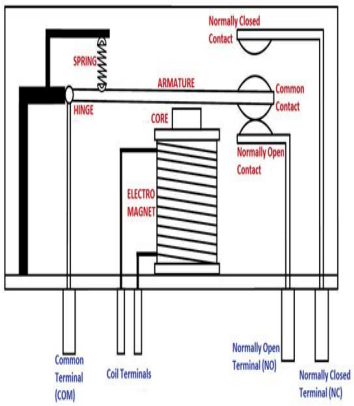

Fig.4 Relay

As shown in fig. , one end of coil is connected to 5V and other terminal to digital pin of ATmega328 microcontroller. When we supply 0V to digital pin of microcontroller then the potential difference is V= 5V- . So the ON/OFF of Relay depends on input of digital pin.

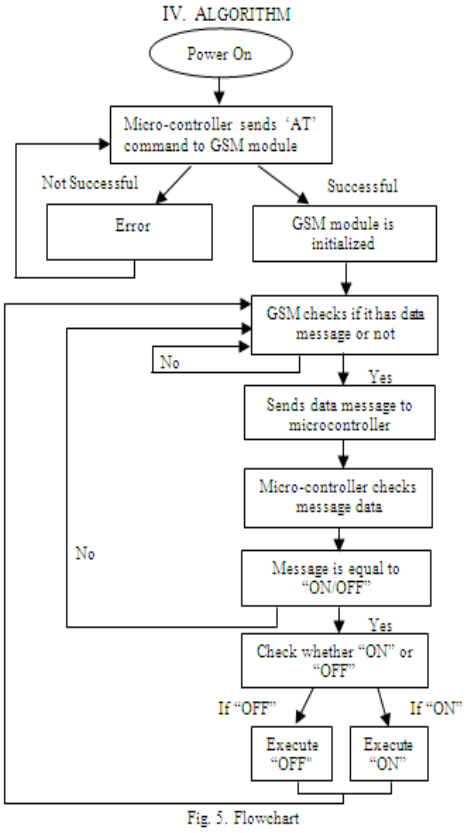

Fig. 5. Flowchart

- Switch on the microcontroller.
- Now, the microcontroller sends 'AT' command to GSM module for establishing serial communication.
- If command is executed successfully, GSM module is initialized and communication between GSM module and the microcontroller is established successfully.
- Else an error message is displayed.

0V=5V. So the relay will be ON. When we supply 5V to digital pin then the potential difference is V= 5V-5V=0V.So the relay will be OFF

- Now, GSM module continuously checks if it has any incoming message data.
- If yes, then it sends the latest message data to the microcontroller.
- If no, it goes to step 5.
- Now, the microcontroller checks that if message data is equal to "on" or "off".
- If no, then it goes back to step 5.
- If yes, ten it checks whether it is "on" or "off"
- If "on", then it executes the "on" statement and if "off" it executes the "off" statement.

system execution

Fig.6 Message displaying the successful initialization of the GSM module by the microcontroller

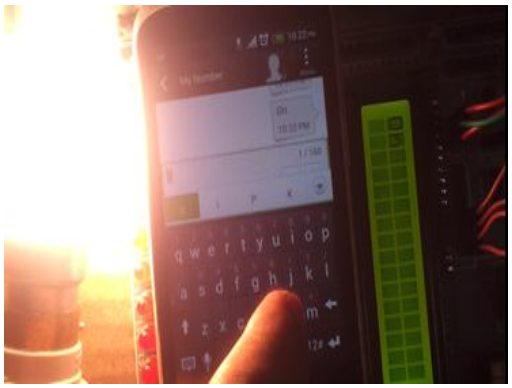

The 12V bulb was successfully switched on by sending a SMS “ON” to the GSM module

Fig.8 Similarly the bulb was switched off sending a SMS “OFF” on the GSM.

Conclusion

This report proposes a low cost, secure, ubiquitously accessible, remotely controlled home automation solution. The approach discussed in the paper is novel and has achieved the target to control home appliances remotely using SMS technology, to meet user expectations, and needs. Deployment of SMS technology in home automation increases system security and is cost-effective as compared to the previously existing systems. Hence author concludes that the required goals and objectives of home automation system has been achieved. The system design and architecture were discussed, and prototype presents the basic level of home appliance control and remote monitoring has been implemented. Finally, the proposed system has a better functionality and security features than the commercially available home automation systems.

References

[1] R. Chutia, D. Sonowal and S. Sharma,” Remote Household Appliance Control System Using GSM” *International Conference on Advanced Computing and Communication Technologies*, 2011.

[2] Faisal Baig, Saira Beg and Muhammad Fahad Khan,” Zigbee Based Home Appliances Controlling Through Spoken Commands Using Handheld Devices” Federal Urdu University of Arts, Science and Technology, Islamabad, Pakistan, *International Journal of Smart Home* Vol. 7, No. 1, January, 2013.

[3] A. R. Al-Ali and M. Al-Rousan, "Java-based home automation system", *IEEE Transactions on Consumer Electronics*, vol. 50, no. 2, pp. 498-504, 2004.

[4] Delgado, A. R., Picking, R., & Grout, V. (2006) Remote-controlled home automation systems with different network technologies. *Proceedings of the 6th International Network Conference (INC 2006)*, University of Plymouth, 11-14 July 2006, pp. 357-366.

[5] Alkar, A. Z., & Buhur, U. (2005). An Internet Based Wireless Home Automation System for Multifunctional Devices. *IEEE Consumer Electronics*, *51*(4), 1169-1174

[6] Rifat Shahriyar, Enamul Hoque, S.M. Sohan, Iftekhar Naim; Remote Controlling of Home Appliances using Mobile Telephony, International Journal of Smart Home,Vol. 2, No. 3, July, 2008

[7] Neng-Shiang Liang; Li-Chen Fu; Chao-Lin Wu; “An integrated, flexible, and Internet-based control architecture for home automation System in the Internet era,” Proceedings ICRA 2002. IEEE International Conference on Robotics and Automation, Vol. 2, pp. 1101 –1106, 2002

[8] Khusvinder Gill, Shuang-Hua Yang, Fang Yao, and Xin Lu,”A ZigBee Based Home Automation System”, IEEE Transactions on Consumer

[9] T. Saito, I. Tomoda, Y. Takabatake, J. Ami and K. Teramoto, "Home Gateway Architecture And Its Implementation", *IEEE International Conference on Consumer Electronics*, pp. 194-195, 2000.

[10] Carelin Felix, Jacob Raglend,” Home Automation Using GSM, *International Conference on Signal Processing, Communication, Computing and Networking Technologies*, 2011.

POWER SYSTEM FREQUENCY CONTROL OF MULTI-AREA SYSTEMS USING PID

[1]Nitin Mondloi, [2] Vineet Chandra , [3]Vishal Upadhyay

Electrical & Electronics Engineering Department
IES,IPS Academy
[1]nitin.mandloi@yahoo.com, [2] vchandra1993@rediffmail.com, [3]vishal.9310@gmail.com

ABSTRACT

Load frequency control deals with the control of frequency of the system as the load (demand) varies. Since the frequency of the system does affect the whole operation of the system, especially for interconnected power systems of multi-area, and as the main objective of control in power systems is to generate and deliver power as economically and reliably as possible, then it is important to consider the control of the frequency of the system. In the last two decades, many studies have focused on damping control and voltage stability and the related issues, but there has been much less work on the power system frequency control analysis and synthesis. A fuzzy logic PI controller is designed for load frequency control of four area interconnected power systems. The system dynamic performances are observed via using different controllers.

This paper describe load frequency control (LFC) which is one of the most important issues in interconnected power systems is effectuated by using PID controller. Multi area power systems are more complex and important than one area power system. In this paper, LFC problem defined firstly, and then mathematical models of power systems are explained. Finally PID controllers are described shortly and power system is modeled by using MATLAB-Simulink platform.

Keywords: Load Frequency Control (LFC), Proportional Integral (PI), Proportional Derivative Integral (PID).

I INTRODUCTION

1.1 OVERVIEW OF LOAD FREQUENCY CONTROL

In recent years, power systems have more complicated and nonlinear configurations. Many industrial establishments are affected by operating point variations [1]. Electricity sector and end user are concerned about power quality reliability, efficiency and energy future. There are many reasons about increasing concerns on power quality. The microprocessor based equipments and power electronic devices are more sensitive to power quality. On the other hand, an electric network consists of many interconnected subsystems. If a fault occurs in a subsystem, disturbances and interruptions adversely affecting power quality take place in the power system. Any disharmonies between energy generation and demand cause frequency deviations. Thus, significant frequency deviations lead to system blackouts [2]. Power system loads are usually variable so that controller

system must be designed to provide power system quality As the name (Load Frequency Control) indicates, this topic deals with the control of frequency of the system as the load (demand) varies. Since the frequency of the system does affect the whole operation of the system, especially for interconnected power systems of multi-area, and as the main objective of control in power systems is to generate and deliver power as economically and reliably as possible, then it is important to consider the control of the frequency of the system.

So far there are many studies about load frequency control of interconnected power systems. The aim is a design of feedback controller to realize desired frequency in multi-area power system.

1.2 OVERVIEW OF CONTROLLERS

An automatic control scheme compares a controlled condition value with desired value and automatically corrects any deviation. The controllers are of following types:

i) Proportional controller
ii) Proportional derivative controller
iii) Proportional integral controller
iv) Proportional integral derivative controller

In this report, load frequency control (LFC) is effectuated by using PID controller which is used in many sectors, and also investigated its performance. It is interesting to note that more than half of the industrial controllers in used today are PID controllers or modified PID controllers are used today as they are adjusted on-site. The usefulness of PID controls lies in their general applicability to most control systems. In particular, when the mathematical model of the plant is not known then analytical design methods cannot be used, PID controls prove their necessity.

This type of controller produces an output signal which consists of three terms, one proportional to the actuating signal, second proportional to in its integral and the third proportional to the derivative (rate of change) of the actuating signal. In PID controller the actuating signal consists of proportional error signal added with derivative and integral of the error signal. Hence the actuating signal for a PID controller is given by

$$e_a(t) = e(t) + K_D \frac{de(t)}{dt} + K_I \int e(t)dt \text{ ----------(1.1)}$$

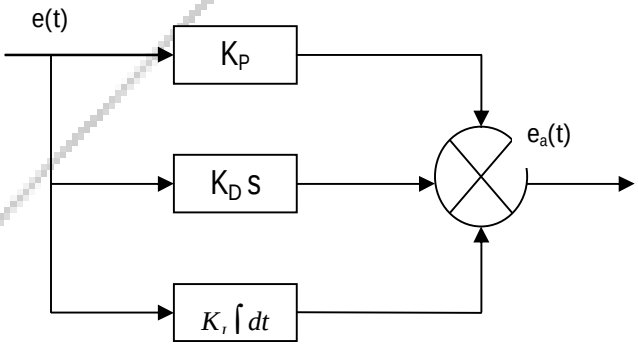

Figure1.1 Simplest Block diagram of PID controller

II Modeling of Single area & Multi-area Power System

2.1 SINGLE AREA SYSTEM MODELING

In Single area system, generation and load demand of one domain is dealt. Any load change within the area has to be met by generators in that area alone through suitable governor action. Thus we can maintain the constant frequency operation irrespective of load change [3].

2.1.1 Generator Model

A single rotating machine is assumed to have a steady speed of ω and phase angle δ_0. Due to various electrical or mechanical disturbances, the machine will be subjected to differences in mechanical and electrical torque, causing it to accelerate or decelerate. We are mainly interested in the deviations of speed, Δω and deviations in phase angle Δδ, from nominal. This can be expressed in Laplace transform operator notation as $\Delta P_{mech} - \Delta P_{elec} = M\ s\ \Delta\omega$-------(2.1) Equation (2.1) can be represented as shown in figure

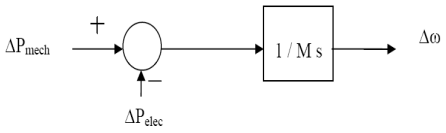

Figure 2.1 Relationship between Mechanical and Electrical power and Speed Change

2.1.2 Load Model

The load on a power system comprises of a variety of electrical devices. Some of them are purely resistive. Some are motor loads with variable power frequency characteristics, and others exhibit quite different characteristics. Since motor loads are a dominant part of the electrical load, there is a need to model the effect of a change in frequency on the net load drawn by the system. The relationship between the changes in load due to the change in frequency is given by

$$\Delta P_{L(freq)} = D\ \Delta\omega \text{ (or)}$$

$$D = \Delta P_{L\,(freq)} / \Delta\omega \quad \text{-------(2.2)}$$

The net change in P_{elec} in figure (2.1) is

$$\Delta P_{elec} = \Delta P_L + D\ \Delta\omega$$

Where ΔP_L=No frequency Sensitive load Change

D Δω= frequency sensitive load change

Incorporating this in the figure2.2,

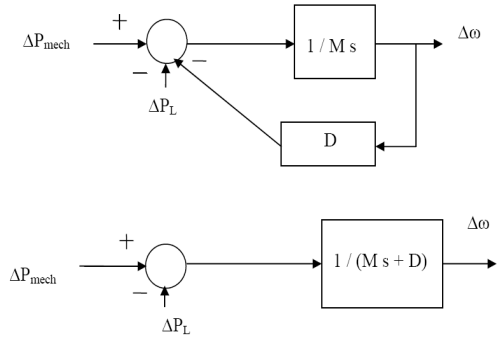

Figure 2.2.Block diagram of rotating mass an load as seen by prime- mover output

2.1.3 Prime-Mover Model

The prime mover driving a generator unit may be a steam turbine or a hydro turbine. The models for the prime mover must take account of the steam supply and boiler control system characteristics in the case of a steam turbine, or the penstock characteristics for a hydro turbine. Here only the simplest prime-mover model, the non reheat turbine, is considered. The model for a non reheat turbine shown in figure 2.3, relates the position of the valve that controls emission of steam into the turbine to the power output of the turbine [4].

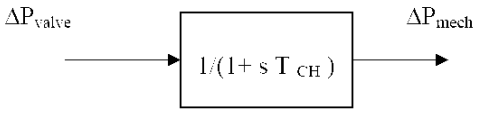

Figure 2.3 Prime-Mover Model

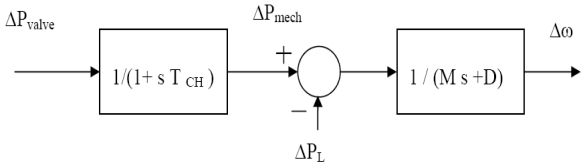

Figure 2.4 Prime mover – generator load model

2.1.4 Governor Model

Suppose a generating unit is operated with fixed mechanical power output from the turbine, the result of any load change would be a speed change sufficient to cause the frequency-sensitive load to exactly compensate for the load change. This condition would allow system frequency to drift far outside acceptable limits. This is overcome by adding mechanism that senses the machine speed, and adjusts the input valve to change the mechanical power output to compensate for load changes and to restore frequency to nominal value.

The earliest such mechanism used rotating "fly balls" to sense speed and to provide mechanical motion in response to speed changes. Modern governors use electronic means to sense speed changes and often use a combination of electronic, mechanic and hydraulic means to effect the required valve position changes.

The simplest governor, is synchronous governor, adjusts the input valve to a point that brings frequency back to nominal value. If we simply connect the output of the speed-sensing mechanism to the valve through a direct linkage, it would never bring the frequency to nominal.

To force the frequency error to zero, one must provide reset action. Reset action is accomplished by integrating the frequency (or speed) error, which is the difference between actual speed and desired or reference speed. Speed-governing mechanism with diagram shown in figure 2.5 and 2.6 The speed-measurement device's output, ω, is compared with a reference, ω_{ref}, to produce an error signal, $\Delta\omega$.

The error, $\Delta\omega$, is negated and then amplified by a gain K_G and integrated to produce a control signal, ΔP_{valve} , which cause main steam supply valve to (ΔP_{valve} position) when $\Delta\omega$ is negative. If, for example, the machine is running at reference speed and the electrical load increases, ω will fall below ω_{ref} and $\Delta\omega$ will be negative. The action of the gain and integrator will be to open the steam valve, causing the turbine to increase its mechanical output, thereby increasing the electrical output of the generator and increasing the speed ω. When ω exactly equals ω_{ref}, the steam valve the new position (further opened) to allow the turbine generator to meet the increased electrical load. The synchronous (constant speed) governor cannot be used if two or more generators are electrically connected to the same system since each generator would have to have precisely the same speed setting or they would fight each other, each trying to pull the system's speed (or frequency) to its own setting. To run two or more generating units in parallel, the speed governors are provided with a feedback signal that causes the speed error to go to zero at different values of generator output. The result of adding the feedback loop with gain R is a governor characteristic as shown in Figure 2.5. The value of R determines the slope of the characteristic. That is, R

determines the change on the unit's output for a given change in frequency.

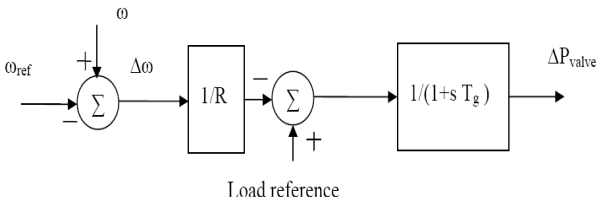

Figure2.5 Block diagram of governor with droop

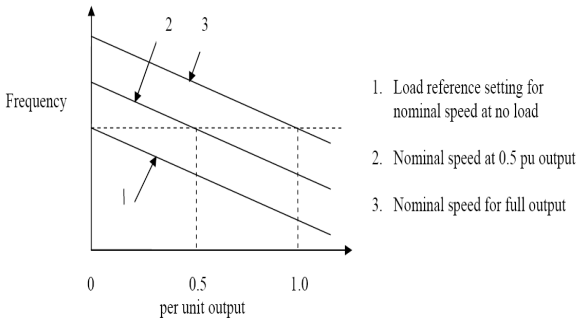

Figure2.6 Governor Characteristics

The basic control input to a generating unit as far as generation control is concerned is the load reference set point. By adjusting this set point on each unit a desired unit dispatch can be maintained while holding system frequency close to the desired nominal value. R is equal to pu change in frequency, divided by pu change in unit output. That is,

$$R = \frac{\Delta w}{\Delta P} \quad \text{p.u.}$$

The combined block diagram of single area system with, governor prime mover – rotatingmass/load model is shown in figure2.7.

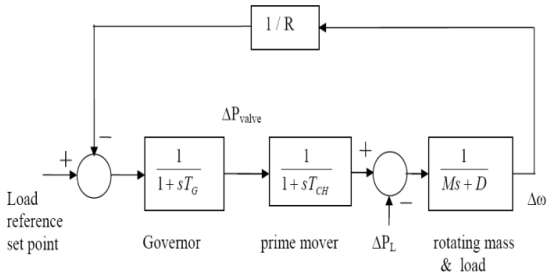

Figure2.7 Block diagram of single area system

Suppose that this generator experience a step increase in load,

$$\Delta P_L(S) = \frac{\Delta P_L}{s}$$

The transfer function relating the load change ΔP_L, to the frequency change $\Delta\omega$ is

$$\Delta w(s) = \Delta P_L(s)\left[\frac{\frac{-1}{Ms+D}}{1+\frac{1}{R}\left(\frac{1}{1+sT_G}\right)\left(\frac{1}{1+sT_{CH}}\right)\left(\frac{1}{Ms+D}\right)}\right] \text{----(2.3)}$$

The steady state value of $\Delta w(s)$ may be found by

$$\Delta w \text{ Steady state} = \frac{\lim}{s-0}[s\Delta w(s)]$$

$$\Delta w \text{ Steady state} = \frac{-\Delta P_L}{\frac{1}{R}+D} \text{----------(2.4)}$$

2.2 MULTI AREA SYSTEM MODELING

In multi area system load change in one area will affect the generation in all other interconnected areas. Tie line power flow should also be taken into account other than change in frequency. We will

discuss two area and three area systems in the following session.

2.2.1 Two Area System

In two-area system, two single area systems are interconnected via the tie line. Interconnection established increases the overall system reliability. Even if some generating units in one area fail, the generating units in the other area can compensate to meet the load demand.

2.2.2 Tie Line Model

The power flowing across a transmission line can be modeled using the DC load flow method as

$$P_{tieflow} = \frac{1}{X_{tie}}(\beta_1 - \beta_2) \text{----------(2.5)}$$

This tie flow is a steady-state quantity. For purposes of analysis here, we will perturb the above equation to obtain deviations from nominal flow as a function of deviations in phase angle from nominal.

$$P_{tieflow} + \Delta P_{tieflow} = \frac{1}{X_{tie}}[(\beta_1 + \Delta\beta_1) - (\beta_2 + \Delta\beta_2)]$$

$$= \frac{1}{X_{tie}}(\beta_1 - \beta_2) + \frac{1}{X_{tie}}(\Delta\beta_1 - \Delta\beta_2) \text{----------(2.6)}$$

Then

$$\Delta P_{tieflow} = \frac{1}{X_{tie}}(\Delta\beta_1 - \Delta\beta_2)$$

Where $\Delta\beta_1$ and $\Delta\beta_2$ are equivalent to $\Delta\delta_1$ and $\Delta\delta_2$. Then equation (2.6) can be expressed as, or can see from figure 2.8

$$\Delta P_{tieflow} = \frac{T}{s}(\Delta\omega_1 - \Delta\omega_2)$$

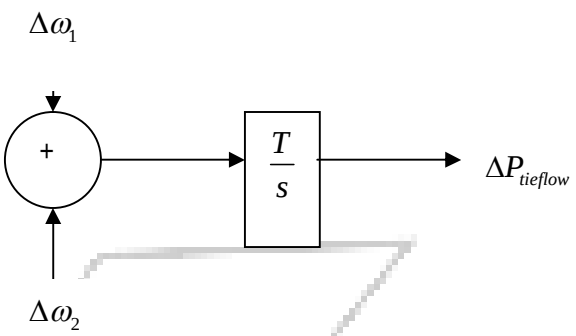

Figure 2.8 Block diagram of inter area tie power

Where T is "tie-line stiffness" coefficient and,

T = (2×3.14×50)× 1 / X_{tie} (for a 50-Hz system).

Suppose now that we have an interconnected power system broken into two areas each having one generator. The areas are connected by a single transmission line. The power flow over the transmission line will appear as a positive load to one area and an equal but negative load to the other, or vice versa, depending on the direction of flow. The direction of flow will be dictated by the relative phase angle between the areas, which is determined by the relative speed -deviations in the areas.

A block diagram representing this interconnection can be drawn as in figure 2.9.

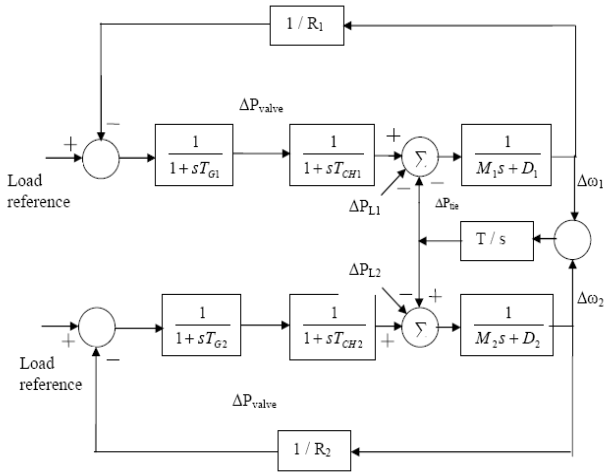

Figure2.9 Block diagram of interconnected areas

It should be noted that the tie power flow was defined as going from area 1 to area 2; therefore, the flow appears as a load to area 1 and a power source (negative load) to area 2. If one assumes that mechanical powers are constant, the rotating masses and tie line exhibit damped oscillatory characteristics are known as synchronizing oscillations.

It is quite important to analyze the steady-state frequency deviation, tie-flow deviation and generator outputs for an interconnected area after a load change occurs. Let there be a load change ΔP_L in area 1.

In the steady state after all synchronizing oscillations have damped out, the frequency will be constant and equal to the same value on both areas.

Then

$\Delta\omega 1 = \Delta\omega 2 = \Delta\omega$ and

$$\frac{d(\Delta\omega_1)}{dt} = \frac{d(\Delta\omega_2)}{dt} = 0 \text{ ----------(2.7)}$$

Finally we have,

$$\Delta\omega = \left[\frac{-\Delta P_{L1}}{\frac{1}{R_1}+\frac{1}{R_2}+D_1+D_2}\right] \text{ ---------- (2.8)}$$

$$\Delta P_{tie} = \left[\frac{-\Delta P_{L1}(\frac{1}{R_2}+D_2)}{\frac{1}{R_1}+\frac{1}{R_2}+D_1+D_2}\right] \text{ ---------- (2.9)}$$

The new tie flow is determined by the net change in load and generation in each area. We do not need to know the tie stiffness to determine this new tie flow, although the tie stiffness will determine how much difference in phase angle across the tie will result from the new tie flow.

III

PID CONTROLLER

3.1DIGITAL PID CONTROLLER IN MATLAB

3.1.1 Description

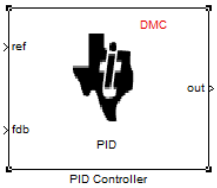

Figure3.1 Basic block diagram of PID Controller

This block implements a 32-bit digital PID controller with anti windup correction. The inputs are a reference input (ref) and a feedback input (fdb) and the output (out) is the saturated PID output. The following diagram shows a PID controller with anti windup.

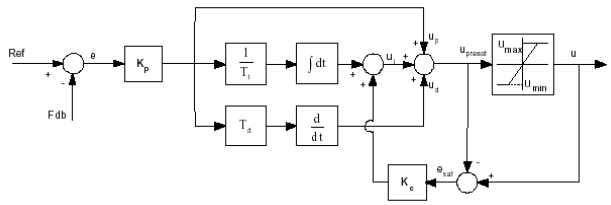

Figure3.2 Basic simulation of PID Controller

The differential equation describing the PID controller before saturation that is implemented in this block is

$$U_{presat}(t) = U_p(t) + U_i(t) + U_d(t)$$

Where U_{presat} is the PID output before saturation, U_p is the proportional term, U_i is the integral term with saturation correction, and U_d is the derivative term.

The proportional term is

$$U_p(t) = K_p e(t)$$

where K_p is the proportional gain of the PID controller and e(t) is the error between the reference and feedback inputs.

The integral term with saturation correction is

$$U_i(t) = \frac{K_p}{T_i}\int_0^t e(t)dt + K_c(U(t) - U_{presat}(t))$$

where K_c is the integral correction gain of the PID controller. The derivative term is

$$U_d(t) = K_p T_p \frac{de(t)}{dt}$$

Where T_d is the derivative time of the PID controller. In discrete terms, the derivative gain is defined as $K_d = T_d/T$, and the integral gain is defined as $K_i = T/T_i$, where T is the sampling period and T_i is the integral time of the PID controller. The above differential equations are transformed into a difference equation by backward approximation.

3.1.2 DIALOG BOX

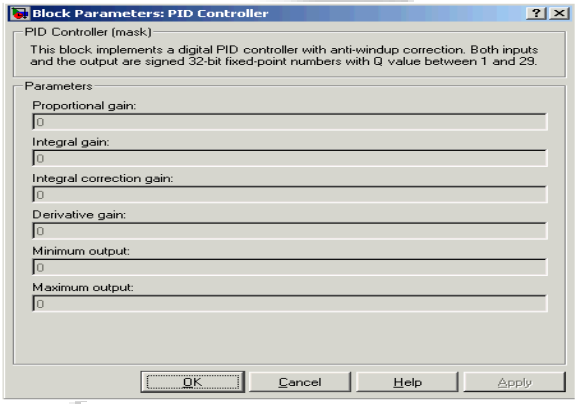

Proportional gain: Amount of proportional gain (Kp) to apply to the PID

Integral gain: Amount of gain (Ki) to apply to the integration equation

Integral correction gain: Amount of correction gain (Kc) to apply to the integration equation

Derivative gain: Amount of gain (Kd) to apply to the derivative equation.

Minimum output: Minimum allowable value of the PID output

Maximum output: Maximum allowable value of the PID output

3.2 DIFFERENT TYPES OF TUNING METHODS FOR PID CONTROLLER

Ziegler and NicholsMethod: The process of selecting the controller parameters to meet given performance specifications is known as controller tuning. Ziegler and Nichols suggested rules for

tuning PID controllers based on experimental step responses or based on the value of Kp that results in marginal stability when only proportional control action is used. Ziegler – Nichols rules, which are briefly presented in the following, are useful when mathematical models of plants are not known. Ziegler – Nichols tuning rules give an educated guess for the parameter values and provide a starting point for fine tuning, rather than giving the final settings for parameters in a single shot.

Ziegler and Nichols proposed rules for determining values of the proportional gain Kp, integral time Ti, and derivative time Td based on the transient response characteristics of a given plant. Such determination of the parameters of PID controllers or tuning of PID controllers can be made by engineers on site by experiments on the plant [5,6].

Genetic Algorithms: GAis a stochastic global search method that mimics the process of natural evolution. It is one of the methods used for optimization. John Holland formally introduced this method in the United States in the 1970 at the University of Michigan. The continuing performance of computational systems has made them attractive for some types of optimization. The GA starts with no knowledge of the correct solution and depends entirely on responses from its environment and evolution operators. The convergence criterion of a genetic algorithm is a user-specified condition [7].

Particle Swarm Optimization Method: PSO was formulated by Edward and Kennedy in 1995. The thought process behind the algorithm was inspired by the social behavior of animals, such as bird flocking or fish schooling. PSO is similar to the continuous GA in that it begins with a random population matrix. Unlike the GA, PSO has no evolution operators such as crossover and mutation. The PSO algorithm updates the velocity vector for each particle then adds that velocity to the particle position or values. Velocity updates are influenced by both the best global solution associated with the lowest cost ever found by a particle and the best local solution associated with the lowest cost in the present population. If the best local solution has a cost less than the cost of the current global solution, then the best local solution replaces the best global solution. The advantages of PSO are that it is easy to implement and there are few parameters to adjust [8].

IV LOAD FREQUENCY CONTROL OF FOUR AREA POWER SYSTEMS WITH PID CONTROLLER

4.1 FOUR-AREA POWER SYSTEM

Power systems have variable and complicated characteristics and comprise different control parts and also many of the parts are nonlinear [9]. These parts are connected to each other by tie lines and need controllability of frequency and power flow [10].

Interconnected multiple-area power systems can be depicted by using circles. A simplified four area interconnected power system used in this study is shown in Figure 4.1 [11].

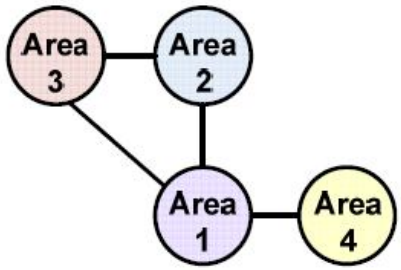

Figure 4.1 Simplified interconnected power system diagram

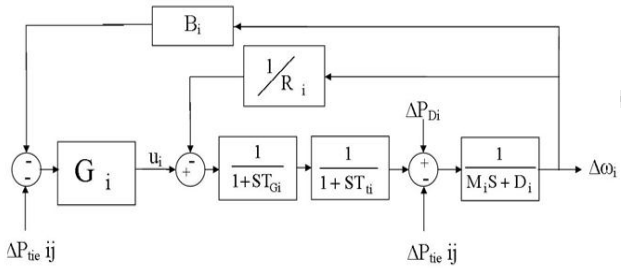

Figure 4.2 Block diagram for one area of system (ith area)

The parameters in Figure 4.2 are defined as follow:

Δ: Deviation from nominal value

M_i=2H: Constant of inertia of ith area

D_i: Damping constant of ith area

R_i: Gain of speed droop feedback loop of ith area

T_{ti}: Turbine Time constant of ith area

T_{Gi}: Governor Time constant of ith area

G_i: Controller of ith area

P_{Di}: Load change of ith area

u_i: Reference load of ith area

$B_i=(1/R_i)+D_i$: Frequency bias factor of ith area

$P_{tie\ ij}$: Inter area tie power interchange from ith area to jth area.

Where: i=1, 2, 3, 4 j=1, 2, 3, 4 and $i \neq j$

By using figure 2.8 and 4.2, the final block diagram of a four area power system is as shown in figure 4.3.

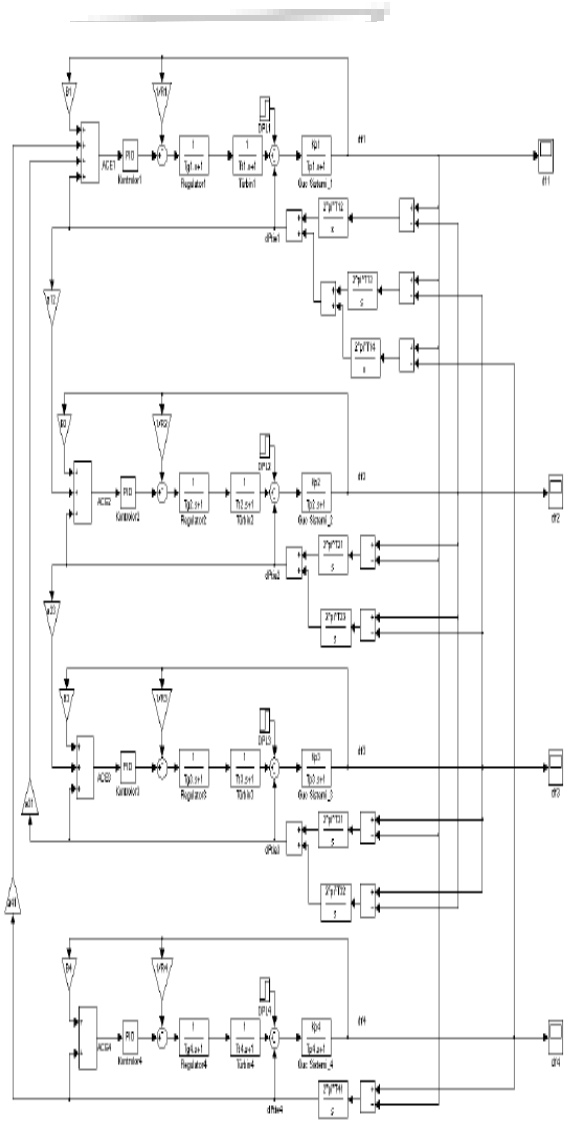

Figure 4.3 Block diagram of a four area power system

4.2 PID CONTROLLER TUNING USING PSO

In this section the parameters of the proposed PID controllers are tuned using PSO. The PID controller has three parameters denoted by K_P, K_I and K_D and for each area there is a PID controller. Therefore in four-area electric power system with four PID

controllers, there are 12 parameters for tuning. These K parameters are obtained based on the PSO. In optimization methods, the first step is to define a performance index for optimal search. In this study the performance index is considered as (4.1). In fact, the performance index is the Integral of the Time multiplied Absolute value of the Error (ITAE) [8].

$$ITAE = \int_0^t t|\Delta\omega_1|dt + \int_0^t t|\Delta\omega_2|dt + \int_0^t t|\Delta\omega_3|dt + \int_0^t t|\Delta\omega_4|dt$$

---------(4.1)

The parameter "t" in ITAE is the simulation time. It is clear to understand that the controller with lower ITAE is better than the other controllers. To compute the optimum parameter values, a 10 % step change in ΔP_{D1} is assumed and the performance index is minimized using PSO. In order to acquire better performance, number of particle, particle size, number of iteration, Γ_1, Γ_2, and Γ are chosen as 24, 12, 40, 2, 2 and 1, respectively. Also, the inertia weight, w, is linearly decreasing from 0.9 to 0.4. It should be noted that PSO algorithm is run several times and then optimal set of parameters is selected. The optimum values of the parameters K_P, K_I and K_D are obtained using PSO and summarized in the Table 1.

Table 1: Optimum values of K_P, K_I and K_D for PSO-PID controllers

	K_P	K_I	K_D
First area PID parameters			12.0818
44.7810	1.0000		
Second area PID parameters			3.3793
67.6872	2.3323		
Third area PID parameters			1.0000
31.9223	1.0000		
Fourth area PID parameters			13.4795
97.3224	1.0000		

Table 2: APPENDIX

Parameters	Values	Parameters	Values
$K_{P\ 1,2,3,4}$	120	$R_{\ 1,2,3,4}$	2.43
$T_{P\ 1,2,3,4}$	20	$B_{\ 1,2,3,4}$	0.425
$T_{g\ 1,2,3,4}$	0.08	$T_{i,j}$	0.086
$T_{t\ 1,2,3,4}$	0.3	a_{ij}	-1

4.3 SIMULATION RESULTS

The system dynamic performance is observed for two different controller structures, PI (Proportional + Integral) and PID controller. The simulation results are shown in Figs. 4.4 to 4.7 in this study.

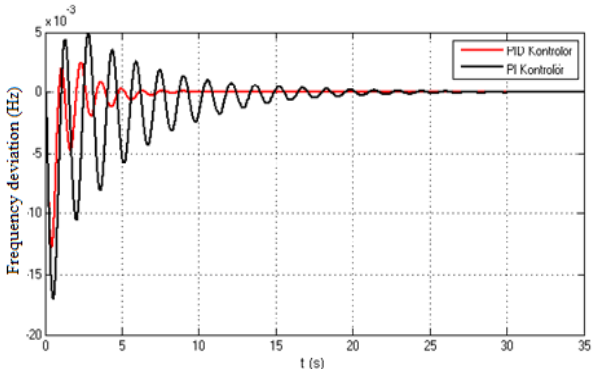

Figure 4.4 Dynamic response of Area1

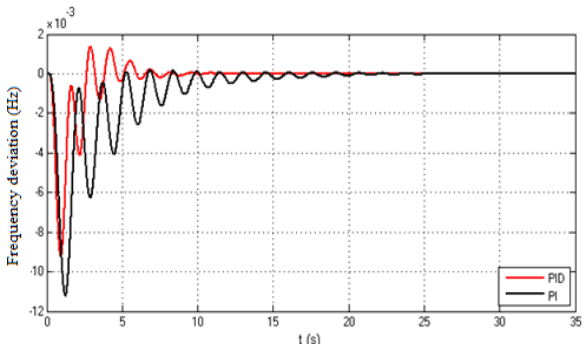

Figure 4.5 Dynamic response of Area2

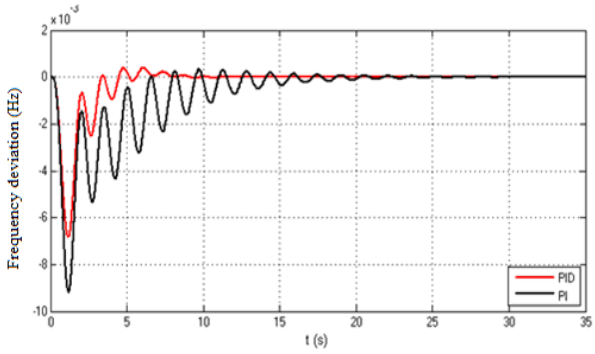

Figure 4.6 Dynamic response of Area3

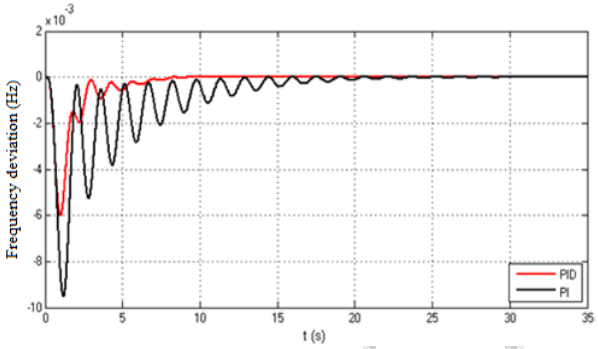

Figure 4.7 Dynamic response of Area4

V CONCLUSION AND FUTURE SCOPE

5.1 CONCLUSION

In this report, modeling and simulation for load frequency control of four-area interconnected power system with PID controller is designed. The tuning of PID controller is done with PSO method. The dynamic performances of different areas are observed via. using PI and PID controller. For investigating the performance, the simulations are carried out in MATLAB/SIMULINK. We see that the response with PID controller is more accurate than the PI controller.

It has been shown that the PSO control algorithms are effective and provides significant improvement in system performance. Therefore, the proposed PID controllers are recommended to generate good quality and reliable electric energy. In addition, the proposed controllers are very simple and easy to implement since it does not require many information about system parameters. Simulations are done by using the same PID parameters for the four different areas because it gives a better performance for the system frequency response than in case of using four different PID parameters for the four areas.

5.2 FUTURE SCOPE

The work is done with a simple four area system but in future the implementation can be done with increased number of areas and with much complicated interconnection tie-lines.

If a power system structure has nonlinear dynamics and parts, the system operating point varies and conventional controllers needing system model must not be used. Thus a modified controller should be deigned. One can design a PID controller with fuzzy logic controller to minimize fluctuation on system outputs.

VI REFERENCES

[1] I. Kocaarslan and E. Cam, “Fuzzy logic controller in interconnected electrical power systems for load-frequency control,” Electrical Power and Energy Systems, vol. 27, no. 8, pp. 542-549, 2005.

[2] V.D.M. Kumar, “Intelligent controllers for automatic generation control,” IEEE Region 10 International Conference on Global Connectivity in Energy, Computer, Communication and Control, TENCON ‘98, vol. 2, pp. 557-574, 1998.

[3] V. Shanmuga Sundaram V. Shanmuga Sundaram, “A Novel Approach of Load Frequency Control in Multi Area Power System” International Journal of Engineering Science and Technology (IJEST), ISSN : 0975-5462, Vol. 3 No. 3 Mar 2011.

[4] Allen J. Wood and Bruce F. Wollenberg, “ Power Generation Operation and Control” ISBN 9814-12-664-0.

[5] Katsuhiko Ogata, “Modern Control Engineering”, 5th Edition, ISBN-978-81-203-4010-7, Chapter 8.

[6] J. G. Ziegler and N. B. Nichols, “Optimum settings for Automatic Controllers”, 1942.

[7] Mohamed M. Ismail, “Load Frequency Control Adaptation using Artificial Intelligent Techniques for one and two different areas Power System”, International Journal of Control, Automation and Systems, Vol. 1, No. 1, Jan. 2012.

[8] Reza Hemmati, Sayed Mojtaba Shirvani Boroujeni, “PID Controller Adjustment using PSO for Multi Ares Frequency Control”, Australian Journal of Basic and Applied Sciences, 5(3): 295-302, 2011, ISSN 1991-8178.

[9] E. Cam and I. Kocaarslan, “Load frequency control in two area power systems using fuzzy logic controller,” Energy Conversion and Management, vol. 46, no. 2, pp. 233-243, 2005.

[10] C.S. Chang and W. Fu “Area load frequency control using fuzzy gain scheduling of PI controllers,” Electrical Power and Energy Systems, vol. 42, no. 2, pp. 145-152, 1997.

[11] T.C. Yang, Z.T. Ding, and H. Yu, “Decentralised power system load frequency control beyond the limit of diagonal dominance,” Electrical Power and Energy Systems, vol. 24, no. 3, pp. 173-184, 2002.

[12] Emre Ozkop, Ismail H. Altas, Adel M. Sharaf, “Load Frequency Control in Four area Power Systems Using Fuzzy Logic PI Contoller”, 16th National Power Systems Conference, December, 2010.

[13] Enes Yalcin, “Load Frequency Control in Four-area Systems Using PID Controller”, IEEE.

TRENDS IN BRUSHLESS DC (BLDC) MOTOR FUNDAMENTALS

[1]Ankit Patidar, [2]Ashish Verma,

Electrical & Electronics Engineering Department
IES,IPS Academy
[1]ankitmpatidar@gmail.com
[2]ashishverma2012@yahoo.in

Abstract-This paper presents a detailed description of recent trends in BLDC motor. As the speed of the various drive application, has been increased to 15000 rpm,the motor is well suited for this, with high performance of industrial applications. The constructional details with control strategy and converter topology are explained. The modeling and analysis of BLDC is also done. The various industrial applications of BLDC motors like engine cooling in automobiles, traction systems, returnless fuel pump, external rotor fan, electric wheel chair with DSP based controller, control of robot arm ,hard disk drive are explained and compared.

***Index Terms**-Back-emf, BLDC drive, Current controller, Hall-Effect sensor, Sensor less, PWM.*

----------***----------

1. INTRODUCTION

The Brushless DC (BLDC) motor is the ideal choice for applications that require high reliability, high efficiency, and high power-to-volume ratio. Generally speaking, a BLDC motor is considered to be a high performance motor that is capable of providing large amounts of torque over a vast speed range. BLDC motors are a derivative of the most commonly used DC motor, the brushed DC motor, and they share the same torque and speed performance curve characteristics. The major difference between the two is the use of brushes. BLDC motors do not have brushes (hence the name "brushless DC") and must be electronically commutated.

Commutation is the act of changing the motor phase currents at the appropriate times to produce rotational torque. In a brush DC motor, the motor assembly contains a physical commutator which is moved by means of actual brushes in order to move the rotor. With a BLDC motor, electrical current powers a permanent magnet that causes the motor to move, so no physical commutator is necessary.

A BLDC motor is highly reliable since it does not have any brushes to wear out and replace. When operated in rated conditions, the life expectancy is over 10,000 hours. For long term applications, this can be a tremendous benefit. Whenever a motor breaks down or needs to be replaced, your project, or part of it, must be shut down. This costs you time and money, perhaps a great deal depending on how long it takes to replace the worn part or parts and get the application started again. Although a BLDC motor may cost more than a brushless motor, it will often more than pay for itself in the amount of work time saved.

2. CONSTRUCTION AND OPERATING PRINCIPLE

BLDC motors are a type of synchronous motor. This means the magnetic field generated by the stator and the magnetic field generated by the rotor rotate at the same frequency. BLDC motors do not experience the “slip” that is normally seen in induction motors. BLDC motors come in single-phase, 2-phase and 3-phase configurations. Corresponding to its type, the stator has the same number of windings. Out of these, 3-phase motors are the most popular and widely used. This application note focuses on 3-phase motors.

2.1 Stator

The stator of a BLDC motor consists of stacked steel laminations with windings placed in the

slots that are axially cut along the inner periphery (as shown in Fig. 3). Traditionally, the stator resembles that of an induction motor; however, the windings are distributed in a different manner. Most BLDC motors have three stator windings connected in star fashion. Each of these windings are constructed with numerous coils interconnected to form a winding. One or more coils are placed in the slots and they are interconnected to make a winding. Each of these windings are distributed over the stator periphery to form an even numbers of poles. There are two types of stator windings variants: trapezoidal and sinusoidal motors. This differentiation is made on the basis of the interconnection of coils in the stator windings to give the different types of back Electromotive Force (EMF). Refer to the "What is Back EMF?" section for more information.

As their names indicate, the trapezoidal motor gives a back EMF in trapezoidal fashion and the sinusoidal motor's back EMF is sinusoidal, as shown in Fig.1 and Fig.2. In addition to the back EMF, the phase current also has trapezoidal and sinusoidal variations in the respective types of motor. This makes the torque output by a sinusoidal motor smoother than that of a trapezoidal motor. However, this comes with an extra cost, as the sinusoidal motors take extra winding interconnections because of the coils distribution on the stator periphery, thereby increasing the copper intake by the stator windings. Depending upon the control power supply capability, the motor with the correct voltage rating of the stator can be chosen. Forty-eight volts, or less voltage rated motors are used in automotive, robotics, small arm movements and so on. Motors with 100 volts, or higher ratings, are used in appliances, automation and in industrial applications.

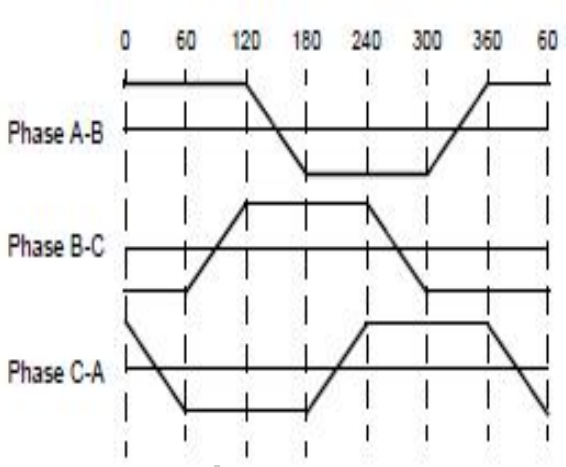

Fig.1. Trapezoidal back emf

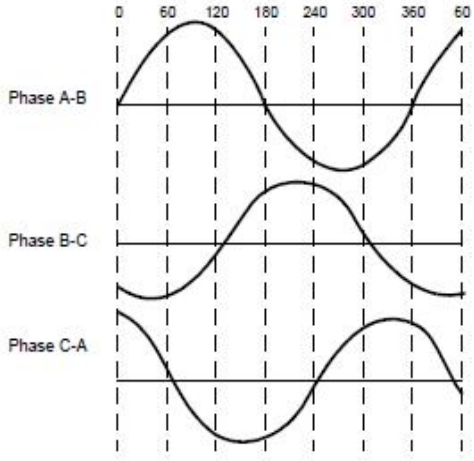

Fig.2. Sinusoidal back emf

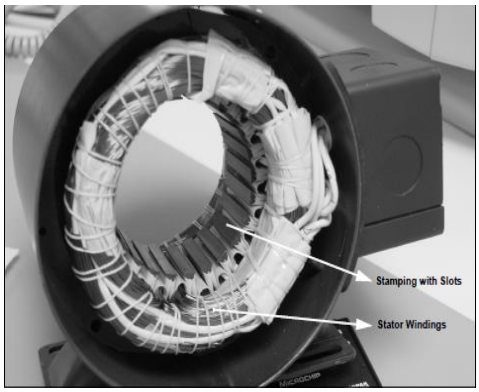

Fig.3. Stator of a BLDC motor

2.2 Rotor

The rotor is made of permanent magnet and can vary from two to eight pole pairs with alternate North (N) and South (S) poles. Based on the required magnetic field density in the rotor, the proper magnetic material is chosen to make the rotor. Ferrite magnets are traditionally used to make permanent magnets. As the technology advances, rare earth alloy magnets are gaining popularity. The ferrite magnets are less expensive but they have the disadvantage of low flux density for a given volume. In contrast, the alloy material has high magnetic density per volume and enables the rotor to compress further for the same torque. Also, these alloy magnets improve the size-to-weight ratio and give higher torque for the same size motor using ferrite magnets. Neodymium (Nd), Samarium Cobalt (SmCo) and the alloy of Neodymium, Ferrite and Boron (NdFeB) are some examples of rare earth alloy magnets. Continuous research is going on to improve the flux density to compress the rotor further. Fig. 4 shows cross sections of different arrangements of magnets in a rotor.

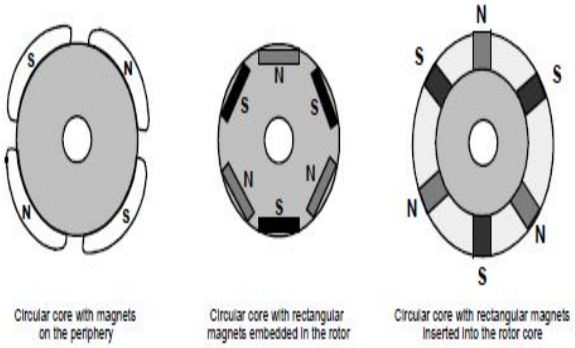

Fig.4. Rotor magnet cross sections

2.3 Hall Sensors

Unlike a brushed DC motor, the commutation of a BLDC motor is controlled electronically. To rotate the BLDC motor, the stator windings should be energized in a sequence. It is important to know the rotor position in order to understand which winding will be energized following the energizing sequence. Rotor position is sensed using Hall effect sensors embedded into the stator. Most BLDC motors have three Hall sensors embedded into the stator on the non-driving end of the motor. Whenever the rotor magnetic poles pass near the Hall sensors, they give a high or low signal, indicating the N

or S pole is passing near the sensors. Based on the combination of these three Hall sensor signals, the exact sequence of commutation can be determined. Figure 5 shows a transverse section of a BLDC motor with a rotor that has alternate N and S permanent magnets. Hall sensors are embedded into the stationary part of the motor. Embedding the Hall sensors into the stator is a complex process because any misalignment in these Hall sensors, with respect to the rotor magnets, will generate an error in determination of the rotor position. To simplify the process of mounting the Hall sensors onto the stator, some motors may have the Hall sensor magnets on the rotor, in addition to the main rotor magnets. These are a scaled down replica version of the rotor. Therefore, whenever the rotor rotates, the Hall sensor magnets give the same effect as the main magnets. The Hall sensors are normally mounted on a PC board and fixed to the enclosure cap on the non-driving end. This enables users to adjust the complete assembly of Hall sensors, to align with the rotor magnets, in order to achieve the best performance. Based on the physical position of the Hall sensors, there are two versions of output. The Hall sensors may be at 60° or 120° phase shift to each other. Based on this, the motor manufacturer defines the commutation sequence, which should be followed when controlling the motor.

2.4 Theory of Operation

Each commutation sequence has one of the windings energized to positive power (current enters into the winding), the second winding is negative (current exits the winding) and the third is in a non-energized condition. Torque is produced because of the interaction between the

magnetic field generated by the stator coils and the permanent magnets. Ideally, the peak torque occurs when these two fields are at 90° to each other and falls off as the fields move together. In order to keep the motor running, the magnetic field produced by the windings should shift position, as the rotor moves to catch up with the stator field. What is known as "Six-Step Commutation" defines the sequence of energizing the windings. See the **"Commutation Sequence"** section for detailed information and an example on six-step commutation.

3. TORQUE/SPEED CHARACTERISTICS

Fig. 5 shows an example of torque/speed characteristics. There are two torque parameters used to define a BLDC motor, peak torque (TP) and rated torque (TR). During continuous operations, the motor can be loaded up to the rated torque. As discussed earlier, in a BLDC motor, the torque remains constant for a speed range up to the rated speed. The motor can be run up to the maximum speed, which can be up to 150% of the rated speed, but the torque starts dropping. Applications that have frequent starts and stops and frequent reversals of rotation with load on the motor, demand more torque than the rated torque. This requirement comes for a brief period, especially when the motor starts from a standstill and during acceleration. During this period, extra torque is required to overcome the inertia of the load and the rotor itself. The motor can deliver a higher torque, maximum up to peak torque, as long as it follows the speed torque curve.

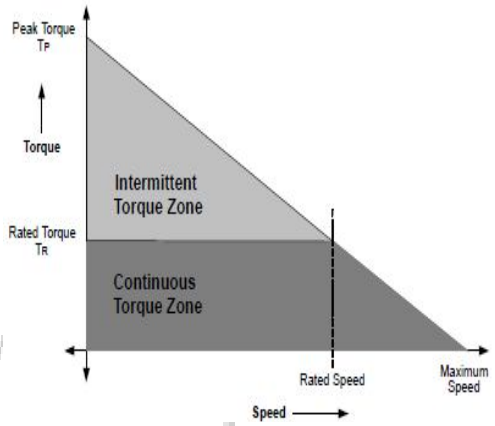

Fig. 5. Torque/speed characteristics

4. COMPARING BLDC MOTORS TO OTHER MOTOR TYPES

Compared to brushed DC motors and induction motors, BLDC motors have many advantages and few disadvantages. Brushless motors require less maintenance, so they have a longer life compared with brushed DC motors. BLDC motors produce more output power per frame size than brushed DC motors and induction motors. Because the rotor is made of permanent magnets, the rotor inertia is less, compared with other types of motors. This improves acceleration and deceleration characteristics, shortening operating cycles. Their linear speed/torque characteristics produce predictable speed regulation. With brushless motors, brush inspection is eliminated, making them ideal for limited access areas and applications where servicing is difficult. BLDC motors operate much more quietly than brushed DC motors, reducing Electromagnetic Interference (EMI). Low-voltage models are ideal for battery operation, portable equipment or medical applications. Table I summarizes the comparison between a BLDC motor and a brushed DC motor. Table II compares a BLDC motor to an induction motor.

TABLE I:

COMPARING A BLDC MOTOR TO A BRUSHED DC MOTOR

Feature	BLDC Motor	Brushed DC Motor
Commutation	Electronic commutation based on Hall position sensors.	Brushed commutation.
Maintenance	Less required due to absence of brushes.	Periodic maintenance is required.
Life	Longer.	Shorter.
Speed/Torque Characteristics	Flat – Enables operation at all speeds with rated load.	Moderately flat – At higher speeds, brush friction increases, thus reducing useful torque.
Efficiency	High – No voltage drop across brushes.	Moderate.
Output Power/ Frame Size	High – Reduced size due to superior thermal characteristics. Because BLDC has the windings on the stator, which is connected to the case, the heat dissipation is better.	Moderate/Low – The heat produced by the armature is dissipated in the air gap, thus increasing the temperature in the air gap and limiting specs on the output power/frame size.
Rotor Inertia	Low, because it has permanent magnets on the rotor. This improves the dynamic response.	Higher rotor inertia which limits the dynamic characteristics.
Speed Range	Higher – No mechanical limitation imposed by brushes/commutator.	Lower – Mechanical limitations by the brushes.
Electric Noise Generation	Low.	Arcs in the brushes will generate noise causing EMI in the equipment nearby.
Cost of Building	Higher – Since it has permanent magnets, building costs are higher.	Low.
Control	Complex and expensive.	Simple and inexpensive.
Control Requirements	A controller is always required to keep the motor running. The same controller can be used for variable speed control.	No controller is required for fixed speed; a controller is required only if variable speed is desired.

TABLE II:

COMPARING A BLDC MOTOR TO AN INDUCTION MOTOR

Features	BLDC Motors	AC Induction Motors
Speed/Torque Characteristics	Flat – Enables operation at all speeds with rated load.	Nonlinear – Lower torque at lower speeds.
Output Power/ Frame Size	High – Since it has permanent magnets on the rotor, smaller size can be achieved for a given output power.	Moderate – Since both stator and rotor have windings, the output power to size is lower than BLDC.
Rotor Inertia	Low – Better dynamic characteristics.	High – Poor dynamic characteristics.
Starting Current	Rated – No special starter circuit required.	Approximately up to seven times of rated – Starter circuit rating should be carefully selected. Normally uses a Star-Delta starter.
Control Requirements	A controller is always required to keep the motor running. The same controller can be used for variable speed control.	No controller is required for fixed speed; a controller is required only if variable speed is desired.
Slip	No slip is experienced between stator and rotor frequencies.	The rotor runs at a lower frequency than stator by slip frequency and slip increases with load on the motor.

5. MATHEMATICAL MODEL

Each active phase in ac motor is describe by a first order differential equation. The general voltage equation of one of active phases is given by, Where v_x is the active phase voltage, R is the phase resistance, i_x is the phase current, θ is the rotor position, $\psi_{kx}(\theta, i_x)$ is the total flux linkage of the active phase and n is the number of phases.

The equivalent circuit of BLDC motor is shown in fig.7. Each phase of the motor is showing its winding resistance, self and mutual inductance and back emfs also.

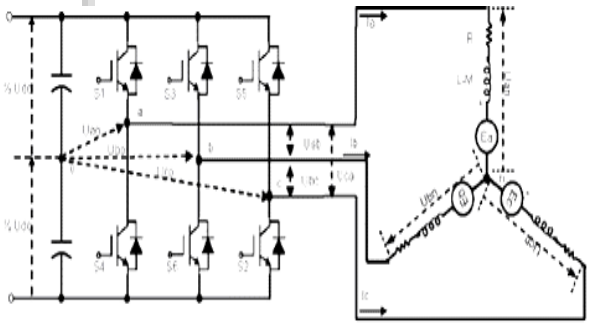

Fig.6. BLDC Equivalent circuit with inverter

A three phase BLDC motor has three winding on stator and permanent magnet on rotor. To model the BLDC motor following assumptions have been made

1. The stator resistance(R) of all windings are equal.
2. The self(L) and mutual(M) inductance's of all winding are equal.
3. Rotor reluctance versus electrical angle are constant.
4. The motor is not saturated.
5. The iron losses are negligible.
6. Power semiconductor devices in the inverter are ideal.

The equivalent circuit of BLDC motor for one phase is shown in fig.7.

Hence the mathematical model is

$$\begin{bmatrix} va \\ vb \\ vc \end{bmatrix} = \begin{bmatrix} R & 0 & 0 \\ 0 & R & 0 \\ 0 & 0 & R \end{bmatrix} \begin{bmatrix} ia \\ ib \\ ic \end{bmatrix} + \begin{bmatrix} L-M & 0 & 0 \\ 0 & L-M & 0 \\ 0 & 0 & L-M \end{bmatrix} \frac{d}{dt} \begin{bmatrix} ia \\ ib \\ ic \end{bmatrix} + \begin{bmatrix} ea \\ eb \\ ec \end{bmatrix} \text{---- (i)}$$

The backemf's are e_a, e_b and e_c have trapezoidal shapes as shown in fig. 6.

The electromagnetic torque is given by :

$$Te = (e_a i_a + e_b i_b + e_c i_c)/\omega \text{ -------(ii)}$$

And mechanical motion equation is :

$$J \frac{d\omega r}{dt} - B \omega r = T_e - T_L \quad \text{(iii)}$$

Where T_L is the load torque, J is the inertia and B is damping co-effiecient.

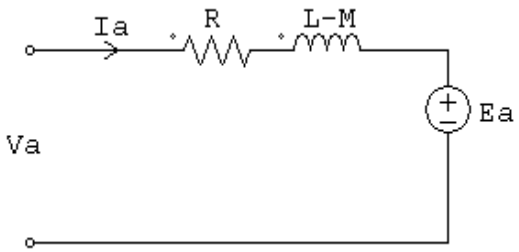

Fig.7. Equivalent circuit of one phase of BLDC motor

6. CONTROL STRATEGY

In a BLDC motor, the position of the rotor is sensed and continually fed back to the commutation electronics to provide for appropriate switching. The BLDC motor is driven by voltage strokes coupled with the given rotor position. The generated stator flux, together with the rotor flux, which is generated by a rotor magnet, defines the torque and thus the speed of the motor. To get the maximum generated torque, the voltage strokes must be applied to the 3-phase winding system, so that the angle between the stator flux and the rotor flux is kept close to 90°. To meet this criterion, the motor requires electronic control for proper operation. This rotor position sensing can be accomplished in many ways.

6.1 Hall Effect

Hall Effect devices which generally provide optimum size and the best environmental capabilities versus cost. The generalized block diagram of this method is shown in fig.8.

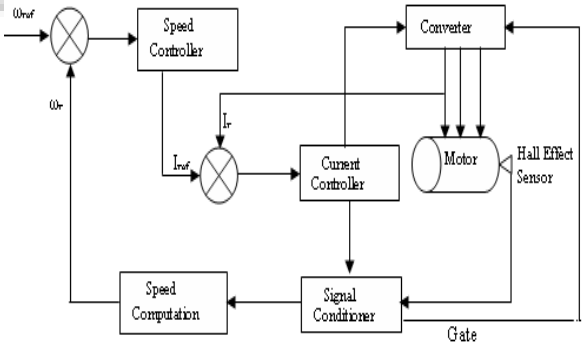

Fig.8. Block Diagram Of Hall Effect Sensor Method

6.2 Back emf detection technique

Back emf detection technique is used for sensorless operation of BLDC motor. The detected back-emf signal is either utilized by DSP, microcontroller, PWM technique for commutation of phases. General block diagram of back emf detection technique is shown in fig 6.

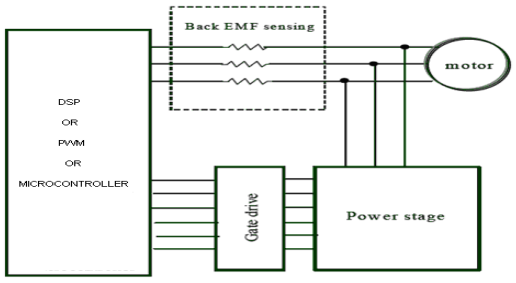

Fig. 6 Block Diagram Of Back EMF Feedback Method

6.3 Digital Control Technique

The BLDC motor will only operates in two predefined States. Within those States and under steady state conditions, the load torque and the developed torque will be constant. Even though alternating of states may occur at every sampling time $t=kT_P$, it is reasonable to assume that the developed mechanical torque will be in steady state. The block diagram for digital control technique is shown in fig.9. The first open loop controller creates state-1 which generates the necessary electromagnetic torque to operate the motor at a speed of low omega (ωL).Operation in state-2, which is attained with the second open loop controller, results in a motor speed of high omega (ωH). where $\omega L<\omega<\omega H$, the digital controller will achieve speed regulation by appropriately alternating states. In other words, the digital controller compares the motor speed to the commanded speed and determines which actuation signal.

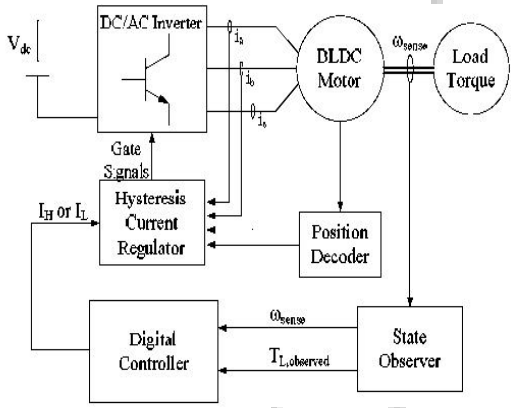

Fig.9 Block Diagram of Digital Control Techniques

6.4 Fuzzy Logic Based Back EMF

Conventional sensorless methods of the BLDC motor have low performance in transient state or low speed range and occasionally require additional circuit. The fuzzy back-EMF observer based on fuzzy function approximation and a novel sensorless control algorithm using this observer. Because fuzzy logic can estimate a variable shape function such as back-EMF of the BLDC motor, both changed and constant back-EMF are excellently estimated by the fuzzy back-EMF observer.

7. BLDC MOTOR APPLICATIONS

Brushless motors fulfill many functions originally performed by brushed DC motors, but cost and control complexity prevents brushless motors from replacing brushed motors completely in the lowest-cost areas. Nevertheless, brushless motors have come to dominate many applications, particularly devices such as computer hard drives and CD/DVD players. Small cooling fans in electronic equipment are powered exclusively by brushless motors. They can be found in cordless power tools where the increased efficiency of the motor leads to longer periods of use before the battery needs to be charged. Low speed, low power brushless motors are used in direct-drive turntables for gramophone records.

A. Transport

High power brushless motors are found in electric vehicles and hybrid vehicles. These motors are essentially AC synchronous motors with permanent magnet rotors. The Segway Scooter and Vectrix Maxi-Scooter use brushless technology. A number of electric bicycles use brushless motors that are sometimes built into the wheel hub itself, with the stator fixed solidly to the axle and the magnets attached to and rotating with the wheel.

B. Heating and ventilations

There is a trend in the HVAC and refrigeration industries to use brushless motors instead of various types of AC motors. The most significant reason to switch to a brushless motor is the dramatic reduction in power required to operate them versus a typical AC motor. While shaded-pole and permanent split capacitor motors once dominated as the fan motor of choice, many fans are now run using a

brushless motor. Some fans use brushless motors also in order to increase overall system efficiency.

C. Motion control systems

Brushless motors are commonly used as pump, fan and spindle drives in adjustable or variable speed applications. They can develop high torque with good speed response. In addition, they can be easily automated for remote control. Due to their construction, they have good thermal characteristics and high energy efficiency. To obtain a variable speed response, brushless motors operate in an electromechanical system that includes an electronic motor controller and a rotor position feedback sensor.

D. Positioning and actuation systems

Brushless motors are used in industrial positioning and actuation applications. For assembly robots, brushless stepper or servomotors are used to position a part for assembly or a tool for a manufacturing process, such as welding or painting. Brushless motors can also be used to drive linear actuators.

E. RC Cars

Their popularity has also risen in the radio controlled car sector. Brushless motors have been legal in North American RC car racing in accordance to ROAR since 2006. These motors provide a great amount of power to RC racers and if paired with appropriate gearing and LiPo Batteries, these cars can go up to 100 Miles/Hour (161km/h).

F. **Electric Traction Application**

Electromagnetic load per volume ratio becomes larger according to the needs of new application fields of motors, such as vehicle tractions and development of motorized systems, which are to replace the existing hydraulic machinery like break by wire and electric compressor. According to the recent higher output design trend and with the help of pwm power conversion circuits and advanced control techniques, permanent magnet (PM) excited motors can be regarded as one of the best solutions and they have increasingly gained much interests. The spoke type BLDC motor (SPOKE-BLDC) as a high power motor. The rotor structure of SPOKE-BLDC is an interior type PMs with higher saliency ratios. The magnetic flux generated by PMs becomes concentrated, resulting in increase of higher torque density per volume. [14]

G. Automotive Fuel Pump

This motor is well suited for automotive return less fuel pump. In a return less fuel system the fuel pump speed is adjusted to maintain constant fuel pressure over the fuel demand/load range. This requires some level of feedback and control. This control is typically performed by a microcontroller. Since a microcontroller is already in use, incorporating brushless commutation to the mix is incremental in cost. [12]

H. Cooling Fan Application in automotive

The automobile is undergoing a revolution in the design of its electrical system. The electrical power demand in automobiles is rising steadily, especially in luxury vehicles, due to new electrical systems that enhance passenger comfort and safety. In buses of the future, throttle actuation, power assist steering, active suspension and air-conditioning and electrically cooling system will all benefit from the electrical power system. Therefore, the main electrical bus of the future will be 42V, and it will be buffered by a 36V battery. 42V BLDC motor for Cooling Fan Application which is predicted a main Power Load in future Automotive Electrical System. For the designing of High Efficiency and Low Noise of Cooling Fan Motor.

8. CONCLUSION

In conclusion, BLDC motors have advantages over brushed DC motors and induction motors. They have better speed versus torque characteristics, high dynamic response, high

efficiency, long operating life, noiseless operation, higher speed ranges, rugged construction and so on. Also, torque delivered to the motor size is higher, making it useful in applications where space and weight are critical factors. With these advantages, BLDC motors find wide spread applications in automotive, appliance, aerospace, consumer, medical, instrumentation and automation industries.

REFERENCES

[1] S.X.Chen,M.A.Jabbar,Q.D.Zang and Z.J.Liu "New challenges: electromagnetic design of BLDC motors for high speed fluid film bearing spindles used in hard disk drives" IEEE transaction on magnetics vol 32, No 5, sept. 1996. Pp 3854-3856.

[2] J.S. Ko "Asymptotically stable adaptive load torque observer for precision position control of BLDC motor" IEE proceeding power application. Vol 145,No 4 July 1998.Pp 383-386.

[3] C.Bi,Z.J.Liu and S.X. Chen "Estimation of Back-Emf of PM BLDC motors using derivative of FE solutions" IEEE transaction on magnetics vol 36, No 4, july2000 Pp 697-700.

[4] Byoung-Heekang, Choel-ju Kim, Hyung-su Mok,Gyu-Hachoe "Analysis of torque ripple in BLDC motor with commutation time" ISIE conf. 2001 Pusan, Korea.Pp 1044-1048.

[5] G.H.Jang, J.H.Park and J.H.Chang. "Position detection and start-up algorithmof a rotor in a sensorless BLDC motor utilising inductance variation." IEEProc.-Electr.Power Appl. Vol 149, No. 2 March 2002.pp 137-142.

[6] S.M. Madani Lei Hao Hamid A.Toliyat. "A Low Cost Four-Switch BLDC Motor Drive with Active Power Factor Correction." 07803-7474-6/02 2002 IEEE Conf. Pp 579-584.

[7] Andrar lelkes Jens Krotsch RikW. De Doncker. " Low – Noise External rotor BLDC Motor for Fan Applications." 0-7803-7420-7/02 2002 IEEE Conf.Pp 2036-2042 **.**

[8] Sung-In Park,Tae- Sung Kim, Sung-Chan ahn*, Dong-Seok Hyun. "An Improved Curent Control Method For Torque Improvement Of High-Speed BLDC Motor" 7803-7768-0/03 2003 IEEE Conf.Pp 294-299**.**

[9] Tae-Hyung Kim, and Mehrdad Ehsani. "An Error Analysis of the Sensorless Position Estimation for BLDC Motors". 0-7803-0/03 2003 IEEE Conf. Pp 611-617 .

[10] John E. Makaran, and Joe Lo Vetri. "BLDC Motor and Drive Conducted RFI Simulation for Automotive Applications." IEEE Transactions On Electromagnetic Compatibility. Vol.45.No.2, May 2003. Pp. 316-329.

[11] Quan Jiang, ChaoBi, Abdullah Al Mamum. "An Effective Approach to Predict Performances of High Speed BLDC Motors in Hard DiskDrives." 0-7803-7906-3/03 2003. IEEE Conf. Pp.2120-2125.

[12] Jianwen Shao, Dennis Nolan,and David Swanson. "A Novel Microcontroller-Based Sensorless Brushless DC (BLDC)Motor drive for Automotive Fuel Pumps.IEEE Transactions on Industry Applications,Vol. 39, No.6,November/December2003. Pp1734-1740.

[13] Ki-Hong Park, Tae-Sung Kim, Sung- Chan Ahn, Dong-Seok Hyun. "Speed Control Of High- Performance Brushless DC Motor Drives by Load Torque Estimation." 0-7803-7754-0/03 2003 IEEE Conf., Pp 1677-1681.

[14] Byoung-Kuk Lee,Gyu-HoungKang, Jin Hur and Dong-Wook You. "Design of Spoke Type BLDC Motors with High Power density for Traction Applications." IEEE IAS Conf 2004 Pp 1068-1074.

[15] Jun-Uk Chu, In-Hyuk Moon Gi-Won Choi, Jei-Cheong Ryu,and Mu-Seong Mun "Design of BLDC Motor Controller for Electric Power wheelchair."0-7803-8599-3/04 2004,IEEE Conf. Pp. 92-97.

[16] Tae-Hyung Kim, Hyung-Woo Lee and Mehrded Ehsani., " Advanced Sensorless Drive Technikque for Multiphase BLDC Motors." The 30th Annual conference of the IEEE Indutrial ElectronicsSociety, November 2-6, 2004, Busan, Korea. 0-7803-8730-9/04 IEEE PP. 926-937.

Lightning strike

Imagine devices that capture electricity from the air — much like solar cells capture sunlight — and using them to light a house or recharge an electric car. Imagine using similar panels on the rooftops of buildings to prevent lightning before it forms. Strange as it may sound, scientists already are in the early stages of developing such devices, according to a report presented at the 240th National Meeting of the American Chemical Society (ACS)."Our research could pave the way for turning electricity from the atmosphere into an alternative energy source for the future," said study leader Fernando Galembeck, Ph.D. His research may help explain a 200-year-old scientific riddle about how electricity is produced and discharged in the atmosphere. "Just as solar energy could free some households from paying electric bills, this promising new energy source could have a similar effect," he maintained.

"If we know how electricity builds up and spreads in the atmosphere, we can also prevent death and damage caused by lightning strikes," Galembeck said, noting that lightning causes thousands of deaths and injuries worldwide and millions of dollars in property damage.

The notion of harnessing the power of electricity formed naturally has tantalized scientists for centuries. They noticed that sparks of static electricity formed as steam escaped from boilers. Workers who touched the steam even got painful electrical shocks. Famed inventor Nikola Tesla, for example, was among those who dreamed of capturing and using electricity from the air. It's the electricity formed, for instance, when water vapor collects on microscopic particles of dust and other material in the air. But until now, scientists lacked adequate knowledge about the processes involved in formation and release of electricity from water in the atmosphere, Galembeck said. He is with the University of Campinas in Campinas, SP, Brazil. Scientists once believed that water droplets in the atmosphere were electrically neutral, and remained so even after coming into contact with the electrical charges on dust particles and droplets of other liquids. But new evidence suggested that water in the atmosphere really does pick up an electrical charge."This was clear evidence that water in the atmosphere can accumulate electrical charges and transfer them to other materials it comes into contact with," Galembeck explained. "We are calling this 'hydroelectricity,' meaning 'humidity electricity'."

In the future, he added, it may be possible to develop collectors, similar to the solar cells that collect the sunlight to produce electricity, to capture hydroelectricity and route it to homes and businesses. Just as solar cells work best in sunny areas of the world, hydroelectrically panels would work more efficiently in areas with high humidity, such as the northeastern and southeastern United States and the humid tropics.

"These are fascinating ideas that new studies by ourselves and by other scientific teams suggest are now possible," Galembeck said. "We certainly have a long way to go. But the benefits in the long range of harnessing hygro electricity could be substantial."National Council for Scientific and Technological Development and The State of São Paulo Research Foundation funded the study.

Prachi Sharma

EX IV Year

Where's the Action?

Electrical engineering covers a wide range of areas in the high-tech sector. “A lot of the areas which are coming up [require a knowledge of] other fields,” Katehi says, referring to the more interdisciplinary shape electrical engineering will take in the future. Take for example, biomedical engineering. Bruce Wooley, chairman of the Department of Electrical Engineering and a professor of electrical engineering at Berkeley, hints at the possibilities that lie before electrical engineers in biology, trying to understand the body as a system. “The core of electrical engineering is the ability to process signals and information,” he says. “Extending that signal processing into other domains will be characteristic [of the future].” Another example is nanotechnology, manipulating and replicating materials on a molecular scale, which requires the pooled resources of chemists and electrical engineers. And there will be plenty of opportunities and expansion in electrical engineering itself. Wireless continues to be a buzzword for the telecommunications industry, and with optical networks stretching across the country and around the world, the industry shows little sign of slowing. “We're seeing a situation beginning to develop now where many of the large, established high-tech firms are building important market niches in the telecommunications area,” Albertson says. “That is going to be a very important growth trend as we move more into this decade.“ Many expect optics (the use of thin strands of glass to carry information by lasers) and photonics (capturing photonic energy to transmit information by light), both important facets of telecommunications technology, to thrive in the years to come. Says Steadman, who is also head of the Department of Electrical and Computer Engineering at the University of Wyoming, “We will hopefully see the development of true optical switching and optical repeating, so that bandwidths can be maintained over larger distances and with large networks.“

Aishwarya Sinha

EX III Year

Large selection of engineering paths gives career flexibility

Entering an engineering program opens the door to multiple branches of engineering. Many schools require the student to complete a general first-year curriculum (math, science, English, and computer skills) before moving forward in an engineering specialty. This allows the student to explore and firm up his or her engineering interest. A typical college may have the following engineering majors: aeronautics and astronautics, agricultural, biological and food processing, biomedical, chemical, civil, computer, construction, electrical, environmental and ecological, materials, mechanical, and nuclear.

Nupur Rawat

EX III Year

Engineering work is challenging.

Engineers work in a professional environment where there is an opportunity to learn and grow through on-the-job and formal training using the most up-to-date technologies. There will never be a shortage of new challenges, as engineers are constantly faced with having to adapt solutions and change technology to move with the trends and needs.

Based on the above reasons, if any young person has strong STEM aptitudes, has completed the STEM coursework, and has a desire to work in problem solving and help the world, entering the engineering program is the right choice as a means to a better life economically, job satisfaction, and a good career.

Ashumendra Singh Chandel

EX IV Year

SUCCESS GRAPH

Harsh Gujrati

EX IV Year

Students Achievements:

2014-15					
S. No	**Year**	**Name of student**	**Name of event**	**Award/Prize**	**Organizer**
1	2014-15	Rajat S. Chandel	Taekwondo / Karate tournament.	1) Awarded as FIRST DAN in taekwondo 2) Registered as INTERNATIONAL TRAINER in kukkiwon korea 3) Secured GOLD MEDAL in second annual international gosoku ruo championship in indore . 4) Awarded referee in state karate tournament. 5) Gold Medal in State Karate Tournament. 6) 1st position in Gold Cup at Gwalior. 7) Attended Interstate Training Camp at	World Taekwondo federation /Taekwondo federation of India/ SCKFI(Shotokan chidokan karate do federation India) India Karate association of India

				Mandu. 8) Official Referee of Inter Dojo Karate Competition at Gujrat.	
		Parvez Khan	Hockey Shot put	1Representing RGPV M.P. Hockey Team in Inter University to be held at Bhopal. 2) Runner up of Inter College Hockey Nodal in 2014. 3) Runner up in Shot put in Swaranjali 2014 Special achievement award in sport in Swaranjali 2014	
	(30Jan to 2Feb2015)	Abhishek Kumar	KSHITIJ'2015 Open Soft (30Jan to2Feb2015)	2 Position	IIT Kharagpur